

**REPORT DOCUMENTATION PAGE**

Form Approved OMB No. 0704-0188

Public reporting burden for this collection of information is estimated to average 1 hour per response, including the time for reviewing instructions, searching existing data sources, gathering and maintaining the data needed, and completing and reviewing the collection of information. Send comments regarding this burden estimate or any other aspect of this collection of information, including suggestions for reducing this burden to Washington Headquarters Services, Directorate for Information Operations and Reports, 1215 Jefferson Davis Highway, Suite 1204, Arlington, VA 22202-4302, and to the Office of Management and Budget, Paperwork Reduction Project (0704-0188), Washington, DC 20503.

1. AGENCY USE ONLY (Leave blank)	2. REPORT DATE 1994	3. REPORT TYPE AND DATES COVERED Final Report	
4. TITLE AND SUBTITLE 2D High Resolution Shock Wave Physics Code		5. FUNDING NUMBERS F6170893W0972	
6. AUTHOR(S) O.Yu.Vorobiev, A.V.Shutov, A.V.Zharov, A.L.Ni, V.E.Fortov			
7. PERFORMING ORGANIZATION NAME(S) AND ADDRESS(ES) HEDRC		8. PERFORMING ORGANIZATION REPORT NUMBER SPC-93-4075	
9. SPONSORING/MONITORING AGENCY NAME(S) AND ADDRESS(ES) EOARD PSC 802 BOX 14 FPO AE 09499-0200		10. SPONSORING/MONITORING AGENCY REPORT NUMBER SPC-93-4075	
11. SUPPLEMENTARY NOTES			
12a. DISTRIBUTION/AVAILABILITY STATEMENT Approved for public release; distribution is unlimited.		12b. DISTRIBUTION CODE A	
13. ABSTRACT (Maximum 200 words)  In the present work, we used Godunov's scheme for computations. Godunov's method in moving grids provides great possibilities and includes both Lagrangian and Eulerian approaches as partial cases. It should be marked that this scheme has been intensively explored for simulations of aerodynamic problems, where high accuracy of calculations is necessary.			
<b>DTIC QUALITY INSPECTED</b>			
<b>19980312 065</b>			
14. SUBJECT TERMS		15. NUMBER OF PAGES 62	16. PRICE CODE N/A
17. SECURITY CLASSIFICATION OF REPORT UNCLASSIFIED	18. SECURITY CLASSIFICATION OF THIS PAGE UNCLASSIFIED	19. SECURITY CLASSIFICATION OF ABSTRACT UNCLASSIFIED	20. LIMITATION OF ABSTRACT UL

2D HIGH RESOLUTION SHOCK WAVE PHYSICS CODE

3-month technical report

*Godunov's scheme on moving grids  
for high velocity impact simulation.*

Participants:

O. Yu Vorobiev

A. V. Shutov

A. V. Zharov

A. L. Ni

V. E. Fortov

# CONTENTS

I. Introduction.....	
II. Physical model.....	
III. Algorithm of computations.....	
1. Scheme of integration on moving grid	
2. Movement of boundaries	
3. Boundary's type checking	
4. Node distribution along the boundary and grid generation	
5. Riemann problem solution and recalculation of flow parameters	
6. Conclusion remark	
IV. Demonstrative examples.....	
1. TEST № 1: impact of a plane aluminum plate onto a semiinfinite aluminum target	
2. TEST № 2: influence of the grid refinement on the results of numerical simulation of penetration problems	
3. Interaction of spherical projectile with two layered aluminum target	
4. Hypervelocity impact of iron projectile on a target with a conical hole	
V. REFERENCES.....	

## I. Introduction

Problems of hypervelocity impact attract attention of scientists during the last thirty years and occupy a significant part in scientific literature. The urgency of investigations of these problems follows from the practice. It concerns, for example, evaluation of effectiveness of spacecraft debris shields, analysis of asteroid impact events, problems of atomic power stations safety and so on. From the other side the possibility of numerical simulations of these phenomena becomes real owing to progress in theoretical and experimental high pressure high temperature physics. The success of numerical simulation of hypervelocity impact depends on two factors: physical model (including mechanical, kinetic, thermodynamic, etc. properties of matter) and numerical methods for integration of governing equations. The second part of the problem will be discussed below. As to the first one, the review of various substances models is given, for example, in [1, 2].

The most widespread numerical methods for hypervelocity impact (HVI) simulation are based on Lagrangian and particle techniques [3-7]. Huge experience has been stored up to now in this area. It becomes clear, that the main drawback of Lagrangian codes is the restriction on deformations of flow and that of for the PIC codes is the necessity of keeping of "superfluous" information about flow parameters in additional numerical grid cells into which substance can get. Of course, these difficulties are algorithmic and can be overcome by some additional measures. For example, a usual procedure for Lagrangian techniques is reinterpolation of flow parameters into a new grid, when the grid deformations become large [8]. As to Eulerian techniques, one can mention about tracking methods [9], that are used to increase the accuracy of calculations near matter-vacuum and contact boundaries and to restrict the domain of computations. Unfortunately Eulerian codes have one more disadvantage associated with mass dispersion problems, that makes it difficult to calculate debris cloud evolution. There are several ways to decrease this dispersion. For example in [10] both the projectile and the shield were proposed to have nonzero initial velocities moving towards each other to minimize

advection of materials between cells in the Eulerian mesh. In order to decrease dispersion in Eulerian computations high-order accurate advection schemes also were used [11, 12].

As both pure Lagrangian and Eulerian codes have their own drawbacks, it is naturally to develop arbitrary Lagrange-Euler (ALE) codes combining the advantages of these approaches. Following this idea, numerical simulation of penetration of a hypervelocity projectile through multi-plate shield was done [13] using two codes: one for computing of penetration stage (Eulerian) and another (Lagrangian) for debris cloud transport calculation. In recent years, some algorithms of computation of real matter dynamics (including elasto-plastic and damaged matter) developed previously only for Lagrangian frame have been extended to the Eulerian frame of reference [12, 14, 15]. This opens new possibilities for HVI simulations using more flexible ALE codes.

In the present work we used Godunov's scheme for computations [16]. Godunov's method in moving grids provides great possibilities and includes both Lagrangian and Eulerian approaches as partial cases. It should be marked that this scheme has been intensively explored for simulations of aerodynamics problems, where high accuracy of calculations is necessary.

In 1968 S.K.Godunov, A.V.Zabrodin and G.P.Prokopov [17] formulated a programmatic approach to numerical integration of nonsteady Euler equations on moving grids. During several years the authors of this report have been working on realization of this approach. Results of this activity are presented below. For simplicity the consideration is given for the Euler equations omitting of strength effects. Applications of this approach to the problems of high velocity impact illustrate possibilities of 2D code developed. As distinct from the most illustrations of possibilities of this method given in [17], the problems of hypervelocity impact are characterized by strong deformations of matter and wide range of matter state parameters: from initially shock-compressed or strongly heated condensed state to finally expanding gaseous or spalled substance. Large variations of density lead to an enormous increase of geometrical sizes of computed fields occupied by the substance. Contacts separating the substance from vacuum are

the physical boundaries of computational region. Therefore the choice of Lagrangian meshes seems to be a preferable strategy for simulations of this class of problems. Unfortunately Lagrangian meshes crash, when the deformations become large, because the cells deform, twist and finally get tangled. The first factor leads to great restrictions on calculation time step and the second makes further calculations impossible. As to the Eulerian grid the marked above uncertainty in computational region leads to the necessity of keeping additional grid cells and to corresponding increase of computational time. The other problem of Eulerian techniques is the problem of contacts between substances.

Methods based on the use of computational regions with moving boundaries and generation inside of these regions of grids connected only with the boundaries seems to unify the advantages of Eulerian and Lagrangian meshes allowing to overcome their drawbacks. In the most examples given below the emphasis is placed on demonstration of possibilities of application of moving grids for treating the flows with strong deformations. Thus, for example, simulations of impact problems presented in this report have been performed on moving grids with fitting all contacts between different media including the boundaries with vacuum. During the process of interaction the structure and configuration of boundaries change: segments of contacts can disappear, for example because of rebound, and new segments can originate due to involving of new bodies into the process of interaction. The flow region under consideration can be subdivided into several subregions. Boundaries of subregions can be both as original flow singularities (characteristics, boundary between substance and vacuum, the contact boundary between two substances, the axis (plane) of symmetry, the shock wave) and so moving in accordance with their physical nature. They can be also inserted for some computational reasons.

As it was mentioned above, the basic attention is paid to computational aspects of simulation. Nevertheless, the algorithm developed makes it possible using of different physical models in the frame of Godunov's scheme. It concerns, for example, the Riemann problem solver, designed for the case of arbitrary EOS.

## II. Physical model

### *Governing Equations*

One fluid one temperature hydrodynamic model is used in simulations. Governing Euler equations are written in the form of conservation laws of mass, momentum, energy and porous volume, what is necessary for Godunov's method. The conservative form of the motion equations allows to describe both as continuous and so discontinues flows.

$$\begin{aligned}\frac{\partial \rho}{\partial t} + \nabla \rho \mathbf{u} &= 0, \\ \frac{\partial \rho \mathbf{u}}{\partial t} + \nabla \rho \mathbf{u} \times \mathbf{u} &= -\nabla p(1-V_p), \\ \frac{\partial \rho h}{\partial t} + \nabla \rho \mathbf{u} h &= -\nabla p \mathbf{u}(1-V_p), \\ \frac{\partial \rho V_p}{\partial t} + \nabla \rho \mathbf{u} V_p &= \rho \phi.\end{aligned}\tag{2.1}$$

Here  $\rho$ - density,  $\mathbf{u}$ - mass velocity,  $h$ -total specific energy,  $p$ - pressure,  $V_p$ - porous volume per unit volume,  $\phi$ - porous growth rate. For  $\phi$  we use semiempirical spall damage kinetic built on the base of free surface motion registration [1]. Nevertheless this model of spall fracture is valid only for small (up to several percents) porosity. When the porosity of matter becomes greater then some value, the substance does not resist to expansion. In this case the volume occupied by the solid component are not changed anymore and the porosity grows with the increase of specific volume of matter.

### *Equations of state*

Semiempirical wide-range equations of state (EOS) are used [18] to determine the pressure, the temperature and the sound velocity as functions of internal energy per unit mass  $\varepsilon$  and the density of solid component  $\rho_0$  connected with density  $\rho$  as  $\rho_0 = \rho / (1 - V_p)$ . These equations are built on the base of available Hugoniot data and provide for correct asymptotes in the cases of extremely high energies and small densities.

### III. Algorithm of computations

#### 1. Scheme of integration on the moving grid

Eqs.(2.1) are integrated on the moving grid by Godunov's procedure [19]. The scheme of the algorithm is shown in Fig.1. In comparison with the traditional one ([17]) this algorithm enables a possibility of the numerical region division into many subregions with independent grid generation in every subregion. An important problem which should be solved by that is interaction between the boundaries belonged to different subregions.

#### 2. Movement of boundaries

The first step of the algorithm is the displacement of subregion's boundaries. The boundary of each subregion is represented as a coordinate array of nodes. Any boundary between adjacent subregions represents a unification of nodes belonging to boundaries of these subregions. The coordinates of nodes are also stored in special arrays establishing the sequence of nodes. Nodes corresponding to the beginning and to the end of different segments of boundaries are also marked. It means that each boundary segment is represented as a sequence of points belonging to the boundaries of different subregions and that of special end-points of boundaries. The total number of nodes representing boundary exceeds, generally speaking, the number of cells being in contact from the side of adjacent subregions.

To determine velocity of a boundary rib, the Riemann problem with flow parameters from adjacent cells being in contact along every link is solved. In case the Riemann solver yields a negative pressure a rebound along the link is supposed to be happened. This fact is taken into account by inserting some new special boundary points in the array. In more complex physical model the coupling force can be prescribed to the contact and a rebound can be inserted when the tense strengths exceeds the value of this force.



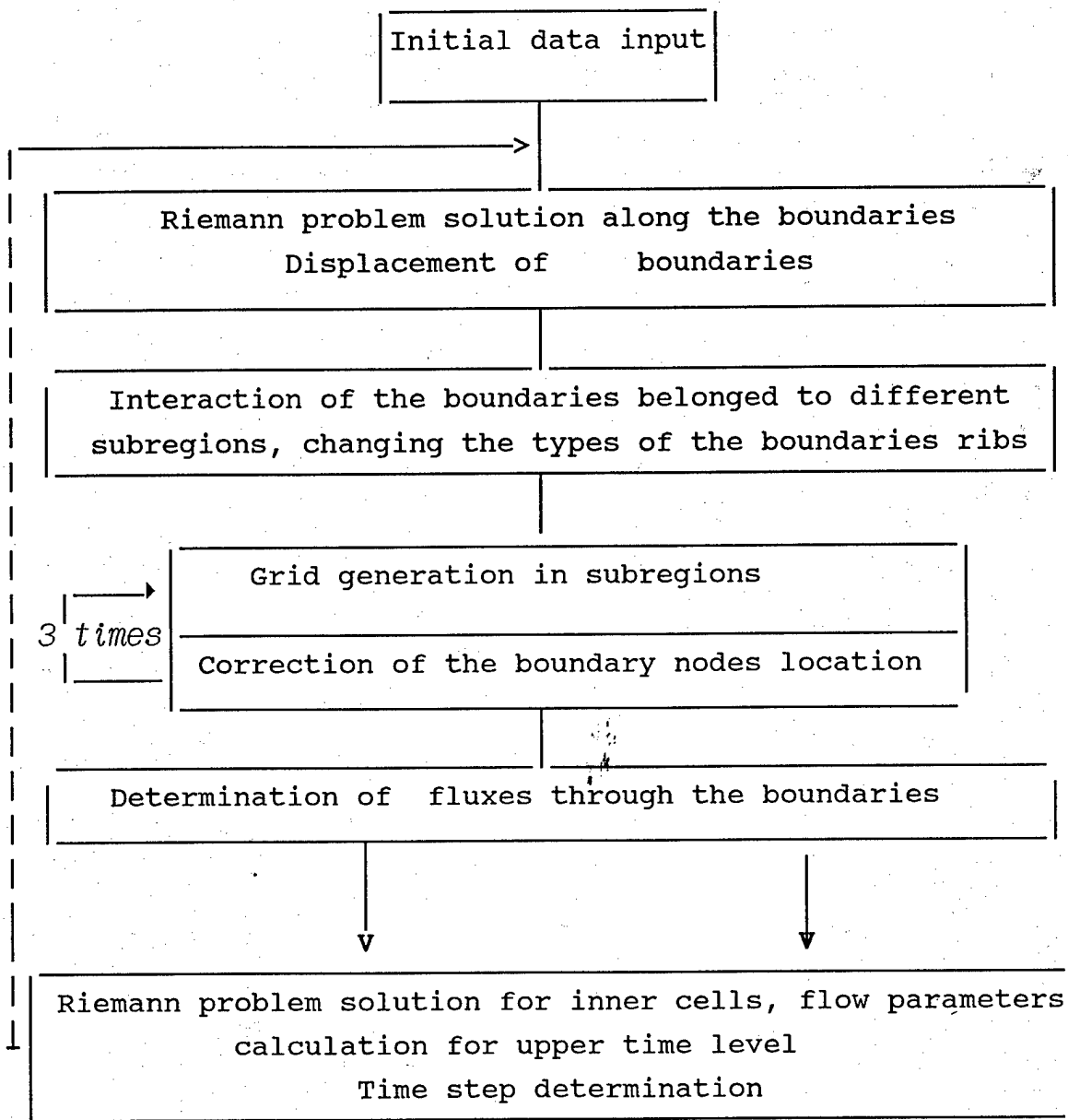


Fig.1 Block-scheme of the algorithm

The velocities of nodes can be calculated after solving of Riemann problem at the rib connecting the nodes. In the Godunov's method the flow parameters; velocity, density, energy are assumed to be uniform inside the meshes. For example, one should take flow parameters from the meshes A and B to calculate velocity  $U_1$  and so from the meshes A and C to calculate velocity  $U_2$ , see fig.2 There may be different ways of nodes velocities interpolation. The linear interpolation proposed by Godunov [17] gives the formula

$$u = \frac{u_1 l_2 + u_2 l_1}{l_1 + l_2} \quad (3.1)$$

How it's seen from (3.1) the shorter the rib is, the more contribution gives it in the node velocity. (For example, if  $l_1 \gg l_2$  then  $u \cong u_2$ ) From another point of view, if we want to minimize the middle-square deviation between the boundary displacement obtained from the Riemann problem solution, when every rib moves with an appropriate "big" velocity, and the boundary displacement determined by the nodes movement one should use the following formula (how it has been shown in [20])

$$u^* = \frac{u_1 l_1 + u_2 l_2}{l_1 + l_2} \quad (3.2)$$

In present algorithm we use an average way of interpolation between (3.1) and (3.2), which leads to a simple formula

$$u = 0.5 * (u + u^*) = 0.5 * (u_1 + u_2) \quad (3.3)$$

The formula (3.3) combines the advantage of (3.1) with simplicity.

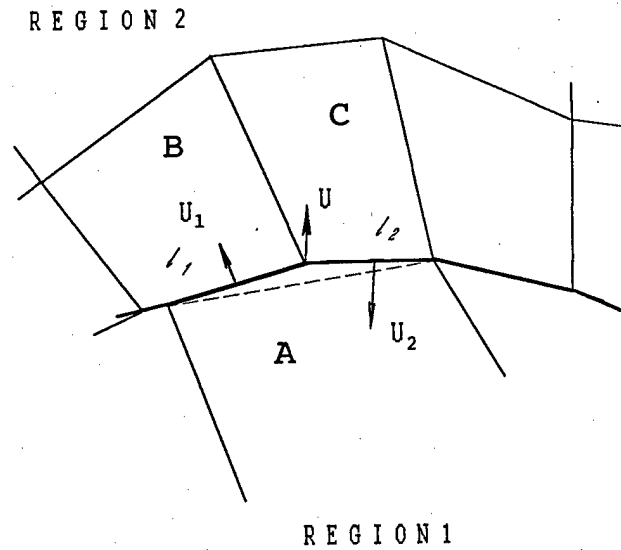


Fig.2 Boundary between the different subregions (solid line)  $U_1, U_2$  - "big" velocities obtained from the Riemann problem solution between the meshes A (region 1) and B (region 2) and so A and C,  $l_1, l_2$  - the lengths of the ribs

### 3. Boundary's type checking

Using of moving grid makes it much more easier setting of boundary condition in comparison with Elerian grid. In accordance with the boundary condition some type of boundary has been assigned to every rib belonged to the boundary. There are five boundary types that have been considered: "free boundary" (boundary with vacuum), "contact" (boundary with another matter), "axes" (axes of symmetry), "hard wall" and so called "special boundary" through which a matter can flow. It's clear, that the type of the boundary can be changed from one time step to another. Therefore a procedure checking the boundary type at each time step has been developed.

#### 4. Nodes distribution along the boundary and grid generation technique

Experience of the numerical simulation on the moving grid shows that some procedure of the nodes distribution along the boundary is required to generate a good grid inside of the region. Interpolation of the boundary plays an important role for displacement of nodes along the boundary. How it has been noticed [19], the sharp angels of the boundary are smoothed from one time step to another, when the nodes move along the straight lines connecting them. To prevent this smoothing on the boundary, we approximate it by arcs linking the boundary nodes.

In the case of strong deformations of numerical region the law of nodes distribution along the boundary influences in a great power on the grid generated inside the region. Previously [20] the law of the nodes distribution along the boundary was chosen anytime in accordance with the specifics of the problem to be solved. Such a way required at least several attempts to find the appropriate law of nodes distribution for problem considered.

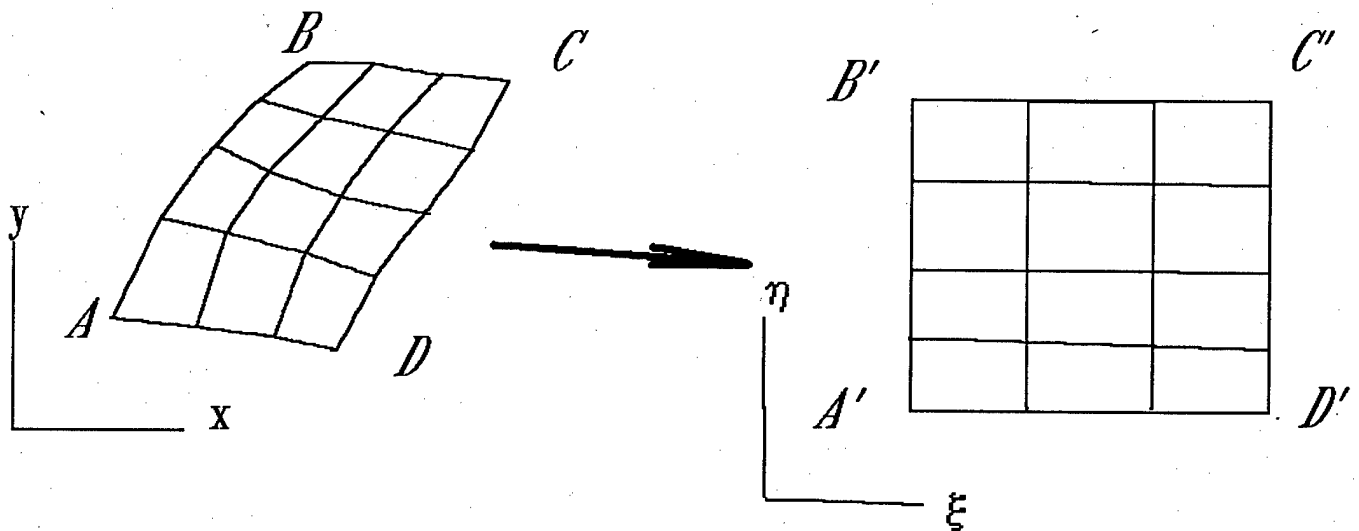


Fig.3 The scheme of the grid mapping

In this version of moving grid code a procedure of boundary node location correction is proposed, which allows to generate orthogonal grids in subregions. For this purpose, boundary nodes are displaced along the boundary at any time step to ensure orthogonality between the boundary and correspondent inner grid line. Nodes shift is limited by settled maximum ratio between adjacent the node rib's lengths. In our calculations the maximum ratio was 1.1. In order to not distort the shape of numerical region during nodes distribution the node is shifted along smooth curve line which approximates the boundary. The curvature of the line is changed from node to node using line interpolation formula for curvature radius. After nodes displacement new grid is generated in subregions.

Grid generation algorithm is based on a univalent mapping of a rectangular region at a parametric plane  $(\xi, \eta)$  onto a subregion under consideration at physical plane  $(x, y)$  of flow. The problem can be formulated mathematically in a following way. The flow region at plane  $(x, y)$  is considered to be a curvilinear quadrangle with tops A, B, C, D (fig.3). The univalent mapping of this quadrangle onto the rectangular  $A', B', C', D'$  is determined by solution of a system of elliptical equations

$$\xi_{xx} + \xi_{yy} = 0 \quad \eta_{xx} + \eta_{yy} = 0 \quad (3.4)$$

It can be easily proved that this mapping is univalent, for example considering the principle of maximum of harmonic function. In reality, to solve the system of equations relative to  $x, y$  as independent variable parameters is more convenient

$$\begin{aligned} a x_{\xi\xi} - 2b x_{\xi\eta} + g x_{\eta\eta} &= 0 & (3.5) \\ a y_{\xi\xi} - 2b y_{\xi\eta} + g y_{\eta\eta} &= 0 \\ a = x_{\eta}^2 + y_{\eta}^2 & \quad b = x_{\xi}x_{\eta} + y_{\xi}y_{\eta} & \quad g = x_{\xi}^2 + y_{\xi}^2 \end{aligned}$$

using the following boundary conditions:

$$\begin{aligned} x(\xi) &= x(\xi, \eta_1) & y(\xi) &= y(\xi, \eta_1) & \text{at AB} & (3.6) \\ x(\eta) &= x(\xi_d, \eta) & y(\eta) &= y(\xi_d, \eta) & \text{at BC} \\ x(\xi) &= x(\xi, \eta_r) & y(\xi) &= y(\xi, \eta_r) & \text{at CD} \\ x(\eta) &= x(\xi_u, \eta) & y(\eta) &= y(\xi_u, \eta) & \text{at DA} \end{aligned}$$

where

$$\xi_d \leq \xi \leq \xi_u \quad \eta_l \leq \eta \leq \eta_r$$

The transition to discrete analog of boundary conditions for this system of quasilinear elliptical equations can be performed easily. If the the grid nodes are given

$$\xi_i = i \quad i=1, \dots, n \quad (3.7)$$

$$\eta_j = j \quad j=1, \dots, m$$

then the boundary conditions are (3.8)

$$x(1) = x(1,1) \quad y(1) = y(1,1) \quad \text{at AB}$$

$$x(j) = x(1,j) \quad y(j) = y(1,j) \quad \text{at BC}$$

$$x(i) = x(i,m) \quad y(i) = y(i,m) \quad \text{at CD}$$

$$x(j) = x(n,j) \quad y(j) = y(n,j) \quad \text{at DA}$$

Different algorithms have been proposed in [17] for solving this problem. Iterations considered to be the most efficient algorithm. We modified this algorithm treating solution of corresponding equations as a result of relaxation of solutions of nonsteady equations. For this purpose "non-steady" terms  $dx/dt$  and  $dy/dt$  are inserted into the right sides of equations for  $x$  and  $y$  correspondingly [21]. The resulted parabolic system is solved by the method of variable directions. At the first half time step terms containing derivatives over  $h$  are considered to be given. At the second half time step derivatives over  $x$  are taken from calculations at the first stage. The problem at the each stage is similar to the one-dimensional heat transport problem. This consideration is similar to iterations, but as any relaxation method it provides more possibilities for the choice of "time-step" or, what is the same, of relaxation parameter. In particular, it can be changed from one grid node to another to accelerate the convergence of the method. The proposed algorithm has demonstrated its reliability. Nevertheless it fails for boundaries of a complex configurations. In order to overcome problems associated with a grid generation the algorithm foresees the possibility of subdividing the flow region into subregions with reasonably regular boundaries.

5. Riemann problem solution and flow parameters  
recalculation for next time level

The basic point of numerical integration of governing equations is the Riemann problem, which is not self similar if any kinetics phenomena is considered (for example, stress relaxation or microporous growth). In the model used the porous growth is also included into consideration. Therefore we take it to be "frozen" when the time of the fracture kinetics  $t_k$  is much more than the time step  $\Delta t$  and on the contrary. Hugoniot adiabates and isoentrops for solid matter are taken for solving Riemann problem in the first case and those for porous matter are used in the second case. This approach has been previously used [22] in calculations of visco-elastic flows by Godunovs method.

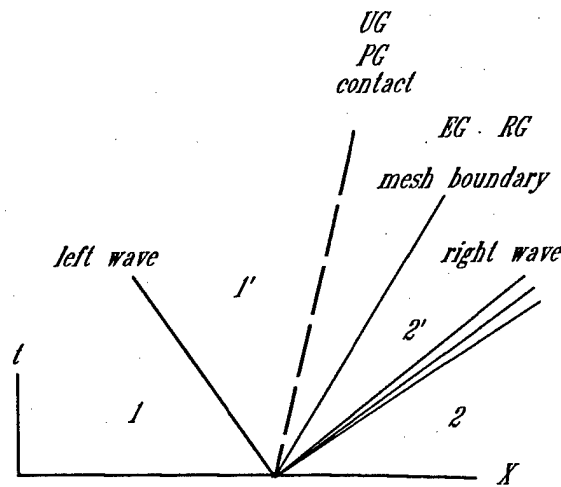


Fig.4 Discontinuity decay: 1 and 2 designate undisturbed regions, 1' and 2' - regions behind the waves, dashed line - contact discontinuity

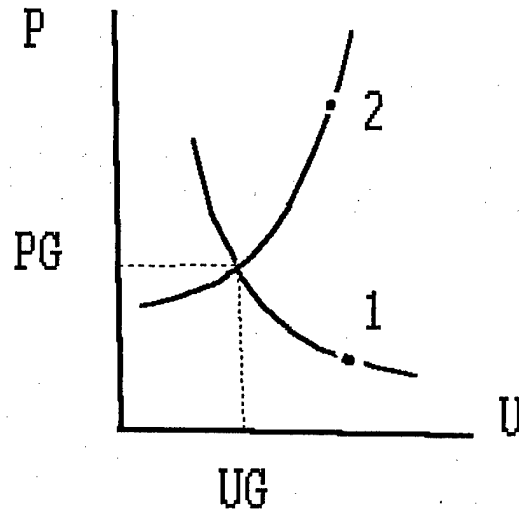


Fig.5 U-P plane. Points 1 and 2 designate initial flow parameters from the left and from the right side of the rib. U means the normal to rib velocity.

Unlike the perfect gas, in the case of an arbitrary EOS the Riemann problem can't be solved exactly by iteration scheme without numerous EOS evaluations. One should mention here about some approximate Riemann solvers [23,24] that can be useful also for the problems considered. Initial flow discontinuity decays into the contact discontinuity, the left wave and the right wave, those may be the shock wave or rarefaction wave depending on the initial parameters (see Fig.4). The mass velocities and the pressures behind the right wave (2-2') are equal those behind the left wave (1-1'). These so called "big parameters" (PG and UG) can be determined as intersection of left and right wave velocities functions in U-P plane (Fig.5 ).

Densities and energies in the regions 1' and 2' can be calculated if velocity UG and pressure PG are known. Velocity functions FL and FR are built using a real equation of state. To build the simple wave velocity function (2'-2) sound velocity as a function of pressure and density is sufficient. In the case of the shock wave (1-1') the energy as a function of pressure and density is necessary. In order to calculate the fluxes of mass, energy, porous volume and momentum the rib velocity has to be



known. Then, the fluxes can be determined choosing the flow parameter from the region where the rib velocity is located (region 2' in the case shown in Fig.4 ). The velocity of the rib  $v$  can be determined if the locations of the rib at the neighboring time levels are known (see Fig.6). Generally speaking, the surface covered by the rib during it's movement is not the plane. For simplicity we replace it by the plane following the way proposed by Godunov [17]. In accordance with this method the normal component of the rib velocity is calculated as

$$V = \frac{\Delta_{abb'a'}}{L_{ab}^{t+\Delta t/2}} \quad (3.9)$$

Here  $\Delta$  - is the area covered by the rib  $ab$  during the time step  $\Delta t$  in the plane  $XY$ ,  $L_{ab}$  - the length of the rib at the time  $t+\Delta t/2$ .

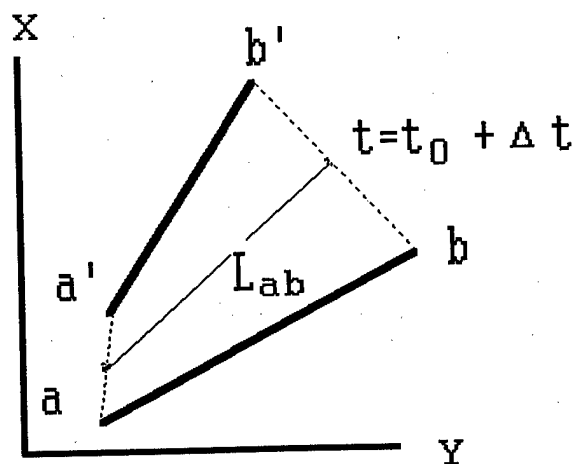


Fig.6 Determination of rib velocity

## 6. Conclusion remark

Naturally the description of the algorithm given above is at least schematic and except of some modifications and details represents only the interpretation of ideas [17]. However we considered the program approach as being already given and the main problem is to put it into practice for specific problems of physics. On this way one can face with a lot of concrete problems of various extent of complexity: mathematical, physical, algorithmic. One of the most important points is an experience of working with given complex of program. We are sure that the difficulties connected with realization of the approach will be rewarded by its huge possibilities. The method allows at least in principle to fit flow singularities : shocks , contacts, characteristics. From this point of view the method unifies main advantages of characteristics methods with the advantages of uniform computational schemes. A promising future we see in integration of this method with analytical methods of gas dynamics. This method provides a possibility to determine dependence and influence domains and to perform calculations at this minimal domains area. From this point of view it can be called economic.

Last years are being marked by the intense activity in developing of high order accuracy modifications of Godunov's methods. Review of these methods can be found for example in [25]. These modifications as a rule can easily be included into the body of the original Godunov's algorithm. Modifications concern the Riemann problem procedure and formulae for recalculation of flow parameters for the new time step. Development of high order resolution schemes in moving grids fitting flow singularities is of great importance [26]. They will be considered more detailly in the next report.

#### IV. Demonstrative examples.

##### 1. TEST № 1: impact of a plane aluminum plate onto a semiinfinite aluminum target

The simplest test problem for 2D code is an impact of a plane projectile on a semiinfinite target. In this case the problem becomes to be one-dimensional and if Hugoniot adiabates of materials are known the pressure and the shock velocity can be easily calculated. The time when rarefaction wave from the back side of the projectile reaches the shock front can be also determined. Results of a plane aluminum- on- aluminum impact with 8 km/s velocity are shown in Fig. 7-8. Region of computations consists of two subregions corresponding to the target and the impactor. Left boundary of the target moves initially with a characteristic velocity (sound speed) inside aluminum target. Then shock from contact reaches this boundary and it becomes moving as shock discontinuity (see fig. 8). This transition from sound to shock regime of boundary movement is automatic because the velocity of the boundary is obtain from Riemann problem solution algorithm. As it can be easily proved, numerical result is agreed well with the analytical calculation of the shock pressure and velocity.

##### 2. TEST № 2: influence of the grid refinement on the results of numerical simulation of penetration problems

Calculation with different levels of accuracy were performed for aluminum sphere of 1 cm diameter penetrating aluminum plate of 2 mm thickness at 10.1 km/s. Numerical grids and levels of constant pressure corresponding the time moment of 710 ns are shown in fig.9-11. In the case presented in fig.11 accuracy was two times more than that in the fig.10 and four times more than in the fig.9. It is seen that the higher the accuracy, the better is shock front resolution in the projectile. More fine grid allows also to resolve the low density vaporized matter blowing off the target during impact. At the following stage of penetration shown in fig.12-13 fine

grid gives less thickness of the target's substance surrounded debris of the projectile. And of course as a consequence of higher pressure there is a higher expansion velocity of debris cloud in this case.

### *3. Interaction of spherical projectile with two layered aluminum target*

Result of computation of spherical aluminum projectile interaction with a spaced two layered aluminum target is presented in fig.14. Impact velocity for the problem considered is 8 km/s. One should note that not more than 1000 meshes is used in this computation. The number of meshes grows during computation to ensure some fixed level of accuracy. Criteria for grid refinement is not pure geometric. When pressure gradient and density of matter decrease some coalescence of meshes takes place.

Using moving grids demonstrates a substantial economy of reserved computer memory in comparison with a fixed eulerian grid. One can calculate that about 30 000 - 40 000 meshes is required to perform computation of this problem using eulerian grid with the same accuracy.

### *4. Hypervelocity impact of iron projectile on a target with a conical hole*

This example demonstrates possibilities of moving grid adaptations to region's form in the case of strong deformations. In the beginning of interaction shock pressure of about 0.5 Mbar is generated in PMMA disk, while pressures in iron target reach about 2 Mbar. Then two jets of liquid PMMA are formed moving along the walls of conical channel (fig. 16). Collision of the jets on the axis leads to cumulation effect. Pressure behind the projectile reaches to 2 Mbar (fig.17). After impacting with the iron projectile these jets breach between the projectile and the walls of the channel accelerating projectile (fig.18).

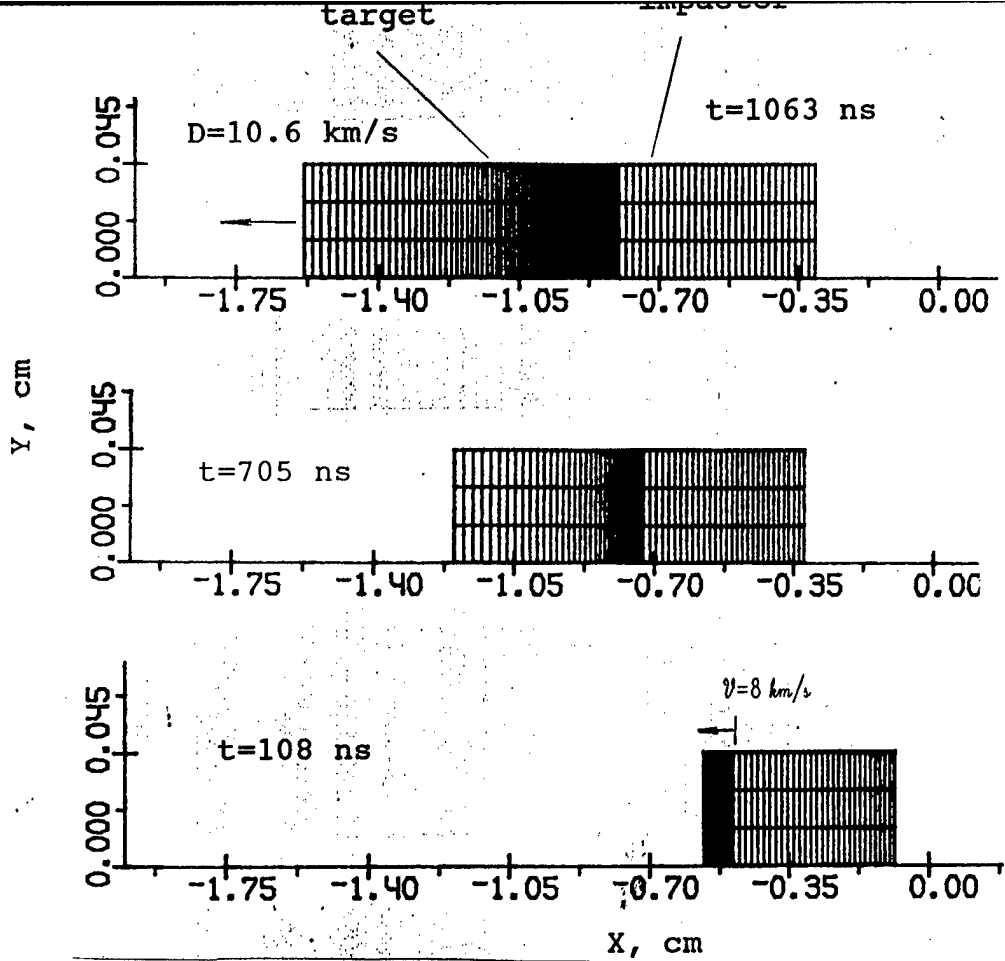


Fig.7 Numerical grid at different time moments

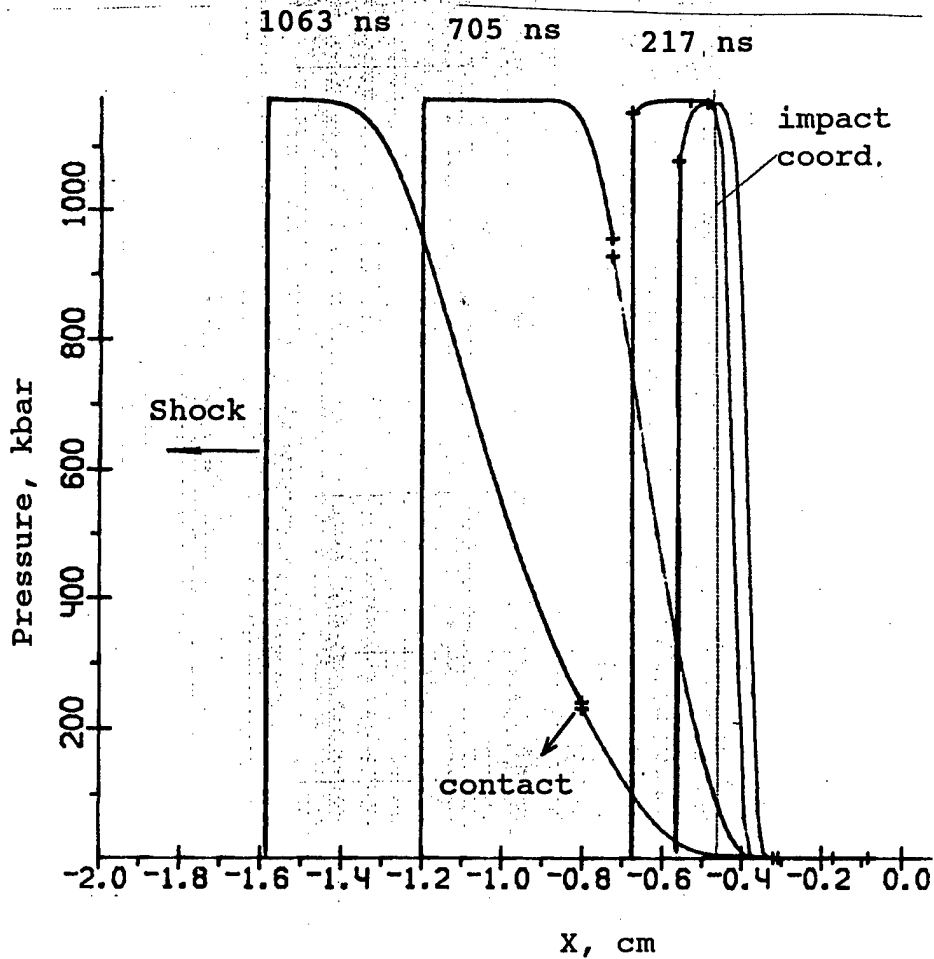


Fig.8 Pressure profiles at different time moments

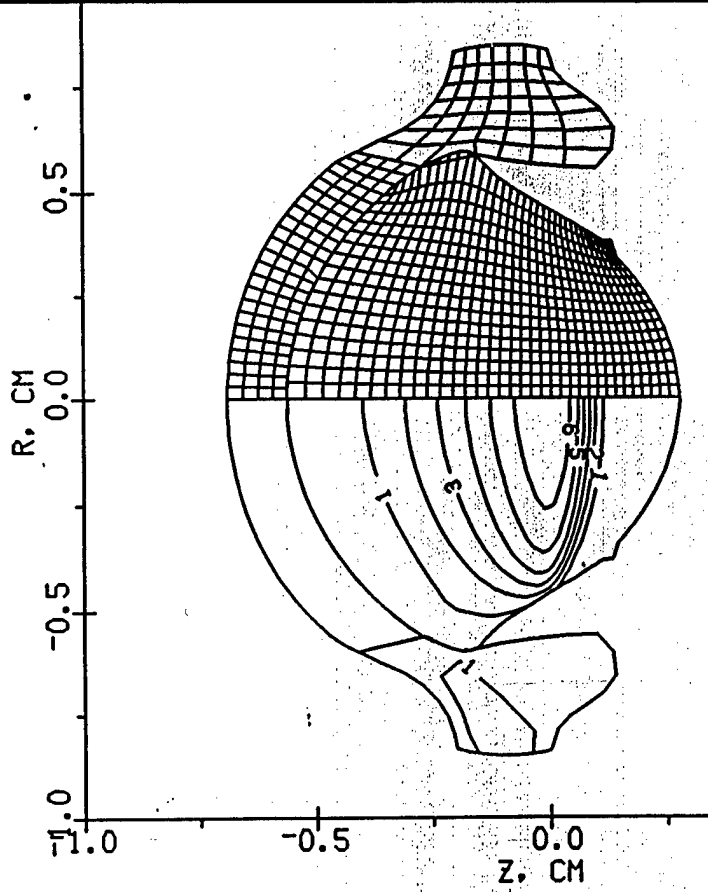


Fig.9 Grid and pressure levels.  
1- 100 kbar, 2- 200 kbar ...  
Time: 710 ns

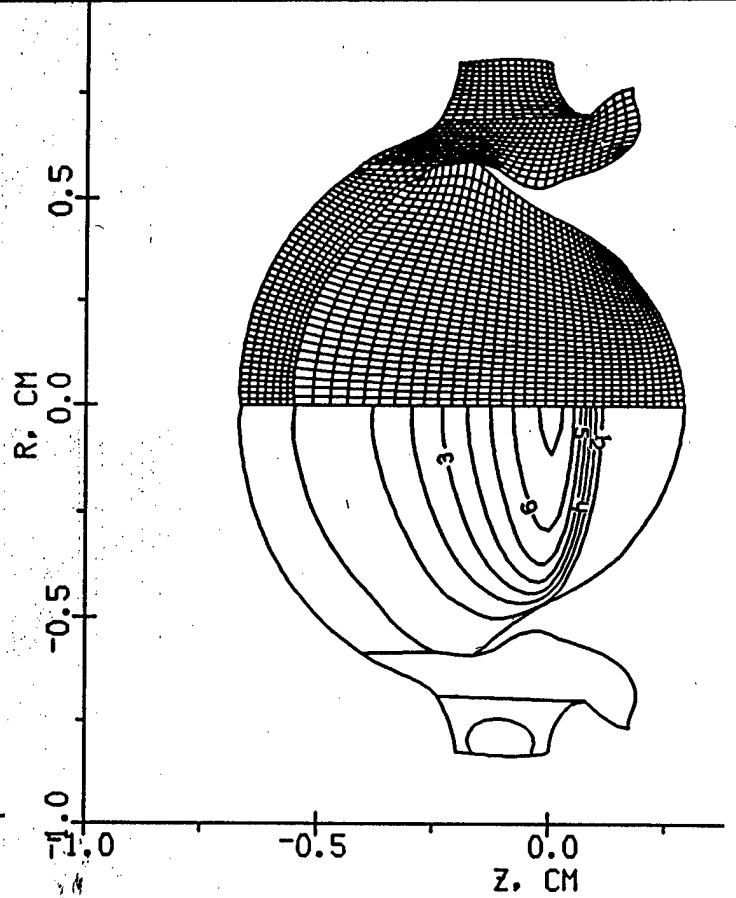


Fig.10 Grid and pressure levels  
1-100 kbar, 2-200 kbar...

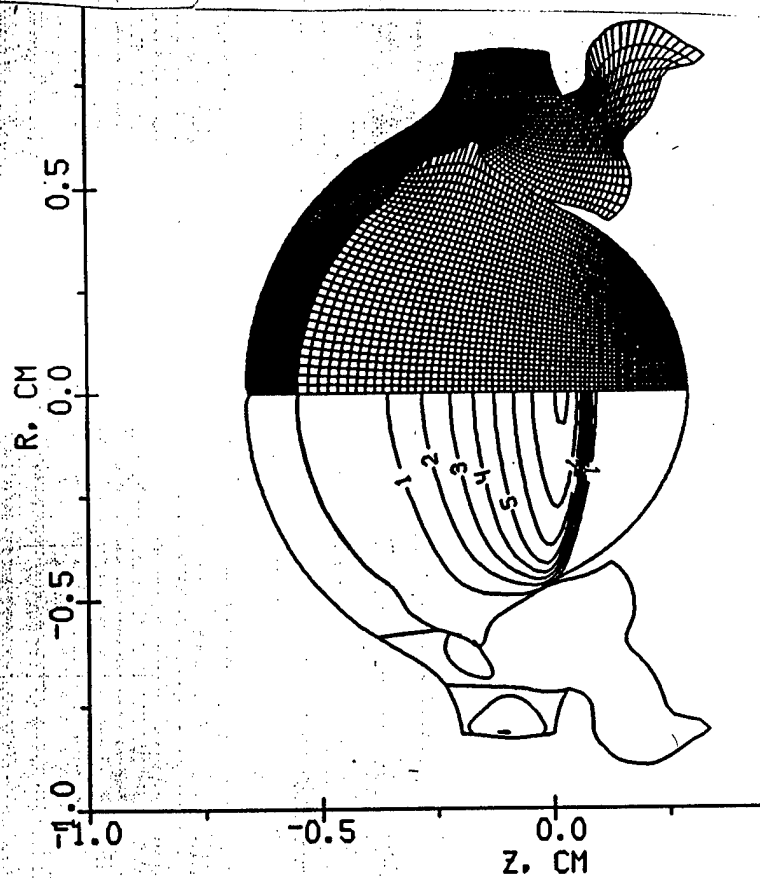


Fig.11 Grid and pressure levels (best accuracy)  
step 100 kbar, time: 710 ns

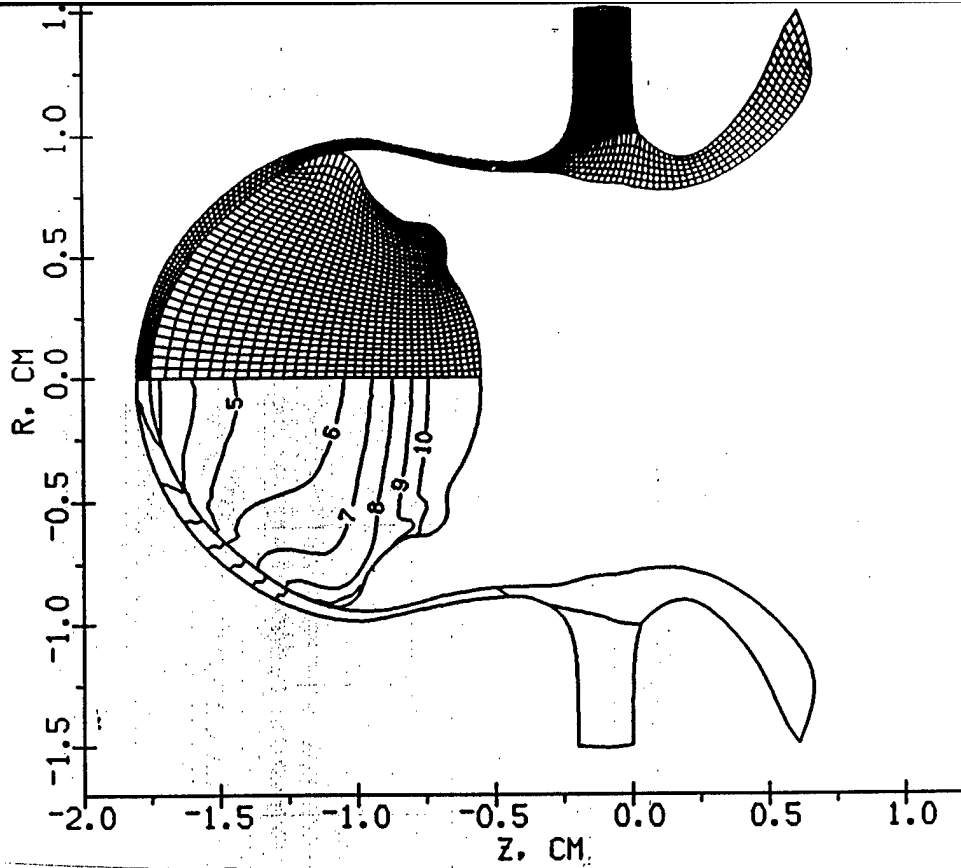


Fig.12 Grid and velocity levels: 1-10.6, 2-10.3, 3-9.9, 4-9.6,  
 5-9.2, 6-8.8, 7-8.5, 8-8.1, 9-7.7, 10-7.4 km/s  
 Time: 1900 ns

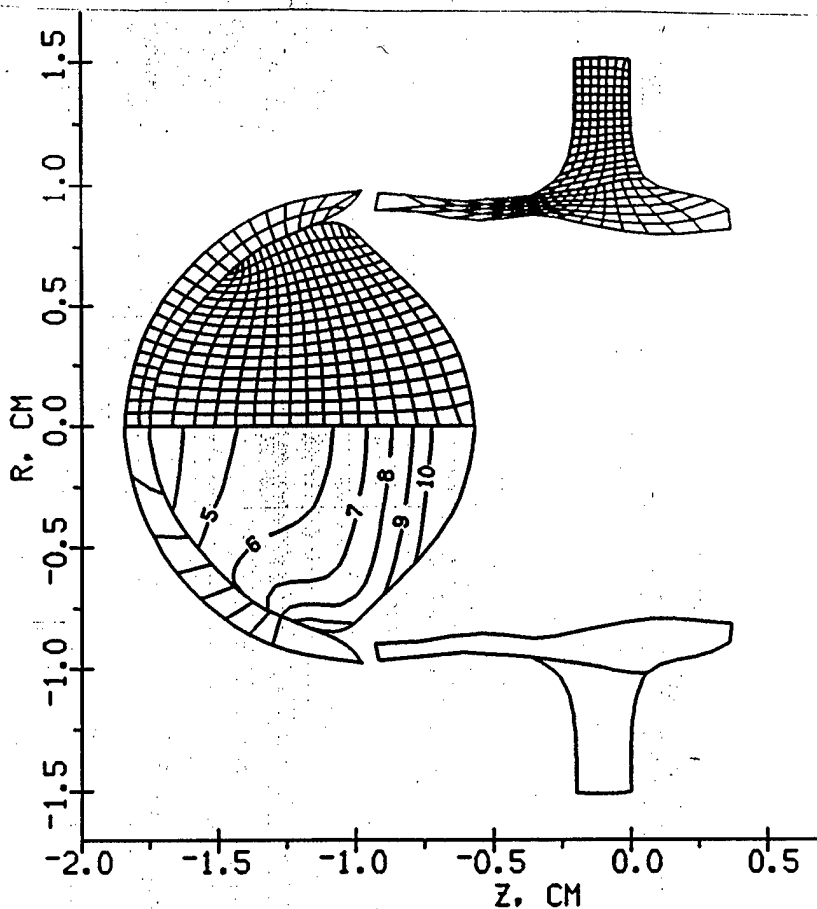


Fig.13 Grid and velocity levels (the same as for fig.12)  
 Time: 1900 ns

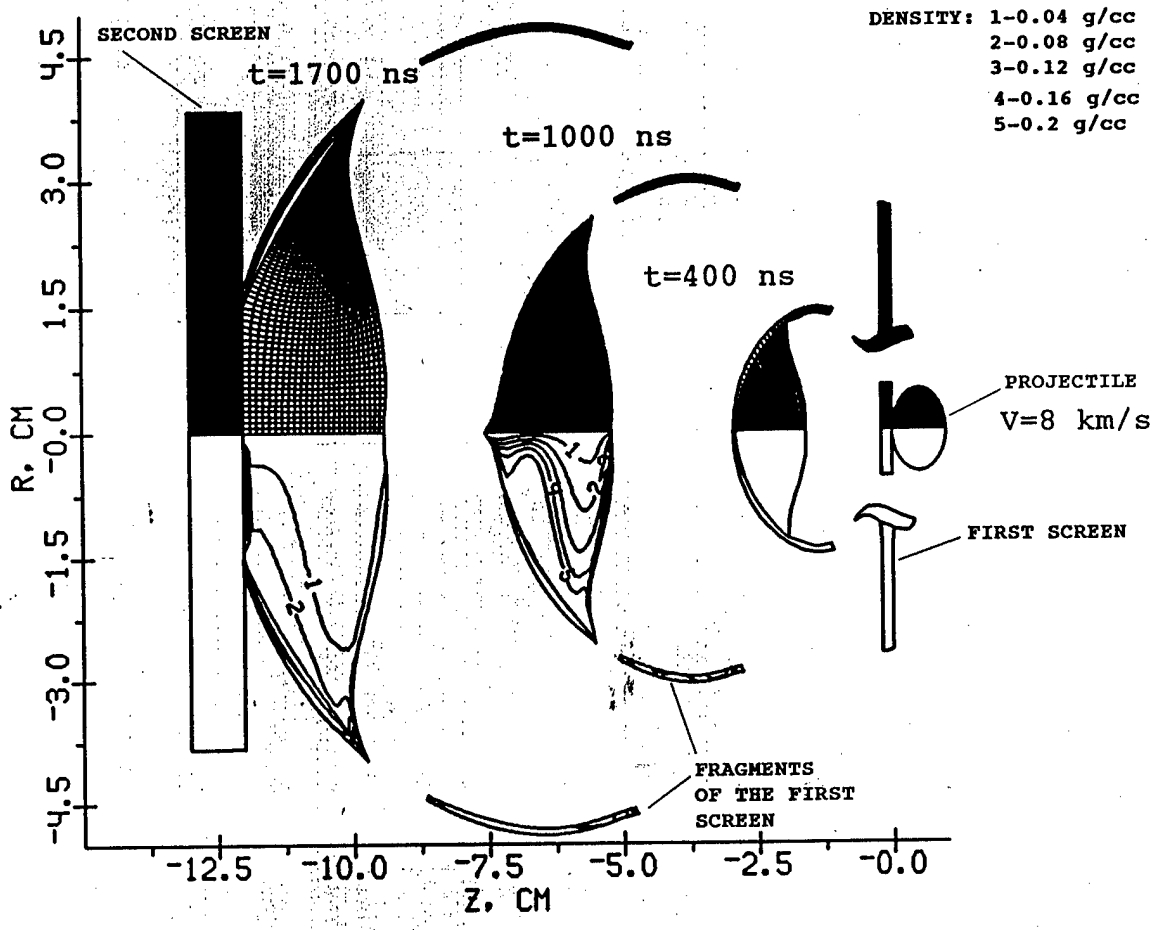


Fig.14 Grids and density levels at different time moments.



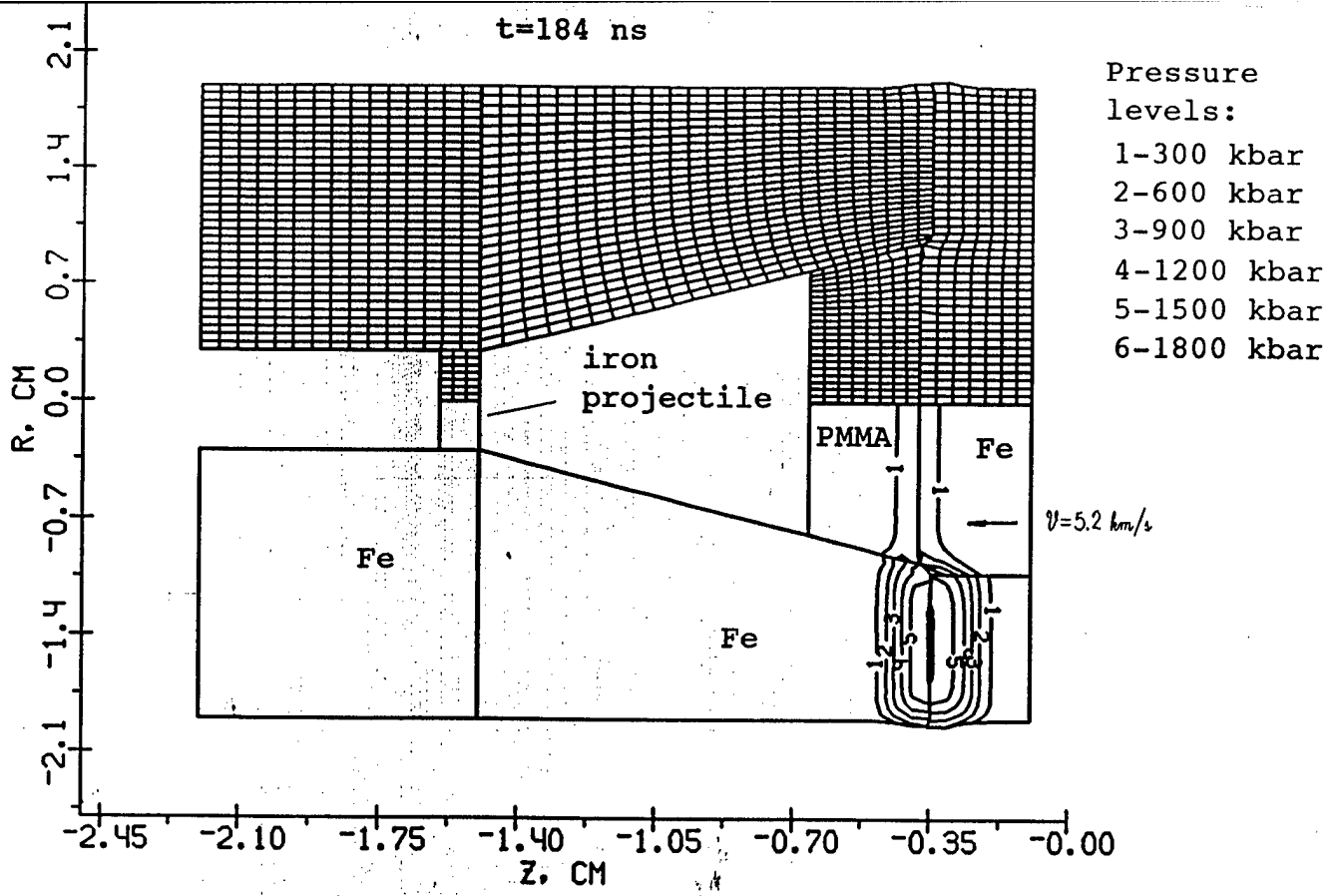


Fig.15 Grid and pressure levels

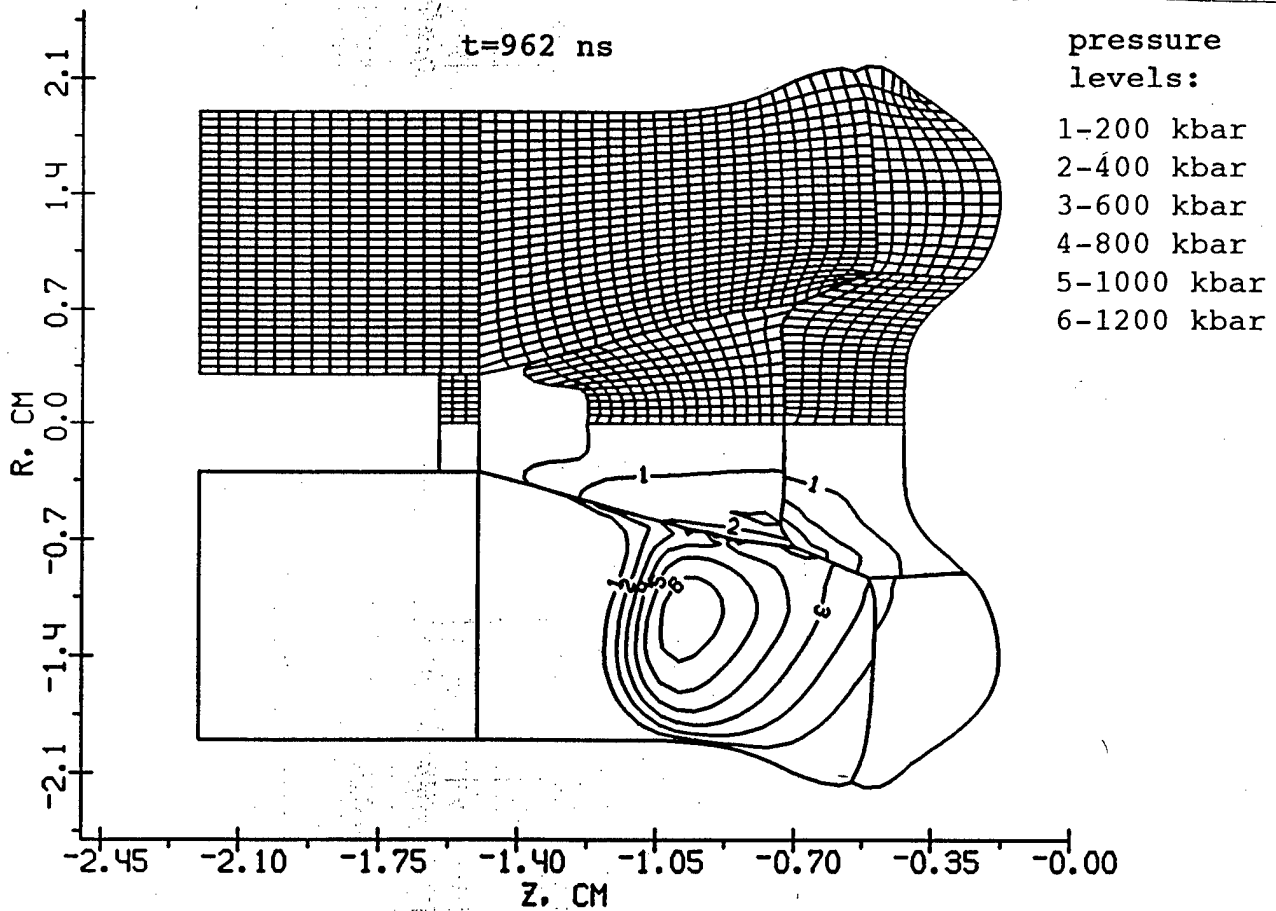


Fig.16 Grid and pressure levels

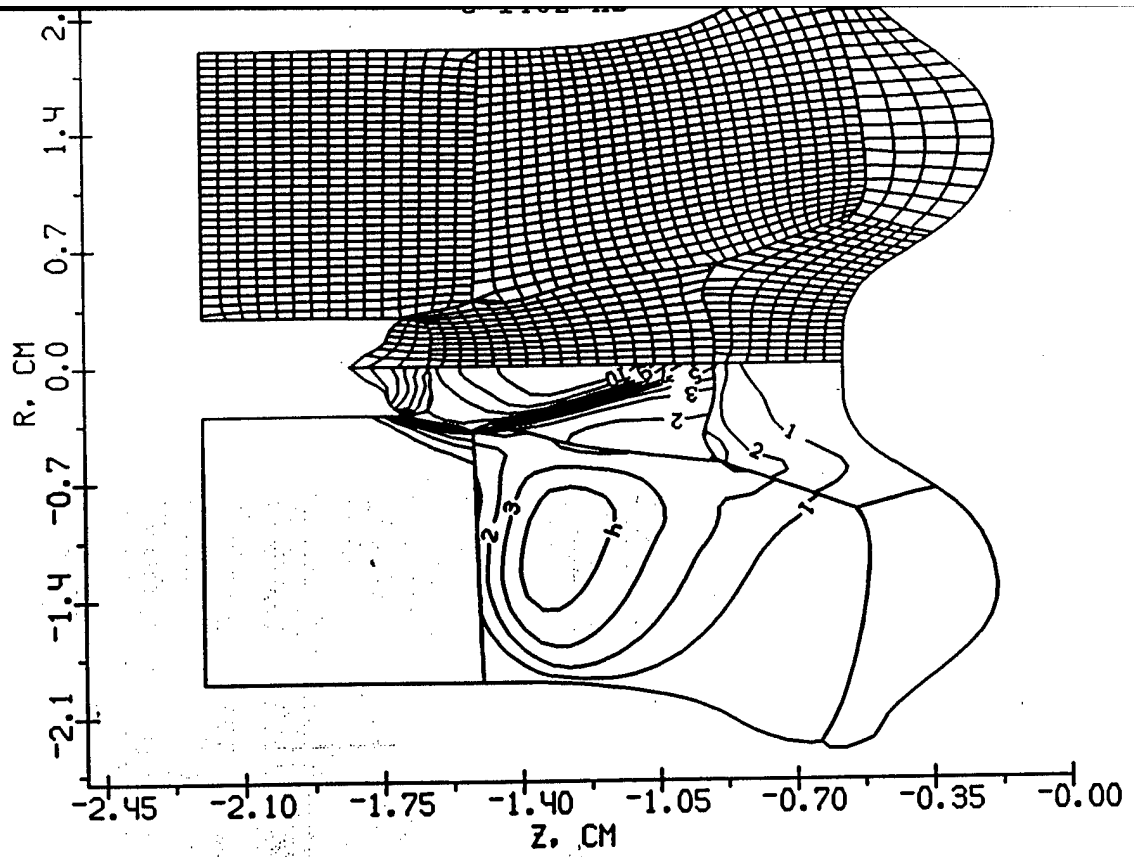


Fig.17 Grid and pressure levels

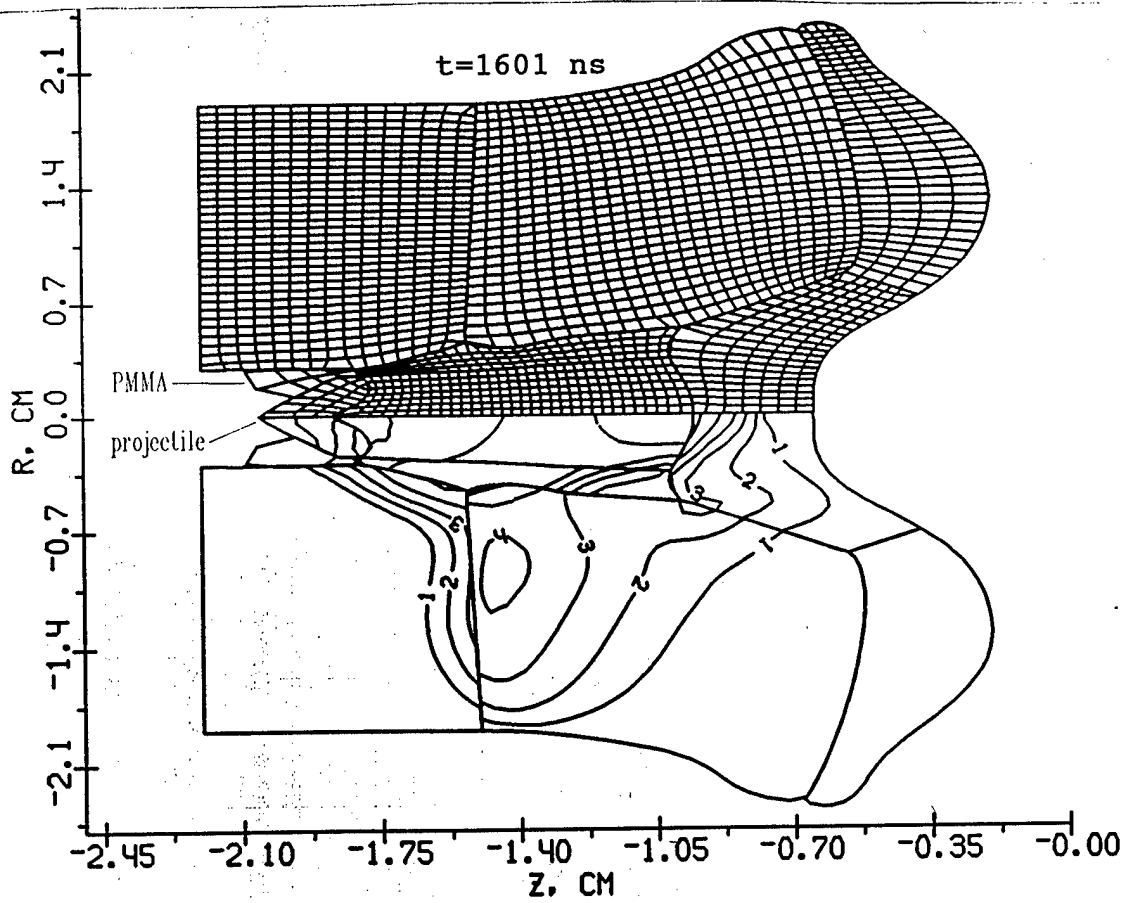


Fig.18 Grid and pressure levels

## V. REFERENCES

1. A.V. Bushman, G.I. Kanel, A.L.Ni, V.E. Fortov, *Thermal Physics and dynamics of Intense Pulse Action*, Inst. of Chemical Physics, Chernogolovka, 1988
2. A.V. Bushman, V.E. Fortov, *Wide-range equations of state for matter under extreme conditions*, Sov.Tech. Rev. B. Term. Phys., vol. 1, p.219, 1987
3. M.L.Wilkins *Calculation of elastic-plastic flow*. In: Adler B, Fernbach S, Rotenberg M (eds) *Methods in Computational Physics* vol. 3, p.211, 1964
4. V.A. Agureikin, B.P.Krukov *Individual particle method for calculations of flows of multi-component matter with strong deformations*, Num.meth.cont.mech (russian), Novosibirsk, vol. 17, No. 1, p.17, 1986
5. O.M.Belocerkovski, Yu.M.Davidov *Big particle methods in fluid dynamics.Computational experiment*. (russian) Moscow, Nauka, 1982
6. F.H.Harlow *The particle-in-cell computing method for fluid dynamics* In: Adler B, Fernbach S, Rotenberg M (eds) *Methods in Computational Physics*, vol. 3, p.319, 1964
7. R.F.Stellingwerf, C.A.Wingate *Impact modelling with smooth particle hydrodynamics*, Int.J.Impact Engng, vol. 14, p.707, 1993
8. Fomin V.M., Shapeev V.P., Yanenko N.N. *Modelling of continuum mechanics problems with large deformations*, Comp.Meth.Appl.Mech. Engng, vol.32, p.157, 1982
9. K.-D.Munz, R.Scheider, M.Goez, A.Herschel *Study of numerical approximations of gas flow into vacuum*, KFK report 5237, 1993
10. J.K. Meier *The sensivity of an eulerian hydrocode impact analysis to user-selected impact parameters*, Int.J. Impact Engng vol. 10, p.361, 1990.

11. T.G. Trucano, J.M. McGlaun Hypervelocity impact calculations using CTH: case studies, *Int.J. Impact Engng.*, 10, p.601, 1990
12. W.W. Predebon, C.E. Anderson, J.D. Walker *Inclusion of evolutionary damage measures in Eulerian wavecodes*, *Computational Mechanics*, No. 7, p.221, 1991
13. E.P. Fahrenthold, *Int.J. Impact Engng*, vol. 14, p.229, 1993
14. J.A. Trangenstein, R.B. Pember *Numerical algorithms for strong discontinuities in elastic-plastic solids*, *J. Comp. Phys.*, vol 103, p.63, 1992
15. A. Suresh, M.S. Liou *Osher's scheme for real gases*, *AIAA Jour.*, vol. 29, No. 6, p.920, 1989
16. S.K. Godunov *A finite difference method for the numerical computation of discontinuous solutions of the equations of fluid dynamics* *Mat.Sb.* 47, p.271, 1959
17. S.K. Godunov *Numerical solution of multi-dimensional problems of gas dynamics* (in russian), Nauka, Moscow, 1976
18. A.V. Bushman, V.E. Fortov, I.V. Lomonosov, *Proc. Enrico Fermi School 1989*, Elsevier Publ. 1989
19. O.Yu. Vorobiev, A.L. Ni, A.V. Shutov, V.E. Fortov *Application of Godunov's method with movable grids for calculations of dynamics of condensed matter under intense impulsive actions*, *Modelling in mechanics* (russian), vol. 6, No 4, p.3., 1992
20. A.L. Ni, T.N. Fortova, K.G. Shkadinski, A.V. Shutov, A.V. Utkin *Numerical simulation of interaction of high velocity impactors with condensed targets*, (in russian) Preprint Institute of Chemical Physics, Chernogolovka, 1989

**HEDRC REPORT**  
contract SPC-93-4075

## **2D HIGH RESOLUTION SHOCK WAVE PHYSICS CODE**

6-month technical report

*Application of 2D code to various hypervelocity impact problems*

*Participants:*  
*Vorobiev O.Yu.*  
*Shutov A.V.*  
*Zharov A.V.*  
*Ni A.L.*  
*Fortov V.E.*

## *Introduction*

In this report we present applications of previously described moving grid Godunov code to several hypervelocity impact problems. This method employs the exact solution of Riemann problem, therefore it is well suited for construction of "nonhomogeneous" computational algorithms fitting flow singularities. It is clear, that to fit all singularities, which can arise in the flow is rather difficult algorithmic problem especially in multidimensional case. That is why the most of widespread computational methods of shock wave dynamics are based on homogeneous algorithms treating in the same fashion both continuous and discontinuous domains of flow.

To better resolve discontinuities so called high resolution shock-capturing schemes are used. Most of them are second order modifications of Godunov scheme [1], which use approximate Riemann problem solvers [2-5]. One should mention in this context so called ENO schemes (essentially non-oscillatory schemes) which allows one to increase the order of accuracy up to fourth or even more [6-7]. Of course, the higher is the order of accuracy, the more complicated is the computational algorithm. For example, as it was found in [8], the cost of the third-order ENO scheme is four times that of the second-order one. It may appear the second order schemes to be more profitable when using refined mesh than the fourth-order ones.

We have chosen another approach to construction of high resolution shock-wave codes, namely, Godunov scheme on a moving grid. The main principles of this approach were described in [9-10] and in the previous HEDRC report. Note that in the framework of moving grid code shock waves, contacts between different materials and matter-vacuum boundaries, can be easily fitted. By that the grid boundaries coincided with these discontinuities are moved in accordance with the solution of Riemann problem.

In the present report we demonstrate the advantages of moving grid approach for solving four different problems.

The first one is an impact of thin plane projectile on a thin screen. A great difference of longitudinal and transverse dimensions leads to a great number of zones when using a Lagrangian grid, which covers all the projectile and the target. Our method allows one to

compute only those domains where the flow is two-dimensional, that gives a substantial economy of computer's resources.

The second example is the numerical simulation of penetration of a cosmic body moving with hypervelocity into gaseous atmosphere with exponentially increasing density. The typical feature of this problem is the presence of various space scales. For examples, the size of the body is much larger than the thickness of compressed gas layer at the face side of the body and on the other side it is much less than the distance which this body passes before it explodes.

The third problem is a debris cloud simulation produced by ball-plate impacts. In this problem the ball and the plate have thicknesses of the same order, that makes it difficult to employ any Lagrangian code because of the great deformations of material. On the other side, it is known that Eulerian codes give a great dispersion of mass due to averaging of flow values over the fixed zone intervals. Application of the moving grid code in which the computational grid moves with material near the boundaries and has a minimal advection error in the central grid region allows one to overcome these difficulties.

The last example is a numerical simulation of detonation of charges of finite diameters. It is well known, that a steady detonation can exist only if the size of the explosive is greater than some minimum value. To find this size for a charge of some specified geometry numerous numerical computations are required. When this size is close to the critical one the time which is necessary for setting up a quasi steady detonation regime is very long. It means that we must be able to track the propagation of the front over a long distance. As the region of computation increases with time, a grid refinement is required to maintain some specified level of computation accuracy.

### **Numerical simulation of impact of projectiles with a great D/L ratio**

Impactors with a great D/L ratio (where D is the diameter and L is the thickness) are used in shock-wave experiments in order to simplify their interpretation reducing the last one to 1D case. Nevertheless, the flow becomes two dimensional when the rarefaction waves from the periphery reach the center of the projectile. To account 2D effects at the late stages of interaction 2D simulation is necessary. In the present report we demonstrate one example of

application of moving grid to effective solution of such a problem. In fig. 1(a-d) numerical grid and levels of constant density are presented for high velocity impact of 1mm thick aluminum disk on 2mm thick aluminum foil at 8 km/s velocity. The diameter of the disk is 4 cm. In the beginning of computation we specify two small numerical regions. One of them represents the edge of the disk and the other corresponds to the fragment of the foil, which is in contact with this edge. Then we move the boundary segment separating the 1D and 2D flow regions with characteristic velocity towards to the axis of symmetry. The other fragments of the boundary are: free boundaries (back sides of the disk and the foil), contact between the disk and the foil and the front of the shock wave running away from the center. Rarefaction waves coming from the back surfaces of the projectile and the target lead to an expansion of shocked material and to generation of tensile stresses. That is why the contact between the disk and the target disappears. The type of the boundary segments is changed automatically from contact boundary to free one (fig. 1b). For the later times the size of the flow under consideration is much more than initial one (see fig. 1d). The straight line fragment of the boundary separates the flow region where the transversal rarefaction waves are important.

In addition to this example one should note, that there is a lot of problems containing different time and space scales which could be effectively solved using moving grid code, for example, investigation of thin foil acceleration with laser and ion beams, perforation of multilayered spaced shields and so on.

### **Computation of large asteroid penetration in Jupiter's atmosphere**

The problems of asteroid hazard are of great interest, because the number of asteroids moving in vicinity of Earth is increasing with time. An impact of periodic comet Shoemaker-Levy 9 on Jupiter took place recently (in July 1994). The consequences of this impact were observed both from the Earth and space satellites. In this report we demonstrate an example of numerical simulation of the penetration of one comet fragment of 1 km diameter into Jupiter's atmosphere. The asteroid was approximated by a spherical incompressible body moving with a velocity of 60 km/s. Due to its high velocity it passes a distance much more than its diameter before it explodes. As the density of the atmosphere grows with distance the flow is unsteady.



Extremely high velocity of impact leads to heating and ionization of a gas flow after shock compression. Since the flow behind the shock front is responsible for ionization and luminosity of gas, which can be observed an accurate resolution in this region is required. It is clear, that application of Eulerian codes to this problem will lead to a great diffusion of shock front and contact interfaces. Eulerian computations also require a great number of computational zones to cover the regions in which the asteroid moves. That is why Eulerian computations of this problem were performed in 'reverse ballistic' sense using an atmosphere moving towards an initially stationary fragment [11].

To avoid computations in undisturbed domains we surrounded the asteroid region by a thin region of the gas, whose boundary moves with the characteristics velocity. The size of the gas region grows in time but we can exclude from consideration those parts of the gas region, which are far from the asteroid and are not of our interest. The results of computation are shown in fig.2-4. In the beginning (fig.2) of penetration the gas detaches from the back side of asteroid and a gas jet appears moving in the opposite direction. Then we cut off the part of gas region corresponding to this jet (fig.3). Fig.4 presents the results of simulation for the time when the asteroid has passed about 80 km in atmosphere. The pressures at the frontal surface of the asteroid become about 0.3-0.5 kbar, that are close to the strength of material. Further computations require to account for the fracture of matter. In accordance with [12], fragmentation of the asteroid leads to a growth of the heat flux inside it, because of significant increase of the effective surface area. This gives rise to the rapid transformation of the asteroid material from the condensed to gaseous state. If we suppose, that the fracture and fragmentation of asteroid is due to the stress gradient at its surface, we obtain the distance of about 100 km, where the explosion takes place. This agrees with recent observations.

### **Numerical simulation of propagation of debris cloud produced by ball-plate impact.**

The results of a computation of a 20 g spherical lead projectile striking a lead plate is

presented in Fig.5(a,b). The impact velocity for this problem is 6.6 km/s. Fig.6 represents the experimental X-ray photograph of the same problem at the time moment 30  $\mu$  m presented in [13]. Simulation results are in accordance with the experiment. The number of zones used grows during the computation to ensure some specified level of accuracy. The criteria for grid refinement are not purely geometric. When the pressure gradient and the density decrease some coalescence of zones takes place.

Using moving grids demonstrates a substantial economy of required computer memory in comparison with a fixed Eulerian grid. One can estimate that about 10 000 - 20 000 meshes is required to perform computation of this problem using Eulerian grid with the same accuracy.

### **Simulation of detonation in high explosive charges of finite diameter.**

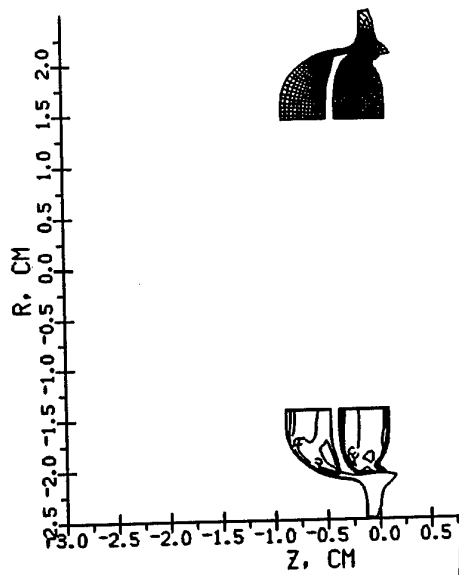
The failure detonation problem is the problem of minimal explosive charge diameter when a self-sustained detonation can exist. We present below an example of determination of this diameter using numerical simulation. The flow is described by Euler equations. The only difference with hypervelocity impact problem is the appearance in the energy equation of a source term which is responsible for heat release. To check whether the detonation becomes steady or not it is necessary to calculate the evolution of detonation process along the distance of at least several (perhaps tens) diameters. As the downstream flow behind the shock is determined by the chemical reaction kinetics and, in particular, by the value of energy release, the shock must be calculated accurately.

The following computational strategy is chosen in accordance with the problems listed above. The computational region represents a curvilinear quadrangle. The sides of the quadrangle are: the leading shock, the segment of contact between detonation products and vacuum, the segment of axis of symmetry, and the forth one is a segment of straight line between the free surface and the axis of symmetry, which is perpendicular to the axis of symmetry. The velocity of this side is assumed to be directed along the axis and to be equal to  $\max(u+a, D)$ , where  $D$  is the shock velocity at the axis of symmetry and  $u+a$  is the velocity of characteristic

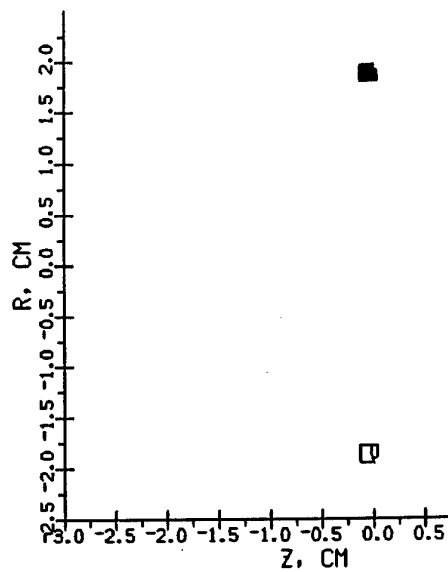
surface moving along the axis and calculated using parameters of the cells adjacent to this side. It means that the boundary moves relative to the matter ahead of it at least with the sonic velocity. Therefore the flow parameters, which determine the fluxes of mass, momentum and energy throughout this side are taken from internal cells. A pressure of 200 kbar, normal density and zero velocity were taken as an initial data for calculations. It was found from simulations, that the critical diameter is somewhere between 2.4 and 3 mm. Results of simulations corresponding to these two cases are shown in Fig.7(a,b) In the case of 2.4 mm diameter detonation decays. Calculations for this diameter were performed with different initial pressures. In all the cases a steady detonation was not obtained. This fact allows to draw a conclusion that the failure diameter of TNT lies within the interval 2.4 and 3 mm. This also agrees with the experiment [14].

## CONCLUSIONS

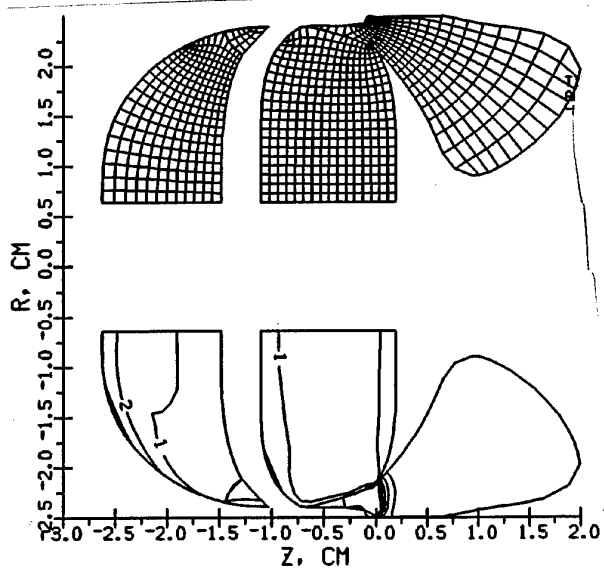
**We have demonstrated the robustness and flexibility of developed 2D code for hypervelocity problem computations. The main advantage of this code in comparison with Eulerian high-order accuracy hydrocodes is an accurate treatment of multimaterial interfaces. On the other side, arbitrary Lagrangian-Eulerian methods (ALE), which utilize lagrangian motion of interfaces and permit an arbitrary mesh motion inside the computation region are not always adapted to dynamically evolving interface shape. It is the main reason to develop ALE codes on unstructured grids [15]. We overcome these difficulties with the help of decomposition of numerical region onto subregions. This decomposition is provided automatically during the computation. By that one can govern this process excluding from computations the regions which are not of our interest.**



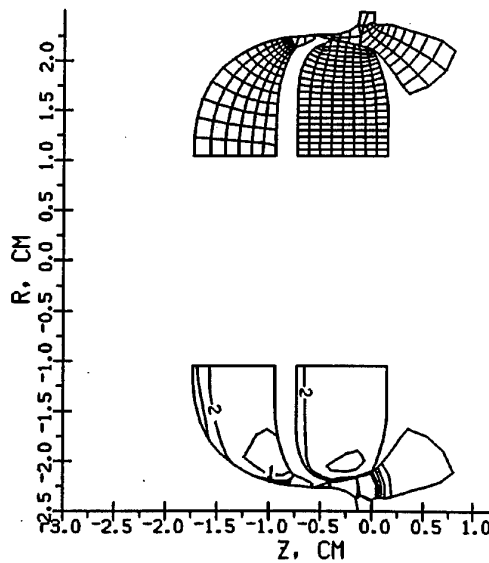
b)



a)



d)



c)

Fig.1(a-d) Numerical grid at different times:  
 a)Time is 51 ns, density level step is 0.5 g/cc  
 b)Time is 1000 ns  
 c)Time is 2010 ns  
 d)Time is 3090 ns

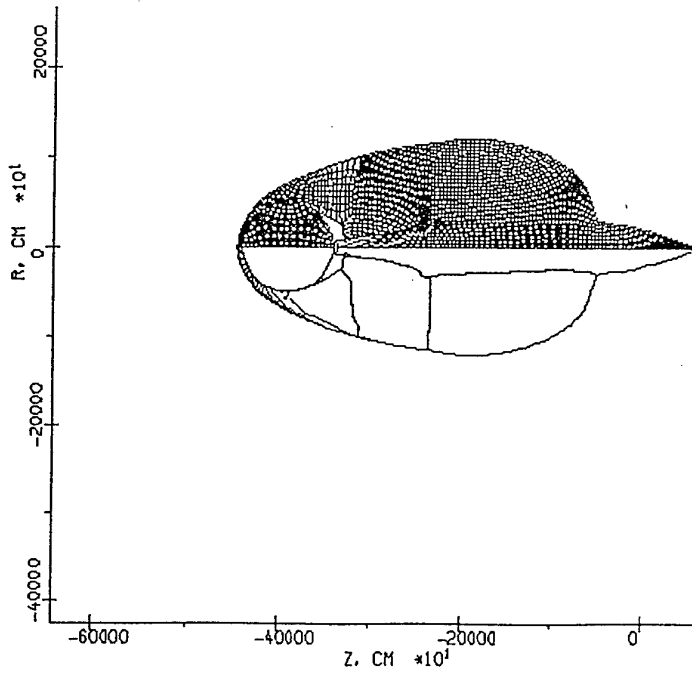


Fig.2. Numerical grid and pressure levels. Pressure level step is 0.001 kbar, maximum pressure is 0.01 kbar. Time is 55  $\mu$ s.

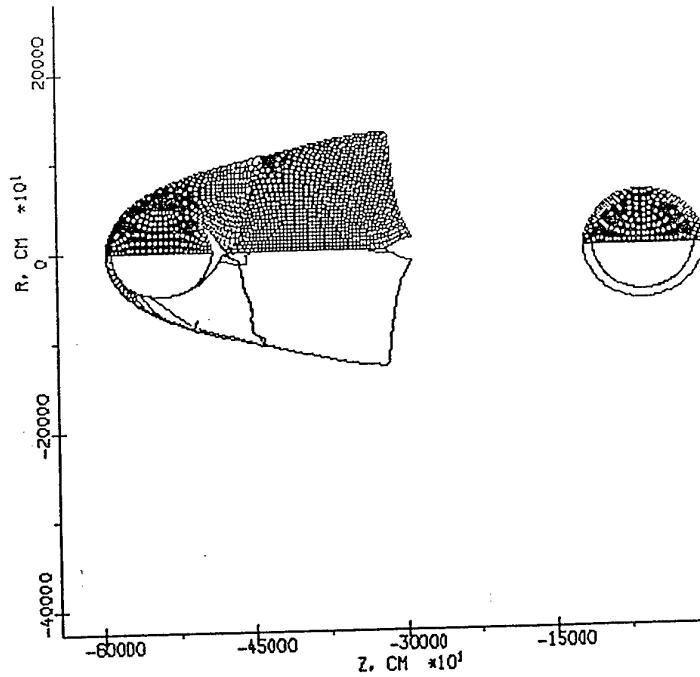


Fig.3. Numerical grid and pressure levels. Pressure level step is 0.001 kbar, maximum pressure is 0.014 kbar. Time is 80  $\mu$ s. Initial configuration is shown on the right side.

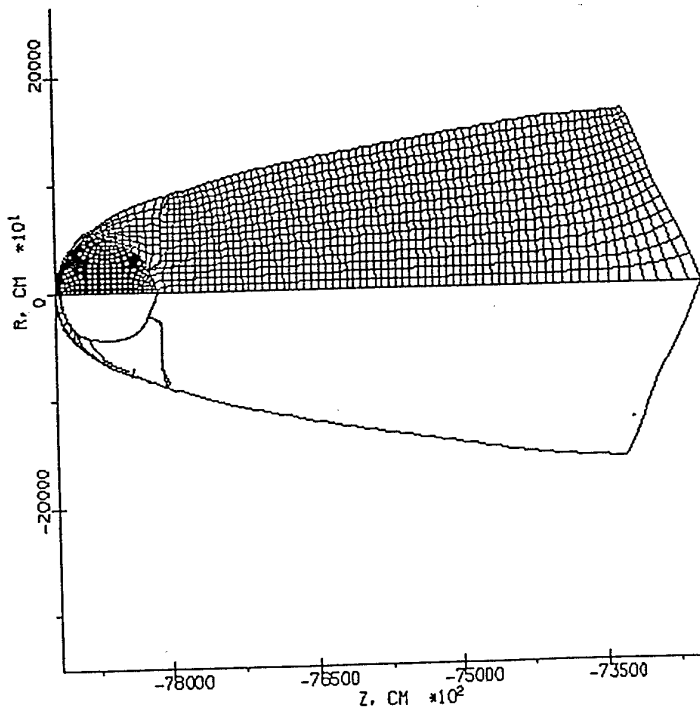
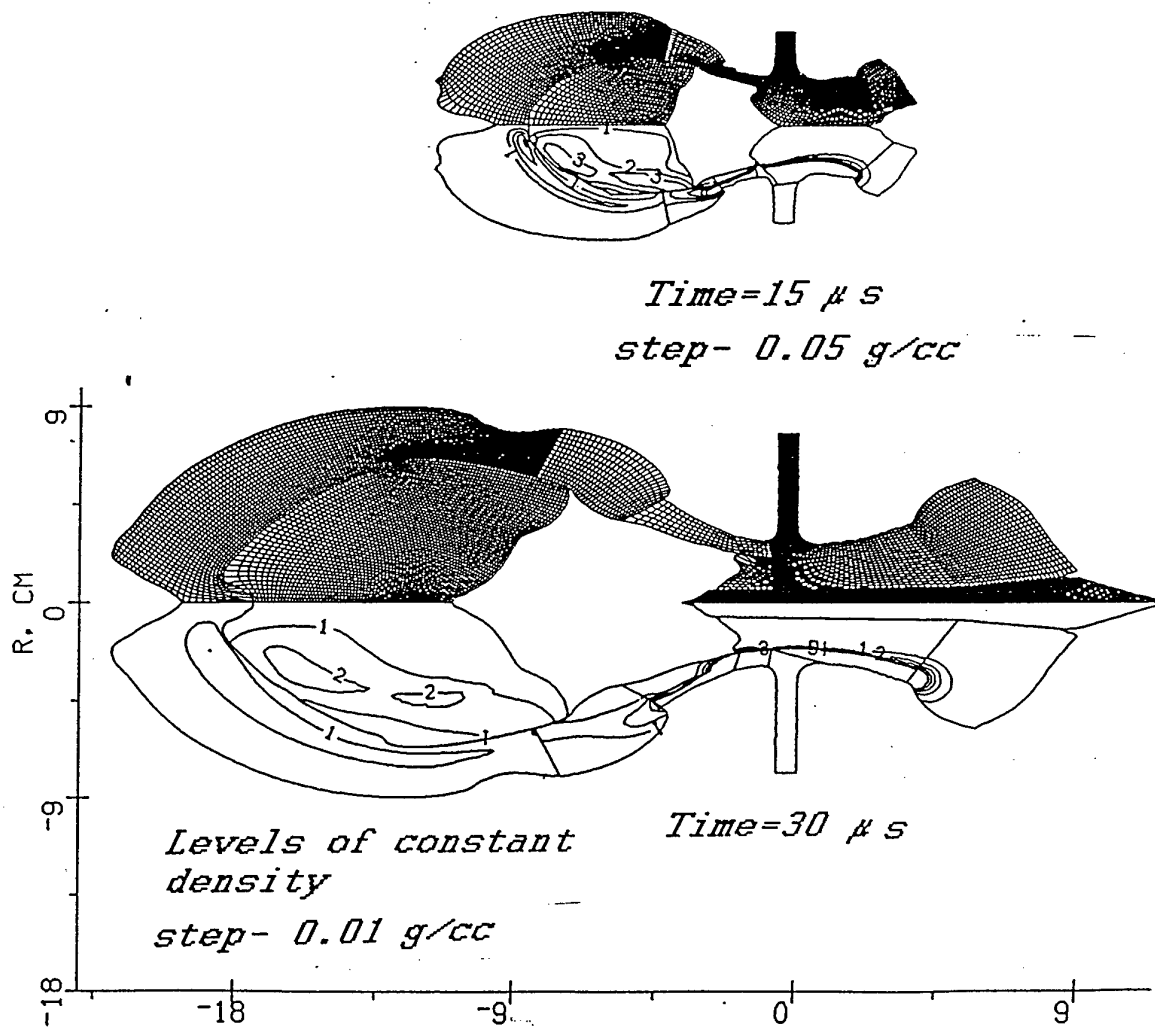
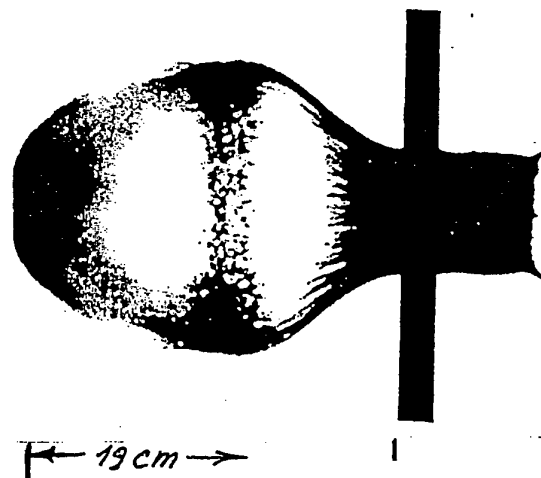


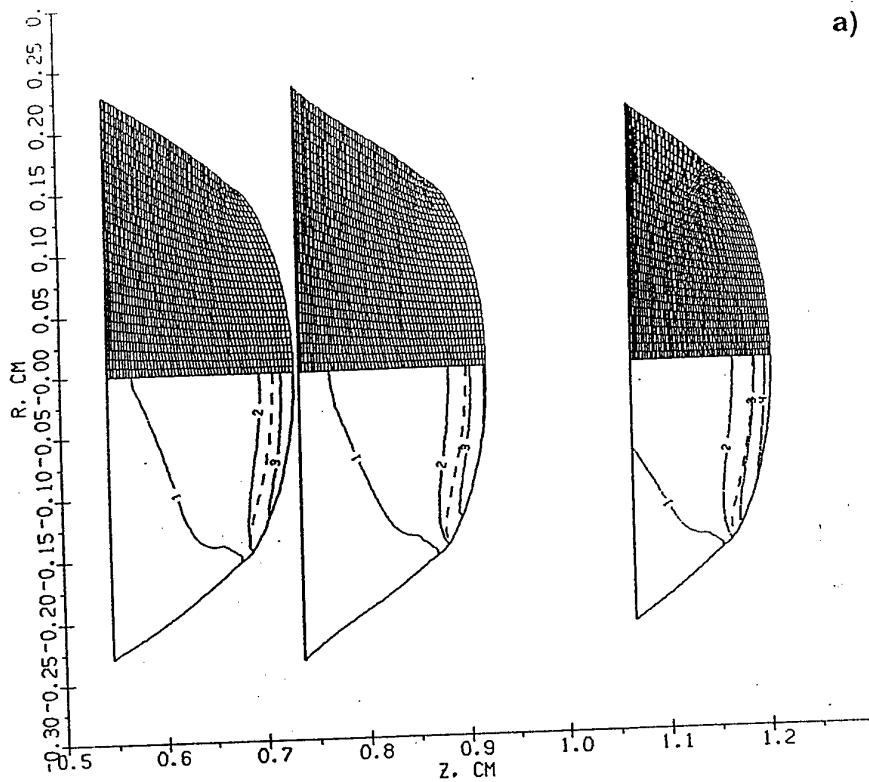
Fig.4. Numerical grid and pressure levels. Pressure level step is 0.06 kbar, maximum pressure is 0.6 kbar. Time is 1.3 s.



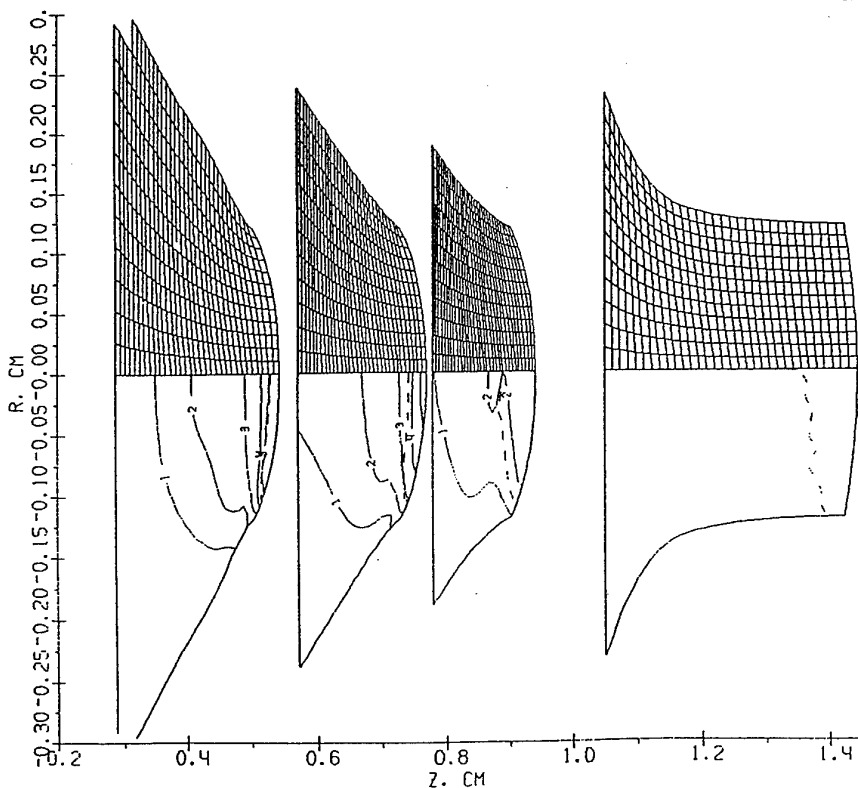
**Fig.5** Numerical grid and levels of constant density.  
 a) Time is 15  $\mu$ s, level step is 0.05 g/cc  
 b) Time is 30  $\mu$ s, level step is 0.01 g/cc



**Fig.6** Experimental X-ray photograph at the time 30  $\mu$ s



a)



b)

**Fig.7(a,b) Computational grids and levels of contact pressure at different times. The dashed line corresponds to Mach number  $M=1$ .  
 a) diameter is 3 mm, levels step is 40 kbar  
 b) diameter is 2.4 mm, levels step is 20 kbar**



## REFERENCES

1. S.K. Godunov (1976) Numerical solution of multi-dimensional problems of gas dynamics (in russian), Nauka, Moscow
2. P.Colella, H.Glaz (1985) Efficient solution algorithm for the Riemann problem for real gases, *J.Comp.Phys.* 59, p.264
3. Ja.Holodov, O.Yu.Vorobiev (1994) Effective methods of integrating 1D gas dynamics problems, *Z.vich.mat. i mat phys.* (russian) to be published
4. J.D. Frey, F.Janicot, X. Garaud, P. Groenenboom, M.Lambert (1993) *Int.J.Impact Engng*, 14, p.255, 1993
5. J.K.Dukowicz (1985) *J.Comput.phys.* 61, pp.119-137.
6. A.Harten (1989) *J.Comput. Phys.* 83, p.148
7. A.Harten and S.Osher (1987) *SIAM J.Numer.Anal.*, 24(2), p.279
8. R.Abgral (1994) *J.Comput Phys.*, 114, p.45
9. O.Yu. Vorobiev, A.L. Ni, A.V. Shutov, V.E. Fortov (1992) Application of Godunov's method with movable grids for calculations of dynamics of condensed matter under intense impulsive actions, *Modelling in mechanics (russian)*, 6(4), p.3
10. A.L Ni, T.N.Fortova, K.G.Shkadinski, A.V.Shutov, A.V. Utkin (1989) Numerical simulation of interaction of high velocity impactors with condensed targets, (in russian) Preprint Institute of Chemical Physics, Chernogolovka
11. D.A.Crawford, M.B.Boslough, T.G.Trucano, A.C.Robinson (1994) The impact of comet Shoemaker-Levy 9 on Jupiter, *Shock Waves*, 4, p.47-50.
12. B.Klumov et al. (1994) Collision of the Shoemaker-Levy-9 Comet with Jupiter: Simulation of Long-Term Consequences, *physics-doklady*, 39, pp.486-493
13. Kathleen S.Holian (1990) Hydrodynamics code calculations of debris clouds produced by ball-plate impacts, *Int.J.Impact Engng.* 10, p.231
14. A.V.Utkin, T.N.Fortova, G.I.Kanel, K.G. Shkadinski.(1988) Calculation of Nonideal Detonation in TNT on the Base of Macrokinetics Empirical Equation", *Chemical Physics, Russia*, 7(9), p.1257.
15. J.K.Dukowicz et al. (1989) A General Topology Godunov Method , *J.Comput.Phys.* 82, p.29

HEDRC REPORT  
contract SPC-93-4075

## 2D HIGH RESOLUTION SHOCK WAVE PHYSICS CODE

9-month technical report

*Second order modification of moving grid hydrocode*

Participants:  
Vorobiev O.Yu.  
Shutov A.V.  
Zharov A.V.  
Ni A.L.  
Fortov V.E.

## Introduction

One of the most important problem of numerical solution of nonlinear hyperbolic conservation equation is to obtain high accuracy of the solution in both discontinuous and continuous regions. In recent years, a lot of so called high resolution schemes have been proposed, for example, second order TVD scheme of Roe [1,2] and Sweby [3]; upwind TVD of Harten [4] and Yee et al. [5]; symmetric TVD of Chakravarthy and Osher [6]; ENO scheme of Harten et al. [7,8], FCT scheme of Zalesak [9] McDonald and Ambrosiano [10]; MUSCL schemes of van Leer [11], Goodman and LeVeque [12], Davis [13], Colella [14], and PPM of Colella and Woodward [15]. The most of schemes mentioned above were originally derived for the case of perfect gas and for 1D geometry (or 2D for fixed Eulerian grids). For numerical simulations of hypervelocity impact problems, when realistic physical models are used, we face with additional problems. This is, for example, a variety of matter properties in different phase states (solid, liquid, gas, plasma), when the compressibility of matter differs up to several orders of magnitude. This difference often gives some unphysical values of variables appearing due to errors of numerical approximation (negative internal energy or density), which lead to a failing of numerical scheme. As it was found in [16], some of Godunov-type second order methods based on approximate Riemann solver are not positively conservative or positively conservative under certain conditions. They can produce non-physical states with negative density or internal energy in rarefaction waves. We based our code on the Godunov's method of numerical integration of Euler equations on a time dependent (so called moving) grid [17]. As it was shown in [16], this scheme is positively conservative for at least in the case of ideal gas EOS.

Let us remind the main principles of this code. In the framework of this approach only the boundaries of numerical grid are moved in Lagrangian fashion. The location of interior grid nodes are determined during grid generation procedure by using of coordinates of boundary nodes. As the material flows through the grid cells there is some diffusion error as well as in any Eulerian method. Nevertheless there exist several possibilities to reduce such errors by generating "near-Lagrangian" grids. In the present version of 2D hydrocode we utilize decomposition of numerical region onto subregions with Lagrangian boundaries, in which grids are generated independently using conformal mapping procedure. This decomposition is provided automatically during the computations. When every subregion consist of only

one cell. This approach resembles Lagrangian method on unstructured quadrilateral mesh. On the other side, such a grid enables all advantages of a regular grid. It is known that the numerical approximation of solution on an orthogonal grid is always better than that one on an arbitrary disturbed grid [17]. The grid generation procedure can be governed by moving the boundary nodes along the boundary. Using such a redistribution of the boundary nodes orthogonal grids are generated in subregions. The other advantage of orthogonal grids is a possibility to simplify a second order extension of Godunov's scheme.

In the present report we consider a second order extension of moving grid code and compare results of calculations of hypervelocity impact problems with shock-fitting calculations. The strategy of shock fitting grids was described in the previous report. Unfortunately, the application of this approach is not possible inside of numerical subregions. It means, that the description of shock wave propagation and interaction inside of disturbed subregion can not be done using shock fitting grids. That is the reason why the second order extension of Godunov's scheme is very important.

### 3. NUMERICAL ALGORITHM

In this report we describe algorithm of computations only briefly. More detailed description one can find, for example, in [18], as well as in the first report. As we have already mentioned, the numerical region is divided into several subregions with Lagrangian boundaries during the computations. Let us consider the main steps of computational algorithm for one subregion.

The first step of computations is the displacement of the boundary of subregion. After shifting the boundary to a new position some segments of the boundary can change their type due to interaction with boundaries of the other subregions. The boundary type determines the boundary condition (what is necessary for Riemann problem initial data) and the law of motion of the boundary. For example, a shock-front boundary moves according to Hugen's principle, rigid wall boundary does not move and so on.

The second step is an iterative procedure of orthogonal grid generation inside of subregion. This procedure is based on the distribution of the boundary nodes. This distribution is performed several times until the grid generated with conformal mapping becomes orthogonal.

The third step is a solution of Riemann problems for inner zones and calculation of fluxes between the neighboring zones. One should remark here,

that for an arbitrary equation of state the Riemann problem can be solved only numerically. Nevertheless, we employ an exact solver of this problem only in vicinity of flow discontinuity. The most of Riemann problem computations are done either in isentropic or in acoustic approximation.

Second order extension of Godunov's scheme can be obtained if we assume a piecewise linear distribution of flow parameters inside of the grid cells. To conserve the monotonicity property of Godunov's scheme we use the "minimum derivative principle" proposed in [19]. The main idea of this principle is to choose the minimum possible derivative when interpolating the values from the zone center to the boundary with the neighboring zone, where the Riemann problem must be solved. If the grid is orthogonal, derivatives only in one direction (either along the grid rows, or along the grid columns) are important when interpolating cell-centered values to the boundaries of the cells. This simplifies the realization of "minimum derivative principle".

#### 4. EXAMPLES OF CALCULATIONS

In the present paper we consider an application of our 2D code to hypervelocity impact problem. One of the most difficult task for any 2D Lagrangian code is to compute hypervelocity penetration of projectile into a thick target. We consider two different approaches to numerical simulation of hypervelocity impact of iron projectile moving with 10 km/s velocity on a thick aluminum target .

First one concludes in a usage of "near-Eulerian" grid, which covers the region of the target where the shock wave propagates.

The second one is fitting of this shock wave by moving the boundary of the grid with shock front velocities obtained by Riemann solver. The second method in fact, is more accurate to resolve the shock front and is more economic, because it does not require a grid in undisturbed regions. On the other hand the shape of numerical region is more complicated and, as a consequence of that, the grid generated is not so orthogonal as in the first case. The results of computations corresponding to these cases together with numerical grids are shown in Fig.1. There were two subregions used in the case of shock-fitting grid. One of them corresponded to the projectile, the other one covered the disturbed region in the target. In the other case (near-Eulerian grid) three subregions were used in computations.

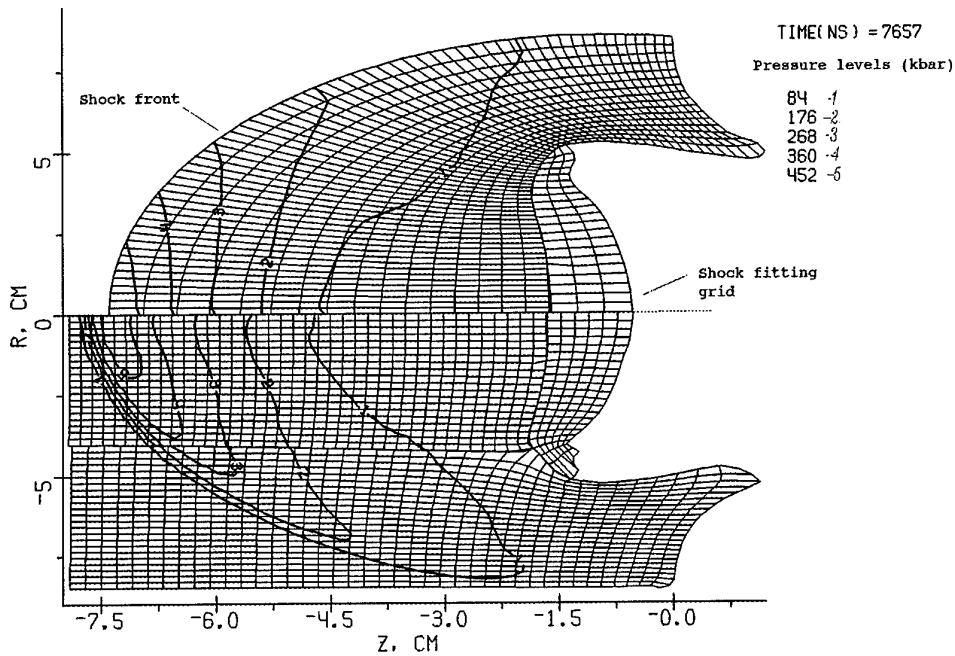


Fig.1 Numerical grid and pressure levels for hypervelocity impact calculations using shock fitting grid (above the axis) and "near-Eulerian" grid (below the axis).

It is known, that first order Godunov's scheme is a very dissipative one. Our experience shows, that this scheme smears out weak discontinuities in the case of realistic EOS much stronger than in the case of perfect gas. Moreover, this dissipation grows in time. Results of computation of hypervelocity impact of iron projectile on aluminum target shown in fig.2-3 confirms this fact. In contrast to the first order scheme, second order calculations exhibit nearly constant width of shock front smoothing.

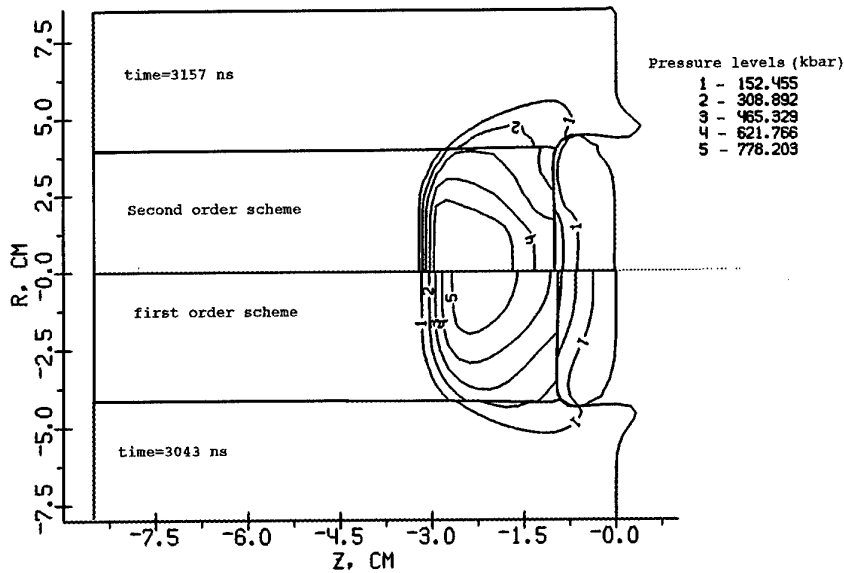


Fig.2 Grid boundaries and levels of constant pressure for the first (below the axis) and second order accuracy calculations of hypervelocity impact of iron projectile (on the right) on an aluminum target.

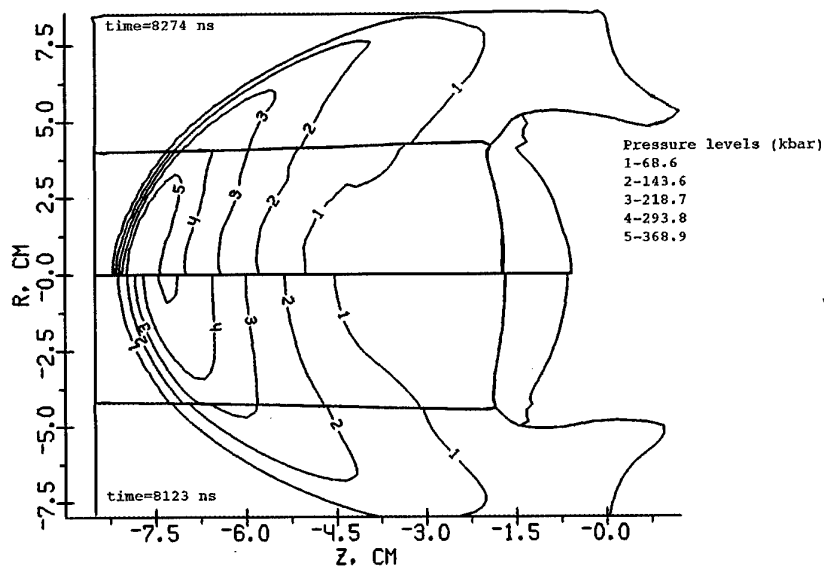


Fig.3 Grid boundaries and levels of constant pressure for the first (below the axis) and second order accuracy calculations of hypervelocity impact of iron projectile (on the right) on an aluminum target.

As it has been shown in [20] for the case of steady gas flow, the second order extension of Godunov's scheme is not so sensitive to distortions of numerical grid as it's first order counterpart. We demonstrate below (Fig.4-5) the results of simulation of hypervelocity impact obtained using the first and the second order Godunov scheme both on the shock fitting grid and on the near-Eulerian grid. Our results generally confirm the conclusions obtained in [20]. For the second order scheme (Fig.5) the difference between the results obtained on the different grids is negligible, while for the first order scheme there is a big difference in the amplitude of the shock wave calculated on the shock fitting and on near-Eulerian grid. It is naturally, that the shock front dissipation is much pronounced in the case of the first order scheme than in the case of the second order one.

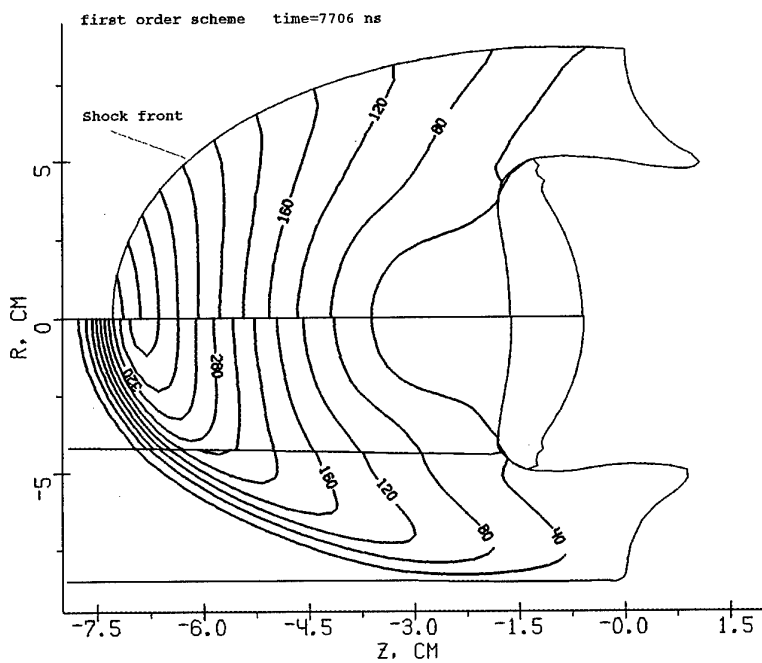


Fig.4 Grid boundaries and pressure levels (in kbars) for shock fitting grid and "near-Eulerian" grid. First order scheme.



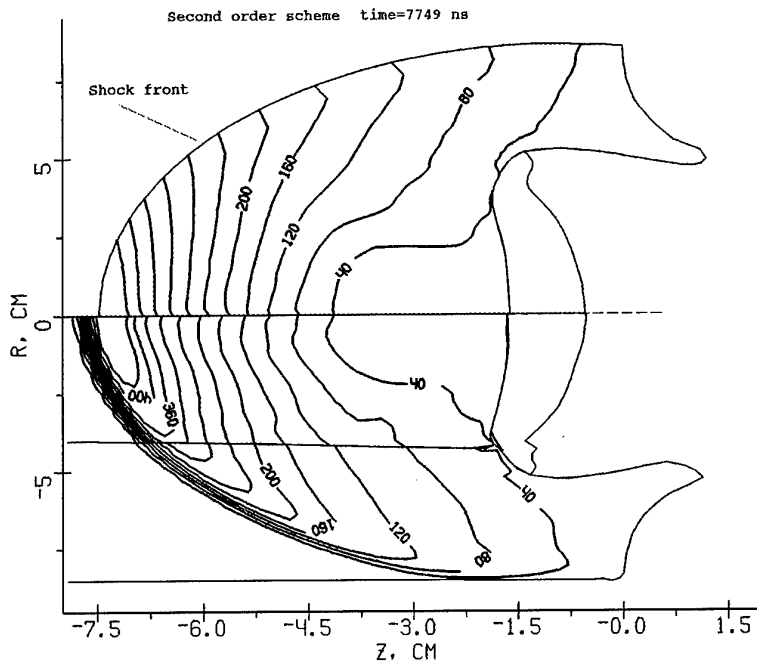


Fig.5 Grid boundaries and pressure levels (in kbars) for shock fitting grid and near-Eulerian grid. Second order scheme.

## CONCLUSIONS

We have considered an application of Godunov's scheme on the moving grids and its second order extension (Kolgan scheme) on the example of hypervelocity impact calculation. We have shown that this scheme coupled with the algorithm of decomposition of numerical region onto subregions shows a good robustness and flexibility for multimaterial problems of computational fluid dynamics with large distortions. The other advantage of decomposition of numerical region of complicated shape is a possibility to generate orthogonal grids in subregions

We have developed second order Godunov's scheme applying Kolgan's algorithm of "minimal derivative". It has been found that Kolgan's scheme is not so sensitive to the form of the moving grid as original Godunov's scheme. The results of second order calculations are much closer to more accurate shock-fitting calculations.

## REFERENCES

- [1] P.L. Roe, *Annu. Rev. Fluid Mech.* 337(1986)

- [2] P.L. Roe, Lectures in Appl. Math. Vol. 22 (Am. Math. Soc., providence, RI , 1985
- [3] P.K.Sweby, SIAM J. Num. Anal. 21,995(1984)
- [4] A. Harten, J.Comput. Phys.49,357(1983)
- [5] H.C.Yee, R.F.Warming, and A. Harten, J.Comput. Phys.57,327(1985)  
ICASE Report No 84-20,June 1984
- [6] S.R.Chakravarthy and S.Osher,"A New Class of High Accuracy TVD Schemes for Hyperbolic conservation Laws",AIAA-98-0363, 1985
- [7] A.Harten and S.Osher,SIAM J.Num.Anal.24,297(1987)
- [8] A.Harten, B.Engquist, S. Osher,S.R.Chakravarthy , "Uniformly High Order Accurate Essentially Non-Oscillatory Schemes", NASA CR-178101,1986
- [9] S.T.Zalesak, J.Comput. Phys.31,335(1979)
- [10] B.E.McDonald and J.Ambrosiano, J.Comput. Phys.56,448(1984)
- [11] B.van Leer, J.Comput. Phys.32,101(1979)
- [12] J.B.Goodman and R. LeVeque, SIAM J. Num. Anal. 25,268(1988)
- [13] S.F.Davis,SIAM J.Sci.Stat.Comput.9.445(1988)
- [14]P.Colella,SIAM J.Sci.Stat.Comput.6.104(1985)
- [15]P.Colella and P.R.Woodward,J.Comp.Phys.54,174(1984)
- [16]B.Einfeldt,C.D.Munz,P.L.Roe,B.Sjoegreen J.Compt.Phys.92,273(1991)
- [17] S.K.Godunov, Numerical solution of multi-dimensional problems of gas dynamics (in russian) (1976) Nauka, Moscow
- [18] O.Yu.Vorobiev, I.N.Lomov,A.V Shutov et al.,Godunov's Scheme on Moving Grids for High Velocity Impact Simulations, to be published in Proc. HVIS94, Santa Fe,NM
- [19] V.P.Kolgan, Scientific Notes of CAGI (in russian),3,68,(1972)
- [20] V.I.Koptchenov, A.V.Kraiko, Zh.Vych.Matem.i Matem Fiz. (in russian) 23,848 (1983)

# HEDRC REPORT

*High resolution shock-wave physics code*  
final report

**USER'S MANUAL**

Participants: Vorobiev O.Yu.  
Shutov A.V.  
Zharov A.V.  
Ni A.L.  
Fortov V.E.

## *Brief description of the code*

The language of the code is standard F77 FORTRAN. So it can be easily installed on any computer with f77 compiler. The code consists of the following program modules:

Module:	Function:
STARTT -	input of initial data and transformation of these data into file NAM.tmp for continuation of calculations by module BIG2T
BIG2T-	carries out calculations, renews data for continuation of calculations (file NAM.tmp) and records results of the calculation
REPT-	modification of the task (possibility to add or delete subregions ). The changed data are rewritten into the file NAM.tmp
UNFTOF-	transformation of NAM.tmp from binary file to ASCII file and back (it may be useful for transmission of calculation results from one computer to other one with different binary data presentation)

This version of 2D hydrocode operates with tabulated equations of state (TABEOS format) as well as with perfect gas analytical EOS. The code loads four EOS tables :ENER\*.TAB,PRES\*.TAB,SND\*.TAB, PHYS\*.TAB, DATA\*.MAN (\* - from 1 to 4), which are energy, pressure, sound velocity, index of state and information about table limits for 1- aluminum, 2-Nickel, 3- tantalum, 4- tungsten correspondingly. If it is required to include another TABEOS tables in computations one need to change the normal densities for substances 1-4 in subroutine readtab (urst.for) in accordance with the tables used.

## *Installation of the code*

To create object modules

- 1) copy all files \*.FOR and \*.INC to one directory on a hard disk  
REMARK: all \*.INC files must be with capital characters

- 2) compile all \*.FOR files

\* before compilation probably may be necessary:

A) to set function which determines CPU time in seconds in  
SUBROUTINE ETIME in the file PC.FOR. (to decomment  
correspondent string may be sufficient)

B) to change parameters in the file BIGPAR.INC  
(dimensions of arrays)

3) create loading module STARTT, using object files:

startt.o, blocka.o, adi.o, arct.o, big.o, contw.o, univer.o, dat0.o,  
dattst.o, disto.o, jup.o, pc.o, shr.o, spect.o, urst.o

4) create loading module BIG2T, using object files:

basica.o, blocka.o, mainxt.o, spect.o, tnew2a.o, urst.o, adi.o, arct.o,  
big.o, buil.o, buil0.o, buil1.o, build.o, contw.o, dat0.o, del.o, disto.o,  
god2.o, grnew.o, jup.o, pc.o, ref.o, shr.o, split.o, split1.o, univer.o

5) create loading module REPT, using object files:

rep.o, blocka.o, spect.o, urst.o, adi.o, arct.o, big.o, contw.o, dat0.o,  
del.o, jup.o, pc.o, ref.o, shr.o, split.o, split1.o, univer.o

\*Note that modules mentioned above (STARTT, BIG2T, REPT) can be  
created using makefile. To generate first order accuracy code (BIG1T),  
one should replace tnew2a.\* by tnew1a.\* in the makefile.

#### *Generation of a new initial data file*

1) Chose one of the existing initial data files from the  
file list below

TST2.DAT

VRB2.DAT

VRB3.DAT

.....

2) Copy the chosen file into file NAM.dat, where NAM is  
any name consisting of 1-4 symbols  
(the names of all the files created during the computation  
of this problem will include NAM as a root word)

3) Correct contents of the file NAM.dat with text editor  
using description of initial data file presented  
below

*Description of the structure of initial data file NAM.dat*

The initial data file consists of two parts:  
First part contains control information. This part has the same format for all files of this type. Let us consider an example shown below, where the first part of initial data file TST.DAT is presented.

```
AL/AL U=10.1KM/C
JSPR-LOS-LST-IRD-ISP-IRA-ICM-AIR
 0 1 1 2 1 00 1 0
NBL--MI-ID1-ID2--IK-IGR-ILENPARIVSP
9900 1 10 10 300 10 -10 6 0
----CMM---:-----H3----:----HDEL---:----T-----:---STABL---:
-1.00000E-03 0.00075E-00 0.01000E+00 1.10000E+05 0.50000E+00
```

The first string is comment. This is usually short information about the problem. (Here this is 10.1 km/s impact of aluminum on aluminum). The next strings consist of title\_strings and contents\_strings. The title\_strings show the names of variables. The contents\_strings are values of these variables. The assignment of the variables is shown in the table

TABLE

---

variables:	meaning:
ispr	controls rebound of different boundary segments 0- calculations without rebound 1- rebound for "contact" type boundaries only 2- rebound for "contacts and rigid walls" type boundaries 3- rebound for all boundary types
los	1- cylindrical symmetry 0- plane symmetry
lst	1- there are rigid walls 0- rigid walls are absent
ird	0- to ignore isp 1- to continue calculations from the restart data 2- to correct in dialog regime the number of time steps after which the splitting of numerical regions into subregions will be switched on
isp	1- to change in dialog regime the type of " contact " between subregions 0- to do nothing

ira energy source (for impact problems ira is equal to 0)

icm 1- automatical choice of time step  
 0- -- ----- ---- time step =  $\text{abs}(\text{cmm}) * \text{stabl}$   
 (cmm, stabl see below.)

nbl is the number of time steps to do before copying of all flow parameters to output file.

mi 1- to search the optimum location of 4 angle tops of rectangular subregion along the boundary

id1, id2 are the numbers of time steps to do before the data record for restart(id1- before the first record)

ok is the maximum number of time steps to do.

igr is the number of time steps to do before printing packed information about all subregion's boundaries.

ilen is the number of time steps to do before the next graphic data record.  
 If ilen less 0 then data for the graphics will be written in time step= $\text{abs}(\text{ilen} * \text{cmm})$  in nanoseconds.  
 (cmm parameter described below)

par is the number of flow parameters which must be written for graphics data. (from 5 to 7 parameters)

ivsp if ivsp is not equal to 0 then ivsp is input parameter for subroutine AUTOSP, which changes types of " contact " between subregions automatically .  
 This automatical regimes must be programmed by user for the concrete task in subroutine AUTOSP.

cmm is parameter which determines time step (stt)  
 $\text{stt} = \text{cmm} * \text{stabl}$  if  $\text{cmm} > 0$ .  
 If  $\text{cmm} < 0$ . then cmm will be read from restart or  $\text{cmm} = \text{abs}(\text{cmm})$  in case of initial data.

h3 space precision.(H3 equals to 0.1 of cell size)  
 H3 is widely used in the code as character space size.

hdel  
 The boundary section with length  $< \text{hdel} * (\text{cell size})$  will be combined with neighboring one.

t time cpu limit in seconds

stabl stability coefficient stt= cmm \* stabl

---

The second part of the initial data file includes an information about geometric configurations of the problem to be solved. The information may be prepared using so called UNIVERSAL INPUT. In this case the first string in the second part of the initial data file must be UNIVER.....

One Universal input starting with UNIVER..and finishing with UNIEND specifies only one subregion (numerical block). To specify several subregions one must use this block of input strings several times.

The boundaries of numerical subregion are specified in accordance with the following rules:

1) If the problem contains the rigid walls and shock fronts they must be specified right after the string UNIVER.... For example, in the case of rigid wall the input looks like this

UNIVER.....

RIGIDRD

IWALL, INW, ITP, AW, BW, CW;STRAIGHT LINE:F=INW\*(AW\*X+BW\*Y-CW)=0.

1 , -1 , 1, 0. , 1., 0.

-1 , -1 , 1, 0. , 1., 0.

Here the second string (after UNIVER) starting as RIGIDRD indicates to the beginning of wall specification, which is finished when the first parameter (IWALL) equals to some negative value (-1 in this example). In the example presented above the rigid wall specified is the straight line (ITP=1) and input parameters are the coefficients which determine it's orientation.

To specify the front one must put the string starting as FRNTREAD either after the UNIVER... or after the rigid wall specification. The front specification looks like the following

FRNTREAD

c1 --- read of front information

ifr,ityp, | the\_number\_of\_front, the\_type\_of\_front

icont, | the\_number\_of\_contour

a,b,c, | the contour is straight line  $a*x+b*y-c=0$  ! icont=nomco+1

ibeg\_end,| 1-begin,2-end

-1

Here the expressions on the right from | are comments. The front input is finished when ifr equals to some negative value (-1 in this example). The beginning and the end of the front move along the stright



lines (called contour). There are not more than two contours corresponding to the same front. The sequence of the numbers of the contours specified must be increasing. Every contour corresponds either to the beginning of the front (ibeg\_end=1) or to the end. Using such an input several fronts can be specified. There are several front types considered (the\_type\_of\_front). The main of them are

- 1- shock front in undisturbed solid media
- 2- shock front in undisturbed porous media

Specification of all fronts and walls must be closed by the string  
END.....

- 2) The next two strings

5., 0., 0.,:--USRT--,---VSTR---,VPOL  
12,:--NUMBER OF URS

give the velocity components (USRT, VSTR), porosity of the subregion (VPOL) and number of material (EOS). Then the boundary segments must be specified. Boundary orientation is counter-clockwise. The boundary segment can be straight line, circle or some other arbitrary curve specified in the table form. The next string gives the coordinates of the first point of the boundary.

0.,0.,:X0,Y0 - THE LOCATION OF THE FIRST POINT FOR A BOUNDARY (CM)

If the first boundary segment is a straight line, then the next two strings are

**STRAIGHT 1**  
0.,1., XE,YE,: IS COORDINATES OF THE END OF THE STRAIGHT SEGMENT (CM)

If the next segment is a fragment of a circle then must be

**CIRCLE**  
XC,YC,ALF,: IS THE CENTER OF THE CIRCLE(CM),ANGLE (0-360 grad)

The boundary segment can be any arbitrary curve. In this case it is specified using the table input

**TABLE**  
XE,YE,: IS THE NODES COORDINATES  
...,... , TABLE INPUT UNTIL INPUT ERROR OCCURES  
END OF THE TABLE

The specification of the boundary of a subregion is closed by the string

**REGEND**

The four angles of subregion must be determined for the purpose of grid generation, when the boundary of the subregion is specified. The angles input looks like this

1---2---3---4 ANGLES LOCATION  
I1,I2,I3,I4,;; TO FIND 4 ANGLES OF THE RECTANGULAR REGION USING  
CORRESPONDENT BOUNDARY SEGMENTS NUMBERS I1,I2,I3,I4

In the example of input shown below

,,5,;;  
the ANGLES with numbers 1,2,4 are determined automatically and the angle 3 is found in the beginning of the boundary segment number 5. Initially all the boundary segments have the type of "FREE BOUNDARY". If one needs to assign some other boundary type to the boundary segment the following strings are necessary:

#### BOUNDARY TYPE INPUT

Then depending on the boundary type can be:

a)in the case of rigid wall

RIGID ,;CHANGES "FREE" TYPE BY "RIGID"  
IREG,IRG ,; IREG-NUMBER OF BOUNDARY SEGMENT  
IRG-NUMBER OF RIGID WALL

b)in the case of shock front

FRONT ,;CHANGES "FREE" TYPE BY "FRONT"  
IREG,IFR ,; IREG-NUMBER OF BOUNDARY SEGMENT  
IFR-NUMBER OF FRONT

c) in the case of contact discontinuity

CONTACT ,;CHANGES "FREE" TYPE BY "CONTACT"  
IREG,N1,IREG1,; IREG-NUMBER OF BOUNDARY SEGMENT FOR CURRENT SUBREGION, N1-  
NUMBER OF SUBREGION WHICH IS IN CONTACT, IREG1-NUMBER OF BOUNDARY  
SEGMENT FOR N1 SUBREGION

The input of data for the current subregion is closed by

UNIEND

#### Remark:

We have described UNIVERSAL INPUT in the text above. If there are special program for more simple input for concrete configuration then the name of this program is the first string in the second part of the input data.

For example:

DATST1 ; -NAME OF THE PROGRAM WHICH TREATS INPUT DATA

### *How to run the code*

- 1) Run the module STARTT in the directory containing file NAM.dat
- 2) Type NAM when the question "ENTER DATA NAME" appears

module STARTT will create the files:

NAM.tmp- for following calculations

NAM000.dat- first file for graphics

NAM.cfg- file containing some parameters (if this file does not exist)

An example of CFG file is presented below

```
-----VRB2.CFG-----  
0.7654392 , PLIM [bar] line 1  
2.7104001E-08, RLIM [G/(CM**3)] line 2  
13.93920 , EPSGAS [M/C] line3  
278.7840 , EPSCON [M/C] line4  
9.9999998E-03, ALMIN line5  
0.3000000 , SINCOND line6  
2.0000000E-02, ALMN line7  
9.9999998E-03, SHISAMI line8  
5.0000001E-02, SHISAMA line9  
0.07000000 , TET line10  
0.000000 , ADP line11  
-----
```

In this file the first two strings are minimal pressure and density, the next two strings are accuracy of calculation of wave velocities for the cases of gas EOS and table EOS correspondingly. Parameters ALMIN, SINCOND (SINCOND is changing from 0 to 1), ALMN are responsible for the movement of boundary nodes on the boundary of "special" type. SHISAMI and SHISAMA are minimum and maximum shift of the boundary nodes during the procedure of boundary node distribution (in relative units). TET is a parameter determining the convergence of grid generation (TET>0) and ADP is a level of grid adaptation to solution. In the present version of the code adaptation is not included (ADP=0)

When the STARTT finishes its work the following message appears

**THE NUMBER OF PICTURE =0**

- 3) Run the module BIG2T (or BIG1T) to continue calculations

- 4) Reply the questions appearing on the screen

To avoid the grid tangle in the cases of large deformations to split the numerical regions into subregions is recommended. The most frequently appearing question concerning that is

**IF YOU DON'T WANT TO SPLIT SUBREGION \***

**ENTER** number of steps without splitting analysis

Enter 0 on this question if you want to split subregion, which the program suggests to split. Then press enter to continue computations.

The question **ENTER N,M ACCORDING TO THE STENCIL** means that you can change the type of contact between subregions N and M. Enter -1,1 to ignore this (and -1,1 for the next question)

The program periodically creates the files NAMxxx.dat for graphics and renews file NAM.tmp for restart.

When the program has done the calculations it starts the dialogue from the beginning (asking "ENTER DATA NAME"). To continue the computations of the same problem enter the same name NAM.

- 5) Analyze the results of computation using graphics modules. For this purpose created graph files NAM\*\*\*.dat (and kNAM\*\*\*.dat) must be copied to IBM PC Then they can be depicted on the screen using and written in TIF file using GR.EXE (See the manual for GR.EXE)
- 6) Continue calculations (point 3) if it is necessary
- 7) Change configuration of the task,if it is necessary if you want to change configuration you must create the file dNAM.dat (see description of the file) and run the program REPT

### *Brief manual for GR.EXE*

*Executing module GR.EXE shows the results of computation on the screen of IBM PC (DOS is required) and writes the pictures shown on the screen in TIF format. Besides the resulting files ROOT\_\*.DAT to be shown, on more file K\_ROOT.DAT is necessary to determine the limits of the picture. This file can be created anytime by coping already existing files of such type. After running GR.EXE one need to answer the questions in the dialog.*

- 1) Type the ROOT name of \*.DAT files to be plotted
- 2) Enter the number of picture N (file ROOT\_N.DAT will be plotted)
- 3) Choose the flow parameter to be plotted (1-density, 2-pressure, 3-porosity, 4,5-velocities, 6-energy)
- 4) Choose the type of picture (I1-levels of constant values and numerical grid, I2-levels of constant values for two different flow parameters, DY-cross sections along the axis of symmetry, DX- perpendicular to the axis)

- 5) When the picture is shown on the screen one can plot over this picture another pictures (if the axes are not plotted yet). For this purpose enter negative number  $-N$  (where  $N$  is the number of picture to be plotted)
- 6) To finish plotting enter any character (for example '.') and axes will be shown. Then type enter, the name of the TIF file where this picture will be saved and CTRL-C to leave the program.
- 7) REMARK: When using DY or DX options (plotting cross sections) use CTRL-Z to return back for plotting pictures after the question I= INPUT Y/X COORDINATE FOR SECTION.

### Example of initial data files

Let us consider some demonstrative examples of initial data generation for hypervelocity impact problems

#### EXAMPLE 1: initial data file VRB3.DAT

```
Impact of W projectile on Al target
JSPR-LOS-LST-IRD-ISP-IRA-ICM-AIR
  1  1  1  2  1  00  1  0
NBL--MI-ID1-ID2--IK-IGR-ILENPARIVSP
9900  1  30  30  300  30-500  6  0
----CMM---:-----H3----:----HDEL---:----T-----:---STABL---:
-1.00000E-03 0.02000E-00 0.06000E+00 1.10000E+05 0.60000E+00
UNIVER      , ; -NAME OF PROGRAM WHICH TREATS INPUT DATA
RIGIDRD      , ; READING AXIS AND RIGID WALLS
C IWALL, INW, ITP, AW, BW, CW ;STRAIGHT LINE: F=AW*X+BW*Y-CW=0.
  1  , -1,  1,  0. ,  1.,  0.
 -1  , -1,  1,  0. ,  1.,  0.  exit,A,A,A,A
END
-5.,  0.,  0.,:--USRT--:---VSTR---,VPOL
44,:--NUMBER OF EOS
0.,0.,: X0,Y0 - THE LOCATION OF THE FIRST POINT FOR THE BOUNDARY (CM)
STRAIGHT  1
1.,0., XE,YE,: COORDINATES OF THE END OF THE STRAIGHT SEGMENT (CM)
STRAIGHT  2
1.,4., XE,YE,: COORDINATES OF THE END OF THE STRAIGHT SEGMENT (CM)
STRAIGHT  3
0.,4., XE,YE,: COORDINATES OF THE END OF THE STRAIGHT SEGMENT (CM)
STRAIGHT  4
0.,0., XE,YE,: COORDINATES OF THE END OF THE STRAIGHT SEGMENT (CM)
REGEND
c-1-2-3-4
  1,2,3,4,
BOUNDARY TYPE INPUT
RIGID      ,;CHANGING "FREE" TYPE BY "RIGID"
  1,1,; IREG-NUMBER OF BOUNDARY SEGMENT,IRG-NUMBER OF RIGID WALL
UNIEND  1
UNIVER      , -NAME OF PROGRAM WHICH TREATS INPUT DATA
```

```

END
0., 0., 0.,::--USRT---VSTR---,VPOL
    41, ::--NUMBER OF EOS
-8.5,0.,:: X0,Y0 - THE LOCATION OF THE FIRST POINT FOR THE BOUNDARY (CM)
STRAIGHT 1
0.,0., XE,YE,:: COORDINATES OF THE END OF THE STRAIGHT SEGMENT (CM)
TABLE 1
0.,0.,
0.,8.5,
0.,8.5,
-8.5,8.5,
-8.5,8.5,
-8.5,0.,
-8.5,0.,
END OF TABLE
REGEN
1--2---3---4
1,2,,,
BOUNDARY TYPE INPUT
RIGID
1,1,
UNIEND 2
ENDINPUT

```

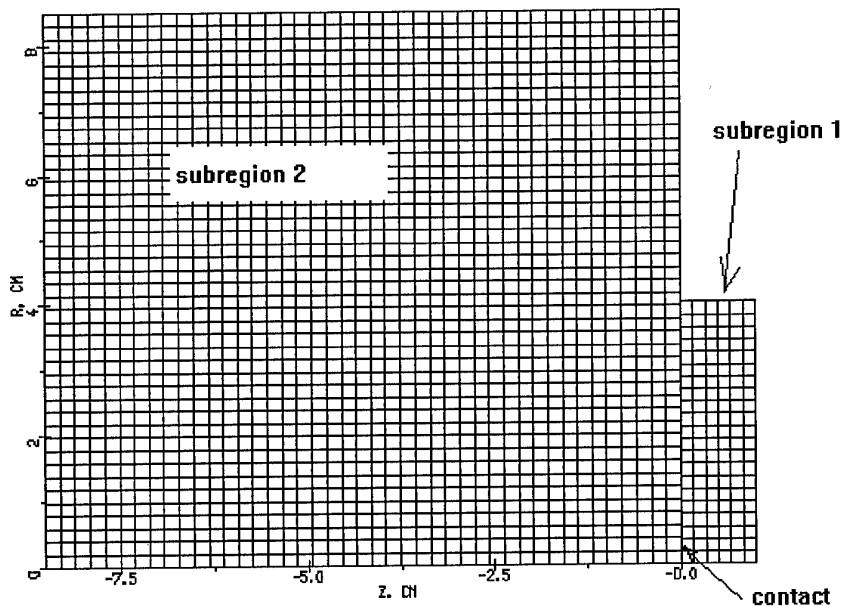


Fig.1 Initial configuration for initial data file VRB3.DAT

EXAMPLE 2: initial data file VRB2.DAT

```

IMPACT with shock fitting
JSPR-LOS-LST-IRD-ISP-IRA-ICM-AIR
1 1 1 2 1 00 1 0

```

```

NBL--MI-ID1-ID2--IK-IGR-ILENPARIVSP
9900 1 30 30 300 30-500 6 0
----CMM---:-----H3-----:----HDEL----:----T-----:---STABL---:
-1.00000E-03 0.02000E-00 0.06000E+00 1.10000E+05 0.60000E+00
UNIVER ;, -NAME OF PROGRAM WHICH TREATS INPUT DATA
FRNTREAD
C1 --- read of the front information
1,1, ;c2 ifr,ityp ;: the_number_of_front, the_type_of_front
1, ;c3 icon,;: the_number_of_contour
1.,0.,0., ;c4 a,b,c,;: the contour is straight line a*x+b*y-c=0 !
icon=nomco+1
1, ;c5 ibeg_end,;: 1-begin,2-end
-1, ;c6 end
RIGIDRD ;, READ OF AXIS AND RIGID WALLS
C IWall, INW, ITP, AW, BW, CW ;STRAIGHT LINE: F=AW*X+BW*Y-CW=0.
1 , -1 , 1, 0. , 1., 0.
-1 , -1 , 1, 0. , 1., 0. exit,A,A,A,A
END
-5., 0., 0.,;--USRT--,---VSTR---,VPOL
44, ;--NUMBER OF EOS
0., 0., :: X0,Y0 - THE LOCATION OF THE FIRST POINT FOR THE BOUNDARY (CM)
STRAIGHT 1
1.,0., XE,YE,;: ARE COORDINATES OF THE END OF THE STRAIGHT SEGMENT (CM)
STRAIGHT 2
1.,4., XE,YE,;: ARE COORDINATES OF THE END OF THE
STRAIGHT SEGMENT (CM)
STRAIGHT 3
0.,4., XE,YE,;: ARE COORDINATES OF THE END OF THE STRAIGHT SEGMENT (CM)
STRAIGHT 4
0.,0., XE,YE,;: ARE COORDINATES OF THE END OF THE STRAIGHT SEGMENT (CM)
REGEND
1---2---3---4 ANGLE LOCATION
1,2,3,4,
BOUNDARY TYPE INPUT
RIGID ;,YOU WILL CHANGE "FREE" TYPE ON "RIGID"
1,1,; IREG-NUMBER OF BOUNDARY SEGMENT,IRG-NUMBER OF RIGID WALL
UNIEND 1
UNIVER ;, -NAME OF PROGRAM WHICH TREATS INPUT DATA
END
0., 0., 0.,;--USRT--,---VSTR---,VPOL
41, ;--NUMBER OF EOS
-0.25, 0., :: X0,Y0 - THE LOCATION OF THE FIRST POINT FOR THE BOUNDARY (CM)
STRAIGHT 1
0.,0., XE,YE,;: ARE COORDINATES OF THE END OF THE STRAIGHT SEGMENT (CM)
STRAIGHT 2
0.,4.1, XE,YE,;: ARE COORDINATES OF THE END OF THE STRAIGHT SEGMENT (CM)
TABLE 3
0.,4.1, XE,YE,;: ARE COORDINATES OF THE END OF THE STRAIGHT SEGMENT (CM)

```

-0.,4.1, XE,YE,:: ARE COORDINATES OF THE END OF THE STRAIGHT SEGMENT (CM)  
 -0.25,3.0, XE,YE,:: ARE COORDINATES OF THE END OF THE STRAIGHT SEGMENT (CM)  
 -0.25,3.0, XE,YE,:: ARE COORDINATES OF THE END OF THE STRAIGHT SEGMENT (CM).  
 -0.25,0., XE,YE,:: ARE COORDINATES OF THE END OF THE STRAIGHT SEGMENT (CM)  
 -0.25,0., XE,YE,:: ARE COORDINATES OF THE END OF THE STRAIGHT SEGMENT (CM)

END OF TABLE

REGEND

1---2---3---4 ANGLE LOCATION

1,2,3,,

BOUNDARY TYPE INPUT

RIGID ;;YOU WILL CHANGE "FREE" TYPE ON "RIGID"

1,1,; IREG-NUMBER OF BOUNDARY SEGMENT,IRG-NUMBER OF RIGID WALL

FRONT

3,1,; IREG-NUMBER OF BOUNDARY SEGMENT,IRG-NUMBER OF FRONT

UNIEND 2

ENDINPUT

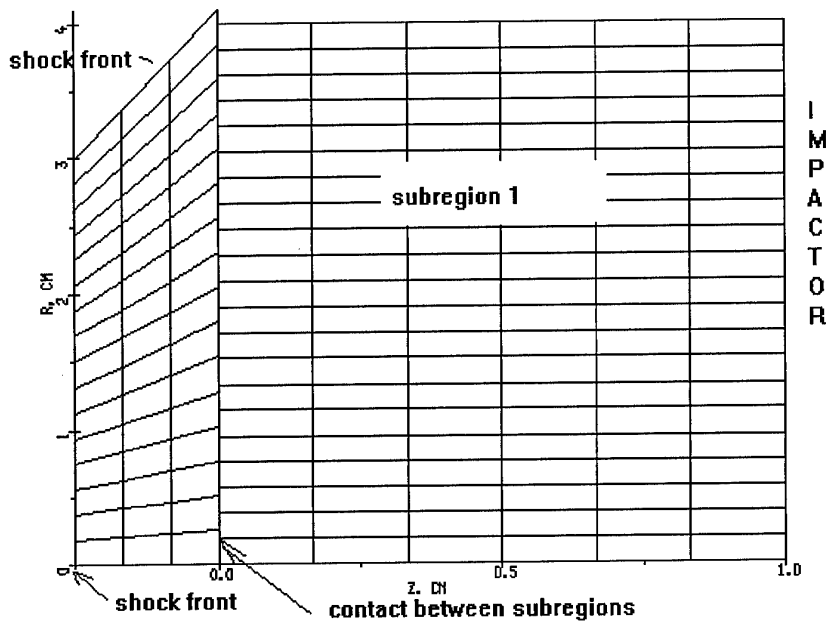


Fig.2 Initial configuration for initial data file VRB2.DAT



HEDRC REPORT  
contract SPC-93-4075

## 2D HIGH RESOLUTION SHOCK WAVE PHYSICS CODE

9-month technical report

*Second order modification of moving grid hydrocode*

Participants:  
Vorobiev O.Yu.  
Shutov A.V.  
Zharov A.V.  
Ni A.L.  
Fortov V.E.

## Introduction

One of the most important problems of numerical solution of nonlinear hyperbolic conservation equations is to obtain high accuracy of the solution in both discontinuous and continuous regions. In recent years, a lot of so-called high-resolution schemes have been proposed, for example, second-order TVD schemes of Roe [1,2] and Sweby [3]; upwind TVD of Harten [4] and Yee et al. [5]; symmetric TVD of Chakravarthy and Osher [6]; ENO scheme of Harten et al. [7,8], FCT scheme of Zalesak [9], McDonald and Ambrosiano [10]; MUSCL schemes of van Leer [11], Goodman and LeVeque [12], Davis [13], Colella [14], and PPM of Colella and Woodward [15]. The most of schemes mentioned above were originally derived for the case of perfect gas and for 1D geometry (or 2D for fixed Eulerian grids). For numerical simulations of hypervelocity impact problems, when realistic physical models are used, we face with additional problems. This is, for example, a variety of matter properties in different phase states (solid, liquid, gas, plasma), when the compressibility of matter differs up to several orders of magnitude. This difference often gives some unphysical values of variables appearing due to errors of numerical approximation (negative internal energy or density), which lead to a failing of numerical scheme. As it was found in [16], some of Godunov-type second-order methods based on approximate Riemann solvers are not positively conservative or positively conservative under certain conditions. They can produce non-physical states with negative density or internal energy in rarefaction waves. We based our code on the Godunov's method of numerical integration of Euler equations on a time-dependent (so-called moving) grid [17]. As it was shown in [16], this scheme is positively conservative for at least in the case of ideal gas EOS.

Let us remind the main principles of this code. In the framework of this approach only the boundaries of numerical grid are moved in Lagrangian fashion. The location of interior grid nodes are determined during grid generation procedure by using of coordinates of boundary nodes. As the material flows through the grid cells there is some diffusion error as well as in any Eulerian method. Nevertheless there exist several possibilities to reduce such errors by generating "near-Lagrangian" grids. In the present version of 2D hydrocode we utilize decomposition of numerical region onto subregions with Lagrangian boundaries, in which grids are generated independently using conformal mapping procedure. This decomposition is provided automatically during the computations. When every subregion consists of only

one cell. This approach resembles Lagrangian method on unstructured quadrilateral mesh. On the other side, such a grid enables all advantages of a regular grid. It is known that the numerical approximation of solution on an orthogonal grid is always better than that one on an arbitrary disturbed grid [17]. The grid generation procedure can be governed by moving the boundary nodes along the boundary. Using such a redistribution of the boundary nodes orthogonal grids are generated in subregions. The other advantage of orthogonal grids is a possibility to simplify a second order extension of Godunov's scheme.

In the present report we consider a second order extension of moving grid code and compare results of calculations of hypervelocity impact problems with shock-fitting calculations. The strategy of shock fitting grids was described in the previous report. Unfortunately, the application of this approach is not possible inside of numerical subregions. It means, that the description of shock wave propagation and interaction inside of disturbed subregion can not be done using shock fitting grids. That is the reason why the second order extension of Godunov's scheme is very important.

### 3. NUMERICAL ALGORITHM

In this report we describe algorithm of computations only briefly. More detailed description one can find, for example, in [18], as well as in the first report. As we have already mentioned, the numerical region is divided into several subregions with Lagrangian boundaries during the computations. Let us consider the main steps of computational algorithm for one subregion.

The first step of computations is the displacement of the boundary of subregion. After shifting the boundary to a new position some segments of the boundary can change their type due to interaction with boundaries of the other subregions. The boundary type determines the boundary condition (what is necessary for Riemann problem initial data) and the law of motion of the boundary. For example, a shock-front boundary moves according to Hugoniot's principle, rigid wall boundary does not move and so on.

The second step is an iterative procedure of orthogonal grid generation inside of subregion. This procedure is based on the distribution of the boundary nodes. This distribution is performed several times until the grid generated with conformal mapping becomes orthogonal.

The third step is a solution of Riemann problems for inner zones and calculation of fluxes between the neighboring zones. One should remark here,

that for an arbitrary equation of state the Riemann problem can be solved only numerically. Nevertheless, we employ an exact solver of this problem only in vicinity of flow discontinuity. The most of Riemann problem computations are done either in isentropic or in acoustic approximation.

Second order extension of Godunov's scheme can be obtained if we assume a piecewise linear distribution of flow parameters inside of the grid cells. To conserve the monotonicity property of Godunov's scheme we use the "minimum derivative principle" proposed in [19]. The main idea of this principle is to choose the minimum possible derivative when interpolating the values from the zone center to the boundary with the neighboring zone, where the Riemann problem must be solved. If the grid is orthogonal, derivatives only in one direction (either along the grid rows, or along the grid columns) are important when interpolating cell-centered values to the boundaries of the cells. This simplifies the realization of "minimum derivative principle".

#### 4.EXAMPLES OF CALCULATIONS

In the present paper we consider an application of our 2D code to hypervelocity impact problem. One of the most difficult task for any 2D Lagrangian code is to compute hypervelocity penetration of projectile into a thick target. We consider two different approaches to numerical simulation of hypervelocity impact of iron projectile moving with 10 km/s velocity on a thick aluminum target .

First one concludes in a usage of "near-Eulerian" grid, which covers the region of the target where the shock wave propagates.

The second one is fitting of this shock wave by moving the boundary of the grid with shock front velocities obtained by Riemann solver. The second method in fact, is more accurate to resolve the shock front and is more economic, because it does not require a grid in undisturbed regions. On the other hand the shape of numerical region is more complicated and, as a consequence of that, the grid generated is not so orthogonal as in the first case. The results of computations corresponding to these cases together with numerical grids are shown in Fig.1. There were two subregions used in the case of shock-fitting grid. One of them corresponded to the projectile, the other one covered the disturbed region in the target. In the other case (near-Eulerian grid) three subregions were used in computations.

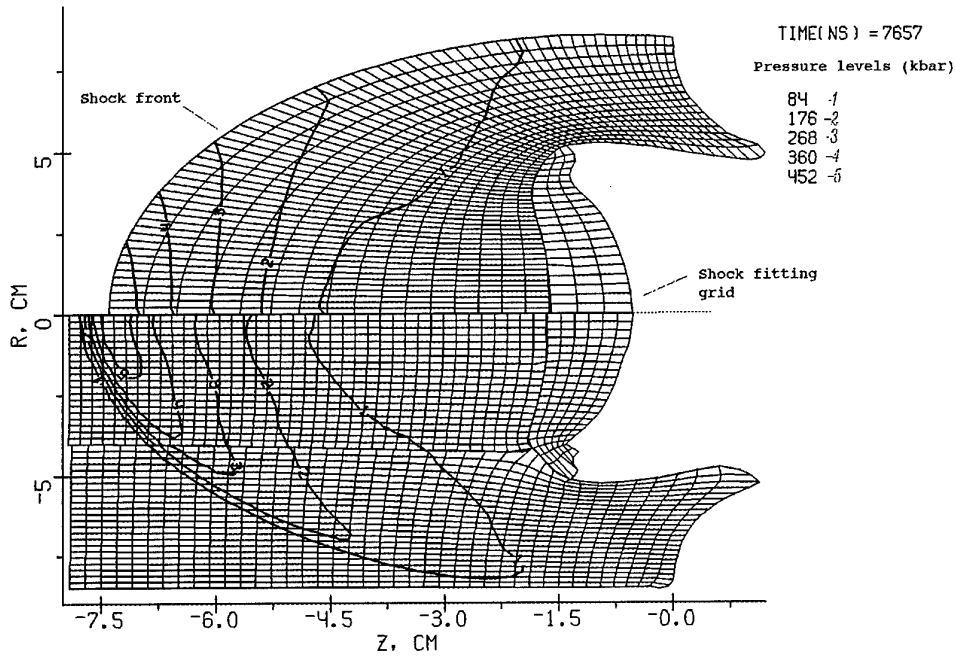


Fig.1 Numerical grid and pressure levels for hypervelocity impact calculations using shock fitting grid (above the axis) and "near-Eulerian" grid (below the axis).

It is known, that first order Godunov's scheme is a very dissipative one. Our experience shows, that this scheme smears out weak discontinuities in the case of realistic EOS much stronger than in the case of perfect gas. Moreover, this dissipation grows in time. Results of computation of hypervelocity impact of iron projectile on aluminum target shown in fig.2-3 confirms this fact. In contrast to the first order scheme, second order calculations exhibit nearly constant width of shock front smoothing.

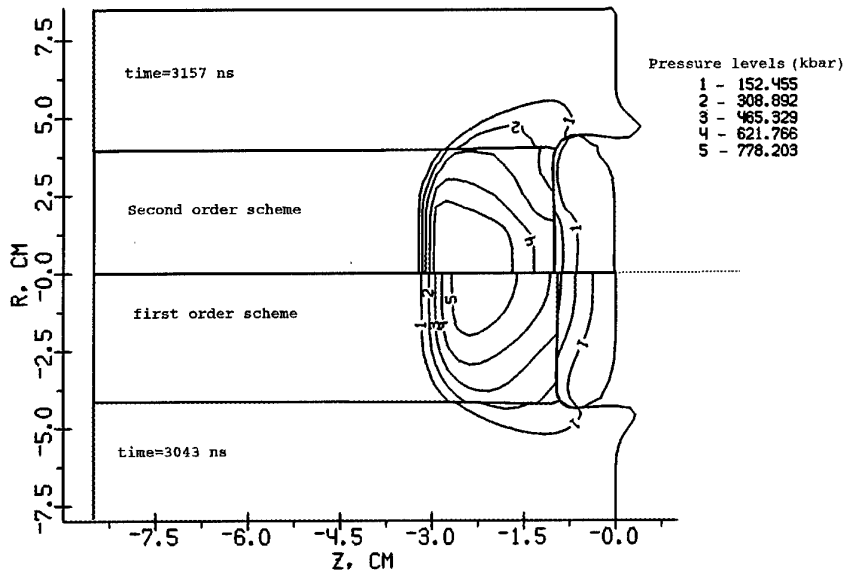


Fig.2 Grid boundaries and levels of constant pressure for the first (below the axis) and second order accuracy calculations of hypervelocity impact of iron projectile (on the right) on an aluminum target.

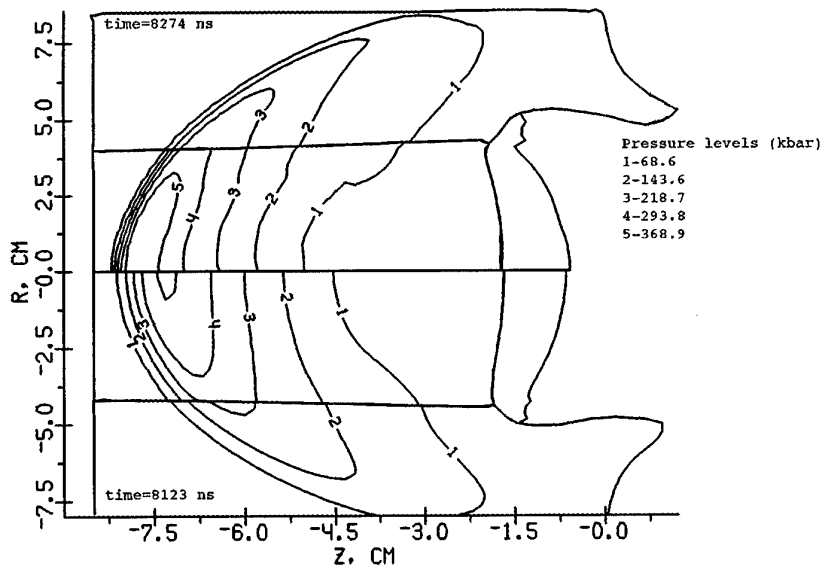


Fig.3 Grid boundaries and levels of constant pressure for the first (below the axis) and second order accuracy calculations of hypervelocity impact of iron projectile (on the right) on an aluminum target.

As it has been shown in [20] for the case of steady gas flow, the second order extension of Godunov's scheme is not so sensitive to distortions of numerical grid as its first order counterpart. We demonstrate below (Fig.4-5) the results of simulation of hypervelocity impact obtained using the first and the second order Godunov scheme both on the shock fitting grid and on the near-Eulerian grid. Our results generally confirm the conclusions obtained in [20]. For the second order scheme (Fig.5) the difference between the results obtained on the different grids is negligible, while for the first order scheme there is a big difference in the amplitude of the shock wave calculated on the shock fitting and on near-Eulerian grid. It is naturally, that the shock front dissipation is much pronounced in the case of the first order scheme than in the case of the second order one.

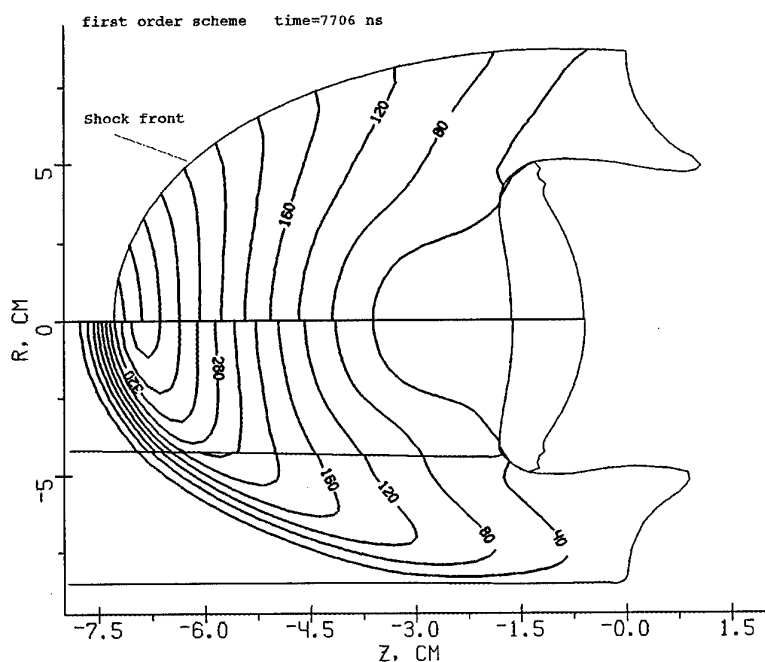


Fig.4 Grid boundaries and pressure levels (in kbars) for shock fitting grid and "near-Eulerian" grid. First order scheme.

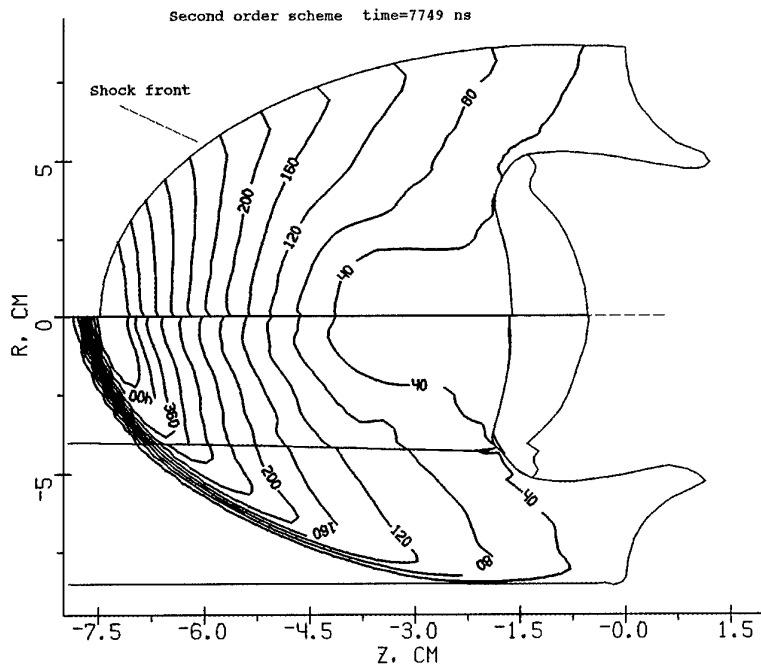


Fig.5 Grid boundaries and pressure levels (in kbars) for shock fitting grid and near-Eulerian grid. Second order scheme.

## CONCLUSIONS

We have considered an application of Godunov's scheme on the moving grids and its second order extension (Kolgan scheme) on the example of hypervelocity impact calculation. We have shown that this scheme coupled with the algorithm of decomposition of numerical region onto subregions shows a good robustness and flexibility for multimaterial problems of computational fluid dynamics with large distortions. The other advantage of decomposition of numerical region of complicated shape is a possibility to generate orthogonal grids in subregions

We have developed second order Godunov's scheme applying Kolgan's algorithm of "minimal derivative". It has been found that Kolgan's scheme is not so sensitive to the form of the moving grid as original Godunov's scheme. The results of second order calculations are much closer to more accurate shock-fitting calculations.

## REFERENCES

- [1] P.L. Roe, *Annu. Rev. Fluid Mech.* 337(1986)



- [2] P.L. Roe, Lectures in Appl. Math. Vol. 22 (Am. Math. Soc., providence, RI , 1985
- [3] P.K.Sweby, SIAM J. Num. Anal. 21,995(1984)
- [4] A. Harten, J.Comput. Phys.49,357(1983)
- [5] H.C.Yee, R.F.Warming, and A. Harten, J.Comput. Phys.57,327(1985)  
ICASE Report No 84-20,June 1984
- [6] S.R.Chakravarthy and S.Osher,"A New Class of High Accuracy TVD Schemes for Hyperbolic conservation Laws",AIAA-98-0363, 1985
- [7] A.Harten and S.Osher,SIAM J.Num.Anal.24,297(1987)
- [8] A.Harten, B.Engquist, S. Osher,S.R.Chakravarthy , "Uniformly High Order Accurate Essentially Non-Oscillatory Schemes", NASA CR-178101,1986
- [9] S.T.Zalesak, J.Comput. Phys.31,335(1979)
- [10] B.E.McDonald and J.Ambrosiano, J.Comput. Phys.56,448(1984)
- [11] B.van Leer, J.Comput. Phys.32,101(1979)
- [12] J.B.Goodman and R. LeVeque, SIAM J. Num. Anal. 25,268(1988)
- [13] S.F.Davis,SIAMM J.Sci.Stat.Comput.9.445(1988)
- [14]P.Colella,SIAMM J.Sci.Stat.Comput.6.104(1985)
- [15]P.Colella and P.R.Woodward,J.Comp.Phys.54,174(1984)
- [16]B.Einfeldt,C.D.Munz,P.L.Roe,B.Sjoegreen J.Compt.Phys.92,273(1991)
- [17] S.K.Godunov, Numerical solution of multi-dimensional problems of gas dynamics (in russian) (1976) Nauka, Moscow
- [18] O.Yu.Vorobiev, I.N.Lomov,A.V Shutov et al.,Godunov's Scheme on Moving Grids for High Velocity Impact Simulations, to be published in Proc. HVIS94, Santa Fe,NM
- [19] V.P.Kolgan, Scientific Notes of CAGI (in russian),3,68,(1972)
- [20] V.I.Koptchenov, A.V.Kraiko, Zh.Vych.Matem.i Matem Fiz. (in russian) 23,848 (1983)

HEDRC REPORT  
contract SPC-93-4075

2D HIGH RESOLUTION SHOCK WAVE PHYSICS CODE

3-month technical report

*Godunov's scheme on moving grids  
for high velocity impact simulation.*

Participants:

O. Yu Vorobiev

A. V. Shutov

A. V. Zharov

A. L. Ni

V. E. Fortov

## CONTENTS

I. Introduction.....	
II. Physical model.....	
III. Algorithm of computations.....	
1. Scheme of integration on moving grid	
2. Movement of boundaries	
3. Boundary's type checking	
4. Node distribution along the boundary and grid generation	
5. Riemann problem solution and recalculation of flow parameters	
6. Conclusion remark	
IV. Demonstrative examples.....	
1. TEST № 1: impact of a plane aluminum plate onto a semiinfinite aluminum target	
2. TEST № 2: influence of the grid refinement on the results of numerical simulation of penetration problems	
3. Interaction of spherical projectile with two layered aluminum target	
4. Hypervelocity impact of iron projectile on a target with a conical hole	
V. REFERENCES.....	

## I. Introduction

Problems of hypervelocity impact attract attention of scientists during the last thirty years and occupy a significant part in scientific literature. The urgency of investigations of these problems follows from the practice. It concerns, for example, evaluation of effectiveness of spacecraft debris shields, analysis of asteroid impact events, problems of atomic power stations safety and so on. From the other side the possibility of numerical simulations of these phenomena becomes real owing to progress in theoretical and experimental high pressure high temperature physics. The success of numerical simulation of hypervelocity impact depends on two factors: physical model (including mechanical, kinetic, thermodynamic, etc. properties of matter) and numerical methods for integration of governing equations. The second part of the problem will be discussed below. As to the first one, the review of various substances models is given, for example, in [1, 2].

The most widespread numerical methods for hypervelocity impact (HVI) simulation are based on Lagrangian and particle techniques [3-7]. Huge experience has been stored up to now in this area. It becomes clear, that the main drawback of Lagrangian codes is the restriction on deformations of flow and that of for the PIC codes is the necessity of keeping of "superfluous" information about flow parameters in additional numerical grid cells into which substance can get. Of course, these difficulties are algorithmic and can be overcome by some additional measures. For example, a usual procedure for Lagrangian techniques is reinterpolation of flow parameters into a new grid, when the grid deformations become large [8]. As to Eulerian techniques, one can mention about tracking methods [9], that are used to increase the accuracy of calculations near matter-vacuum and contact boundaries and to restrict the domain of computations. Unfortunately Eulerian codes have one more disadvantage associated with mass dispersion problems, that makes it difficult to calculate debris cloud evolution. There are several ways to decrease this dispersion. For example in [10] both the projectile and the shield were proposed to have nonzero initial velocities moving towards each other to minimize

advection of materials between cells in the Eulerian mesh. In order to decrease dispersion in Eulerian computations high-order accurate advection schemes also were used [11, 12].

As both pure Lagrangian and Eulerian codes have their own drawbacks, it is naturally to develop arbitrary Lagrange-Euler (ALE) codes combining the advantages of these approaches. Following this idea, numerical simulation of penetration of a hypervelocity projectile through multi-plate shield was done [13] using two codes: one for computing of penetration stage (Eulerian) and another (Lagrangian) for debris cloud transport calculation. In recent years, some algorithms of computation of real matter dynamics (including elasto-plastic and damaged matter) developed previously only for Lagrangian frame have been extended to the Eulerian frame of reference [12, 14, 15]. This opens new possibilities for HVI simulations using more flexible ALE codes.

In the present work we used Godunov's scheme for computations [16]. Godunov's method in moving grids provides great possibilities and includes both Lagrangian and Eulerian approaches as partial cases. It should be marked that this scheme has been intensively explored for simulations of aerodynamics problems, where high accuracy of calculations is necessary.

In 1968 S.K.Godunov, A.V.Zabrodin and G.P.Prokopov [17] formulated a programmatic approach to numerical integration of nonsteady Euler equations on moving grids. During several years the authors of this report have been working on realization of this approach. Results of this activity are presented below. For simplicity the consideration is given for the Euler equations omitting of strength effects. Applications of this approach to the problems of high velocity impact illustrate possibilities of 2D code developed. As distinct from the most illustrations of possibilities of this method given in [17], the problems of hypervelocity impact are characterized by strong deformations of matter and wide range of matter state parameters: from initially shock-compressed or strongly heated condensed state to finally expanding gaseous or spalled substance. Large variations of density lead to an enormous increase of geometrical sizes of computed fields occupied by the substance. Contacts separating the substance from vacuum are

the physical boundaries of computational region. Therefore the choice of Lagrangian meshes seems to be a preferable strategy for simulations of this class of problems. Unfortunately Lagrangian meshes crash, when the deformations become large, because the cells deform, twist and finally get tangled. The first factor leads to great restrictions on calculation time step and the second makes further calculations impossible. As to the Eulerian grid the marked above uncertainty in computational region leads to the necessity of keeping additional grid cells and to corresponding increase of computational time. The other problem of Eulerian techniques is the problem of contacts between substances.

Methods based on the use of computational regions with moving boundaries and generation inside of these regions of grids connected only with the boundaries seems to unify the advantages of Eulerian and Lagrangian meshes allowing to overcome their drawbacks. In the most examples given below the emphasis is placed on demonstration of possibilities of application of moving grids for treating the flows with strong deformations. Thus, for example, simulations of impact problems presented in this report have been performed on moving grids with fitting all contacts between different media including the boundaries with vacuum. During the process of interaction the structure and configuration of boundaries change: segments of contacts can disappear, for example because of rebound, and new segments can originate due to involving of new bodies into the process of interaction. The flow region under consideration can be subdivided into several subregions. Boundaries of subregions can be both as original flow singularities (characteristics, boundary between substance and vacuum, the contact boundary between two substances, the axis (plane) of symmetry, the shock wave) and so moving in accordance with their physical nature. They can be also inserted for some computational reasons.

As it was mentioned above, the basic attention is paid to computational aspects of simulation. Nevertheless, the algorithm developed makes it possible using of different physical models in the frame of Godunov's scheme. It concerns, for example, the Riemann problem solver, designed for the case of arbitrary EOS.

## II. Physical model

### *Governing Equations*

One fluid one temperature hydrodynamic model is used in simulations. Governing Euler equations are written in the form of conservation laws of mass, momentum, energy and porous volume, what is necessary for Godunov's method. The conservative form of the motion equations allows to describe both as continuous and so discontinues flows.

$$\begin{aligned}\frac{\partial \rho}{\partial t} + \nabla \rho \mathbf{u} &= 0, \\ \frac{\partial \rho \mathbf{u}}{\partial t} + \nabla \rho \mathbf{u} \times \mathbf{u} &= -\nabla p(1-V_p), \\ \frac{\partial \rho h}{\partial t} + \nabla \rho \mathbf{u} h &= -\nabla p \mathbf{u}(1-V_p), \\ \frac{\partial \rho V_p}{\partial t} + \nabla \rho \mathbf{u} V_p &= \rho \phi.\end{aligned}\tag{2.1}$$

Here  $\rho$ - density,  $\mathbf{u}$ - mass velocity,  $h$ -total specific energy,  $p$ - pressure,  $V_p$ - porous volume per unit volume,  $\phi$ - porous growth rate. For  $\phi$  we use semiempirical spall damage kinetic built on the base of free surface motion registration [1]. Nevertheless this model of spall fracture is valid only for small (up to several percents) porosity. When the porosity of matter becomes greater then some value, the substance does not resist to expansion. In this case the volume occupied by the solid component does not change anymore and the porosity grows with the increase of specific volume of matter.

### *Equations of state*

Semiempirical wide-range equations of state (EOS) are used [18] to determine the pressure, the temperature and the sound velocity as functions of internal energy per unit mass  $\varepsilon$  and the density of solid component  $\rho_0$  connected with density  $\rho$  as  $\rho_0 = \rho / (1 - V_p)$ . These equations are built on the base of available Hugoniot data and provide for correct asymptotes in the cases of extremely high energies and small densities.

### III. Algorithm of computations

#### 1. Scheme of integration on the moving grid

Eqs.(2.1) are integrated on the moving grid by Godunov's procedure [19]. The scheme of the algorithm is shown in Fig.1. In comparison with the traditional one ([17]) this algorithm enables a possibility of the numerical region division into many subregions with independent grid generation in every subregion. An important problem which should be solved by that is interaction between the boundaries belonged to different subregions.

#### 2. Movement of boundaries

The first step of the algorithm is the displacement of subregion's boundaries. The boundary of each subregion is represented as a coordinate array of nodes. Any boundary between adjacent subregions represents a unification of nodes belonging to boundaries of these subregions. The coordinates of nodes are also stored in special arrays establishing the sequence of nodes. Nodes corresponding to the beginning and to the end of different segments of boundaries are also marked. It means that each boundary segment is represented as a sequence of points belonging to the boundaries of different subregions and that of special end-points of boundaries. The total number of nodes representing boundary exceeds, generally speaking, the number of cells being in contact from the side of adjacent subregions.

To determine velocity of a boundary rib, the Riemann problem with flow parameters from adjacent cells being in contact along every link is solved. In case the Riemann solver yields a negative pressure a rebound along the link is supposed to be happened. This fact is taken into account by inserting some new special boundary points in the array. In more complex physical model the coupling force can be prescribed to the contact and a rebound can be inserted when the tense strengths exceeds the value of this force.



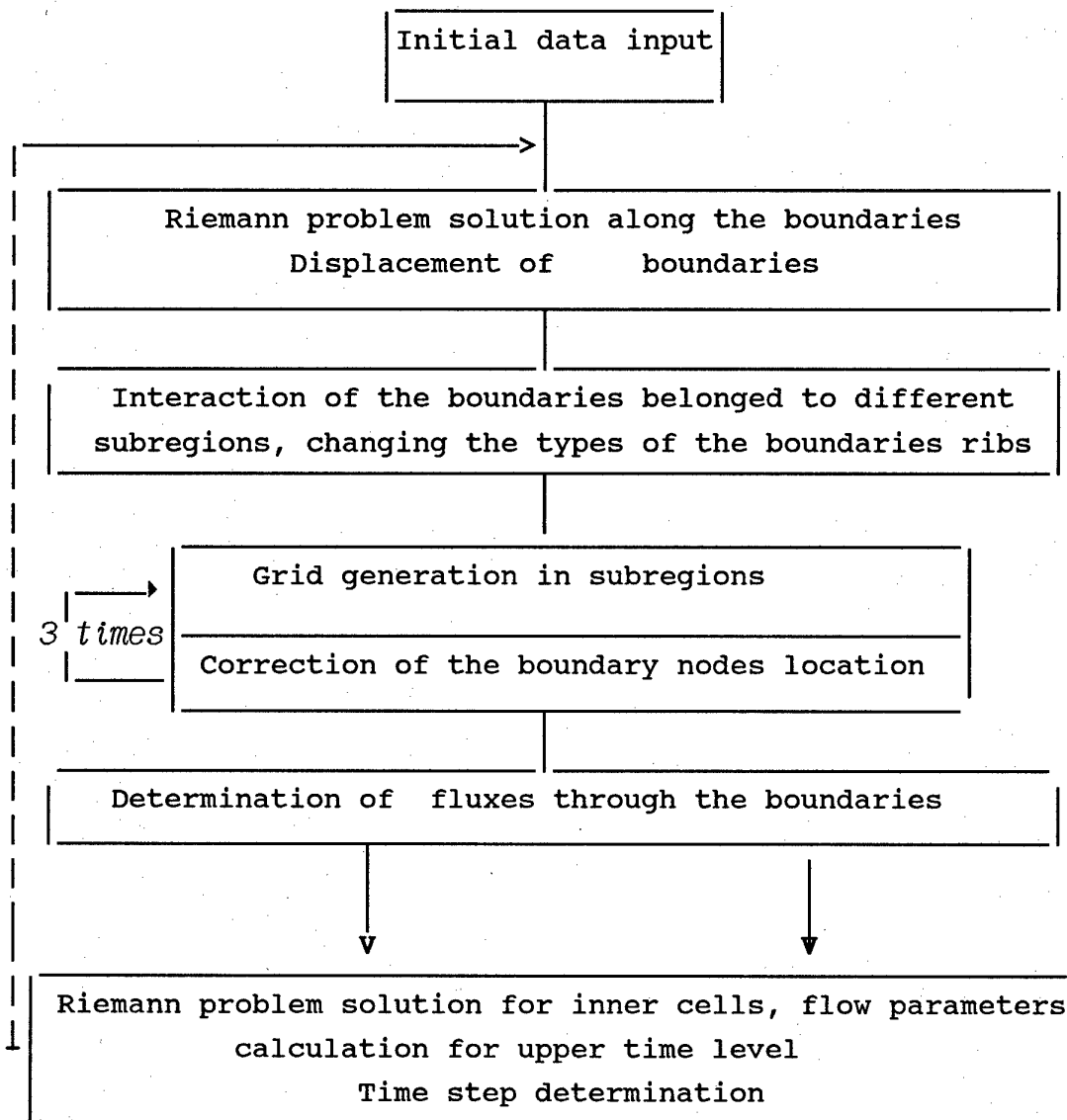


Fig.1 Block-scheme of the algorithm

The velocities of nodes can be calculated after solving of Riemann problem at the rib connecting the nodes. In the Godunov's method the flow parameters; velocity, density, energy are assumed to be uniform inside the meshes. For example, one should take flow parameters from the meshes A and B to calculate velocity  $U_1$  and so from the meshes A and C to calculate velocity  $U_2$ , see fig.2 There may be different ways of nodes velocities interpolation. The linear interpolation proposed by Godunov [17] gives the formula

$$u = \frac{u_1 l_2 + u_2 l_1}{l_1 + l_2} \quad (3.1)$$

How it's seen from (3.1) the shorter the rib is, the more contribution gives it in the node velocity. (For example, if  $l_1 \gg l_2$  then  $u \cong u_2$ ). From another point of view, if we want to minimize the middle-square deviation between the boundary displacement obtained from the Riemann problem solution, when every rib moves with an appropriate "big" velocity, and the boundary displacement determined by the nodes movement one should use the following formula (how it has been shown in [20])

$$u^* = \frac{u_1 l_1 + u_2 l_2}{l_1 + l_2} \quad (3.2)$$

In present algorithm we use an average way of interpolation between (3.1) and (3.2), which leads to a simple formula

$$u = 0.5 * (u + u^*) = 0.5 * (u_1 + u_2) \quad (3.3)$$

The formula (3.3) combines the advantage of (3.1) with simplicity.

In this version of moving grid code a procedure of boundary node location correction is proposed, which allows to generate orthogonal grids in subregions. For this purpose, boundary nodes are displaced along the boundary at any time step to ensure orthogonality between the boundary and correspondent inner grid line. Nodes shift is limited by settled maximum ratio between adjacent the node rib's lengths. In our calculations the maximum ratio was 1.1. In order to not distort the shape of numerical region during nodes distribution the node is shifted along smooth curve line which approximate the boundary. The curvature of the line is changed from node to node using line interpolation formula for curvature radius. After nodes displacement new grid is generated in subregions.

Grid generation algorithm is based on a univalent mapping of a rectangular region at a parametric plane  $(\xi, \eta)$  onto a subregion under consideration at physical plane  $(x, y)$  of flow. The problem can be formulated mathematically in a following way. The flow region at plane  $(x, y)$  is considered to be a curvilinear quadrangle with tops A, B, C, D (fig.3). The univalent mapping of this quadrangle onto the rectangular  $A', B', C', D'$  is determined by solution of a system of elliptical equations

$$\xi_{xx} + \xi_{yy} = 0 \quad \eta_{xx} + \eta_{yy} = 0 \quad (3.4)$$

It can be easily proved that this mapping is univalent, for example considering the principle of maximum of harmonic function. In reality, to solve the system of equations relative to  $x, y$  as independent variable parameters is more convenient

$$\begin{aligned} a x_{\xi\xi} - 2b x_{\xi\eta} + g x_{\eta\eta} &= 0 & (3.5) \\ a y_{\xi\xi} - 2b y_{\xi\eta} + g y_{\eta\eta} &= 0 \\ a = x_{\eta}^2 + y_{\eta}^2 & \quad b = x_{\xi}x_{\eta} + y_{\xi}y_{\eta} & \quad g = x_{\xi}^2 + y_{\xi}^2 \end{aligned}$$

using the following boundary conditions:

$$\begin{array}{lll} x(\xi) = x(\xi, \eta_1) & y(\xi) = y(\xi, \eta_1) & \text{at AB (3.6)} \\ x(\eta) = x(\xi_d, \eta) & y(\eta) = y(\xi_d, \eta) & \text{at BC} \\ x(\xi) = x(\xi, \eta_r) & y(\xi) = y(\xi, \eta_r) & \text{at CD} \\ x(\eta) = x(\xi_u, \eta) & y(\eta) = y(\xi_u, \eta) & \text{at DA} \end{array}$$

where

$$\xi_d \leq \xi \leq \xi_u \quad \eta_l \leq \eta \leq \eta_r$$

The transition to discrete analog of boundary conditions for this system of quasilinear elliptical equations can be performed easily. If the the grid nodes are given

$$\xi_i = i \quad i=1, \dots, n \quad (3.7)$$

$$\eta_j = j \quad j=1, \dots, m$$

then the boundary conditions are (3.8)

$$x(1) = x(1,1) \quad y(1) = y(1,1) \quad \text{at AB}$$

$$x(j) = x(1,j) \quad y(j) = y(1,j) \quad \text{at BC}$$

$$x(1) = x(1,m) \quad y(1) = y(1,m) \quad \text{at CD}$$

$$x(j) = x(n,j) \quad y(j) = y(n,j) \quad \text{at DA}$$

Different algorithms have been proposed in [17] for solving this problem. Iterations considered to be the most efficient algorithm. We modified this algorithm treating solution of corresponding equations as a result of relaxation of solutions of nonsteady equations. For this purpose "non-steady" terms  $dx/dt$  and  $dy/dt$  are inserted into the right sides of equations for  $x$  and  $y$  correspondingly [21]. The resulted parabolic system is solved by the method of variable directions. At the first half time step terms containing derivatives over  $h$  are considered to be given. At the second half time step derivatives over  $x$  are taken from calculations at the first stage. The problem at the each stage is similar to the one-dimensional heat transport problem. This consideration is similar to iterations, but as any relaxation method it provides more possibilities for the choice of "time-step" or, what is the same, of relaxation parameter. In particular, it can be changed from one grid node to another to accelerate the convergence of the method. The proposed algorithm has demonstrated its reliability. Nevertheless it fails for boundaries of a complex configurations. In order to overcome problems associated with a grid generation the algorithm foresees the possibility of subdividing the flow region into subregions with reasonably regular boundaries.

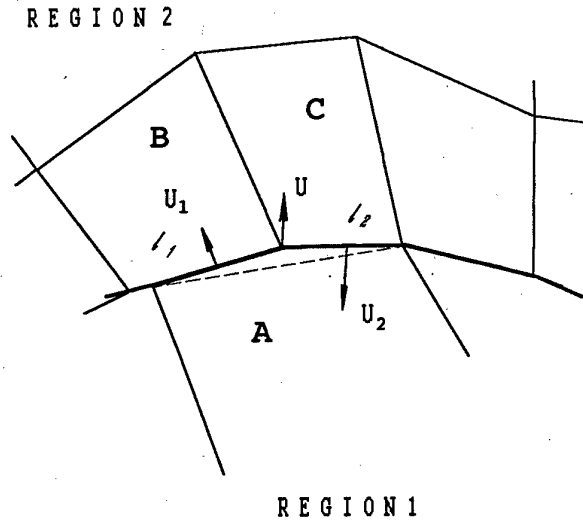


Fig.2 Boundary between the different subregions (solid line)  $U_1, U_2$  - "big" velocities obtained from the Riemann problem solution between the meshes A (region 1) and B (region 2) and so A and C,  $l_1, l_2$  - the lengths of the ribs

### 3. Boundary's type checking

Using of moving grid makes it much more easier setting of boundary condition in comparison with Elerian grid. In accordance with the boundary condition some type of boundary has been assigned to every rib belonged to the boundary. There are five boundary types that have been considered: "free boundary" (boundary with vacuum), "contact" (boundary with another matter), "axes" (axes of symmetry), "hard wall" and so called "special boundary" through which a matter can flow. It's clear, that the type of the boundary can be changed from one time step to another. Therefore a procedure checking the boundary type at each time step has been developed.

#### 4. Nodes distribution along the boundary and grid generation technique

Experience of the numerical simulation on the moving grid shows that some procedure of the nodes distribution along the boundary is required to generate a good grid inside of the region. Interpolation of the boundary plays an important role for displacement of nodes along the boundary. How it has been noticed [19], the sharp angles of the boundary are smoothed from one time step to another, when the nodes move along the straight lines connecting them. To prevent this smoothing on the boundary, we approximate it by arcs linking the boundary nodes.

In the case of strong deformations of numerical region the law of nodes distribution along the boundary influences in a great power on the grid generated inside the region. Previously [20] the law of the nodes distribution along the boundary was chosen anytime in accordance with the specifics of the problem to be solved. Such a way required at least several attempts to find the appropriate law of nodes distribution for problem considered.

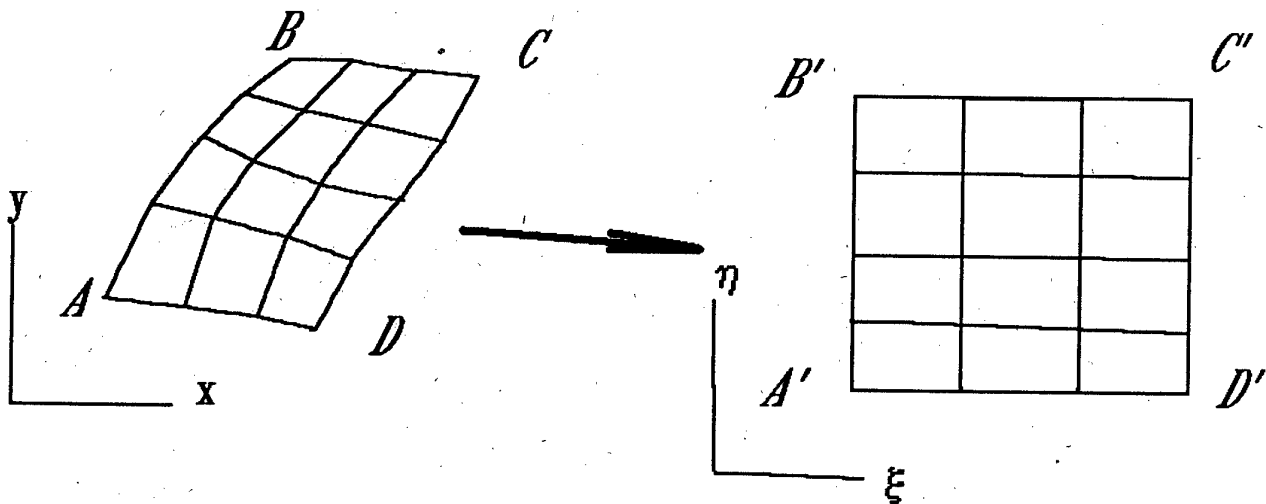


Fig.3 The scheme of the grid mapping

5. Riemann problem solution and flow parameters  
recalculation for next time level

The basic point of numerical integration of governing equations is the Riemann problem, which is not self similar if any kinetics phenomena is considered (for example, stress relaxation or microporous growth). In the model used the porous growth is also included into consideration. Therefore we take it to be "frozen" when the time of the fracture kinetics  $t_k$  is much more than the time step  $\Delta t$  and on the contrary. Hugoniot adiabates and isoentrops for solid matter are taken for solving Riemann problem in the first case and those for porous matter are used in the second case. This approach has been previously used [22] in calculations of visco-elastic flows by Godunovs method.

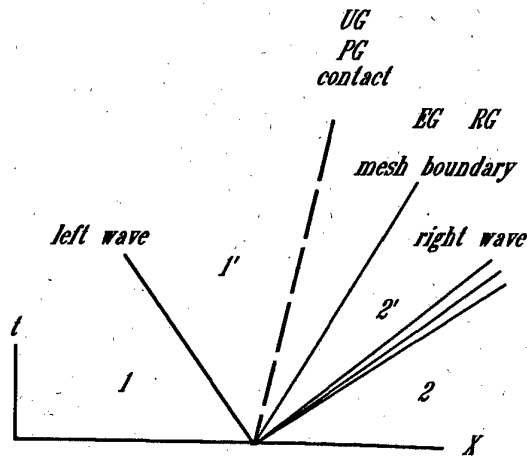


Fig.4 Discontinuity decay: 1 and 2 designate undisturbed regions, 1' and 2' - regions behind the waves, dashed line - contact discontinuity

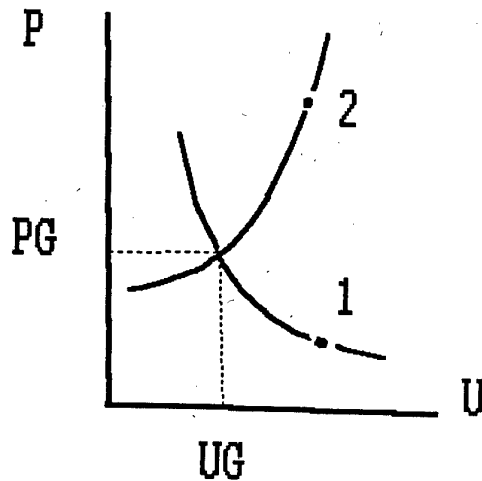


Fig.5 U-P plane. Points 1 and 2 designate initial flow parameters from the left and from the right side of the rib.  $U$  means the normal to rib velocity.

Unlike the perfect gas, in the case of an arbitrary EOS the Riemann problem can't be solved exactly by iteration scheme without numerous EOS evaluations. One should mention here about some approximate Riemann solvers [23,24] that can be useful also for the problems considered. Initial flow discontinuity decays into the contact discontinuity, the left wave and the right wave, those may be the shock wave or rarefaction wave depending on the initial parameters (see Fig.4). The mass velocities and the pressures behind the right wave (2-2') are equal those behind the left wave (1-1'). These so called "big parameters" ( $PG$  and  $UG$ ) can be determined as intersection of left and right wave velocities functions in  $U$ - $P$  plane (Fig.5 ).

Densities and energies in the regions 1' and 2' can be calculated if velocity  $UG$  and pressure  $PG$  are known. Velocity functions  $FL$  and  $FR$  are built using a real equation of state. To build the simple wave velocity function (2'-2) sound velocity as a function of pressure and density is sufficient. In the case of the shock wave (1-1') the energy as a function of pressure and density is necessary. In order to calculate the fluxes of mass, energy, porous volume and momentum the rib velocity has to be



known. Then, the fluxes can be determined choosing the flow parameter from the region where the rib velocity is located (region 2' in the case shown in Fig.4 ). The velocity of the rib  $v$  can be determined if the locations of the rib at the neighboring time levels are known (see Fig.6). Generally speaking, the surface covered by the rib during it's movement is not the plane. For simplicity we replace it by the plane following the way proposed by Godunov [17]. In accordance with this method the normal component of the rib velocity is calculated as

$$V = \frac{\Delta_{abb'a'}}{L_{ab}^{t+\Delta t/2}} \quad (3.9)$$

Here  $\Delta$  - is the area covered by the rib  $ab$  during the time step  $\Delta t$  in the plane  $XY$ ,  $L_{ab}$  - the length of the rib at the time  $t+\Delta t/2$ .

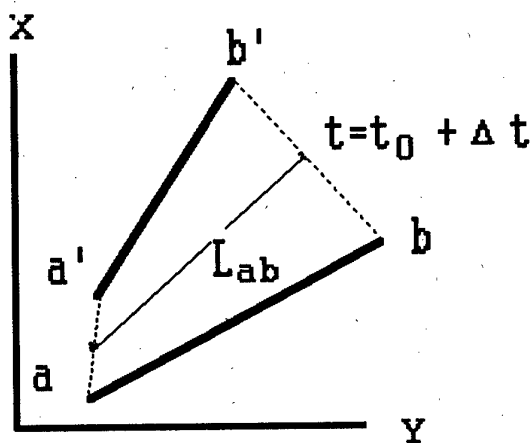


Fig.6 Determination of rib velocity

## 6. Conclusion remark

Naturally the description of the algorithm given above is at least schematic and except of some modifications and details represents only the interpretation of ideas [17]. However we considered the program approach as being already given and the main problem is to put it into practice for specific problems of physics. On this way one can face with a lot of concrete problems of various extent of complexity: mathematical, physical, algorithmic. One of the most important points is an experience of working with given complex of program. We are sure that the difficulties connected with realization of the approach will be rewarded by its huge possibilities. The method allows at least in principle to fit flow singularities : shocks , contacts, characteristics. From this point of view the method unifies main advantages of characteristics methods with the advantages of uniform computational schemes. A promising future we see in integration of this method with analytical methods of gas dynamics. This method provides a possibility to determine dependence and influence domains and to perform calculations at this minimal domains area. From this point of view it can be called economic.

Last years are being marked by the intense activity in developing of high order accuracy modifications of Godunov's methods. Review of these methods can be found for example in [25]. These modifications as a rule can easily be included into the body of the original Godunov's algorithm. Modifications concern the Riemann problem procedure and formulae for recalculation of flow parameters for the new time step. Development of high order resolution schemes in moving grids fitting flow singularities is of great importance [26]. They will be considered more detailly in the next report.

#### IV. Demonstrative examples.

##### 1. TEST № 1: *impact of a plane aluminum plate onto a semiinfinite aluminum target*

The simplest test problem for 2D code is an impact of a plane projectile on a semiinfinite target. In this case the problem becomes to be one-dimensional and if Hugoniot adiabates of materials are known the pressure and the shock velocity can be easily calculated. The time when rarefaction wave from the back side of the projectile reaches the shock front can be also determined. Results of a plane aluminum- on- aluminum impact with 8 km/s velocity are shown in Fig. 7-8. Region of computations consists of two subregions corresponding to the target and the impactor. Left boundary of the target moves initially with a characteristic velocity (sound speed) inside aluminum target. Then shock from contact reaches this boundary and it becomes moving as shock discontinuity (see fig. 8). This transition from sound to shock regime of boundary movement is automatic because the velocity of the boundary is obtain from Riemann problem solution algorithm. As it can be easily proved, numerical result is agreed well with the analytical calculation of the shock pressure and velocity.

##### 2. TEST № 2: *influence of the grid refinement on the results of numerical simulation of penetration problems*

Calculation with different levels of accuracy were performed for aluminum sphere of 1 cm diameter penetrating aluminum plate of 2 mm thickness at 10.1 km/s. Numerical grids and levels of constant pressure corresponding the time moment of 710 ns are shown in fig.9-11. In the case presented in fig.11 accuracy was two times more than that in the fig.10 and four times more than in the fig.9. It is seen that the higher the accuracy, the better is shock front resolution in the projectile. More fine grid allows also to resolve the low density vaporized matter blowing off the target during impact. At the following stage of penetration shown in fig.12-13 fine

grid gives less thickness of the target's substance surrounded debris of the projectile. And of course as a consequence of higher pressure there is a higher expansion velocity of debris cloud in this case.

### *3. Interaction of spherical projectile with two layered aluminum target*

Result of computation of spherical aluminum projectile interaction with a spaced two layered aluminum target is presented in fig.14. Impact velocity for the problem considered is 8 km/s. One should note that not more than 1000 meshes is used in this computation. The number of meshes grows during computation to ensure some fixed level of accuracy. Criteria for grid refinement is not pure geometric. When pressure gradient and density of matter decrease some coalescence of meshes takes place.

Using moving grids demonstrates a substantial economy of reserved computer memory in comparison with a fixed eulerian grid. One can calculate that about 30 000 - 40 000 meshes is required to perform computation of this problem using eulerian grid with the same accuracy.

### *4. Hypervelocity impact of iron projectile on a target with a conical hole*

This example demonstrates possibilities of moving grid adaptations to region's form in the case of strong deformations. In the beginning of interaction shock pressure of about 0.5 Mbar is generated in PMMA disk, while pressures in iron target reach about 2 Mbar. Then two jets of liquid PMMA are formed moving along the walls of conical channel (fig. 16). Collision of the jets on the axis leads to cumulation effect. Pressure behind the projectile reaches to 2 Mbar (fig.17). After impacting with the iron projectile these jets breach between the projectile and the walls of the channel accelerating projectile (fig.18).

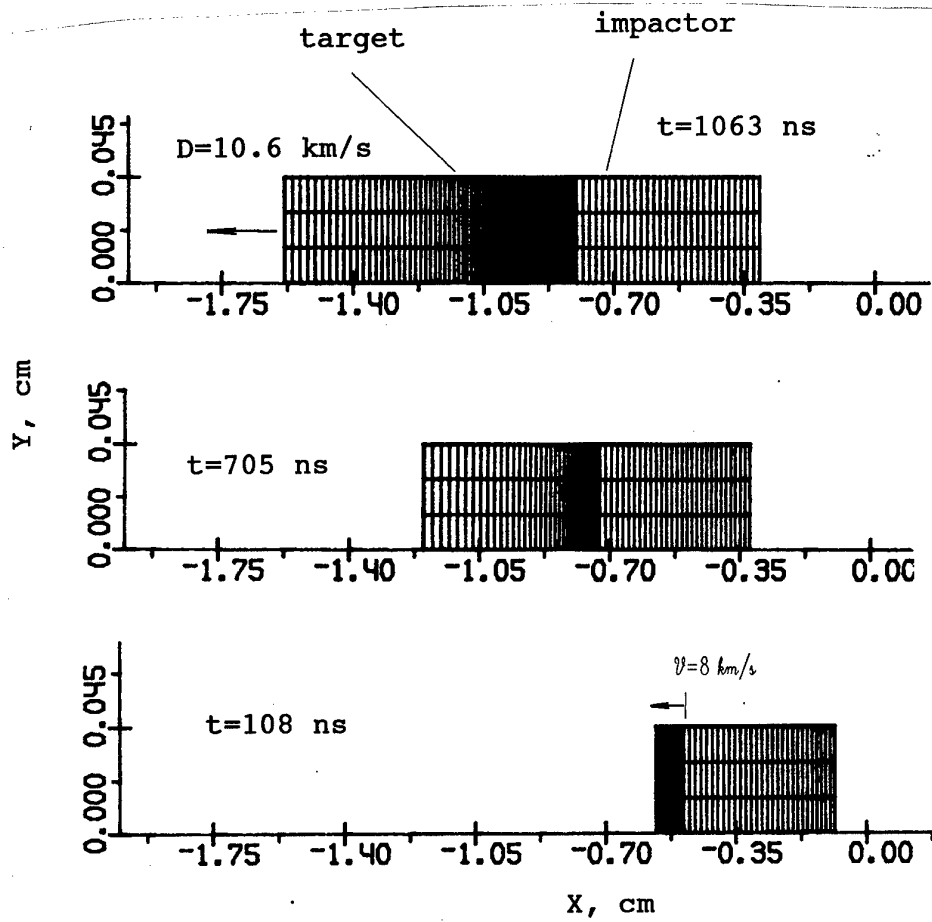


Fig.7 Numerical grid at different time moments

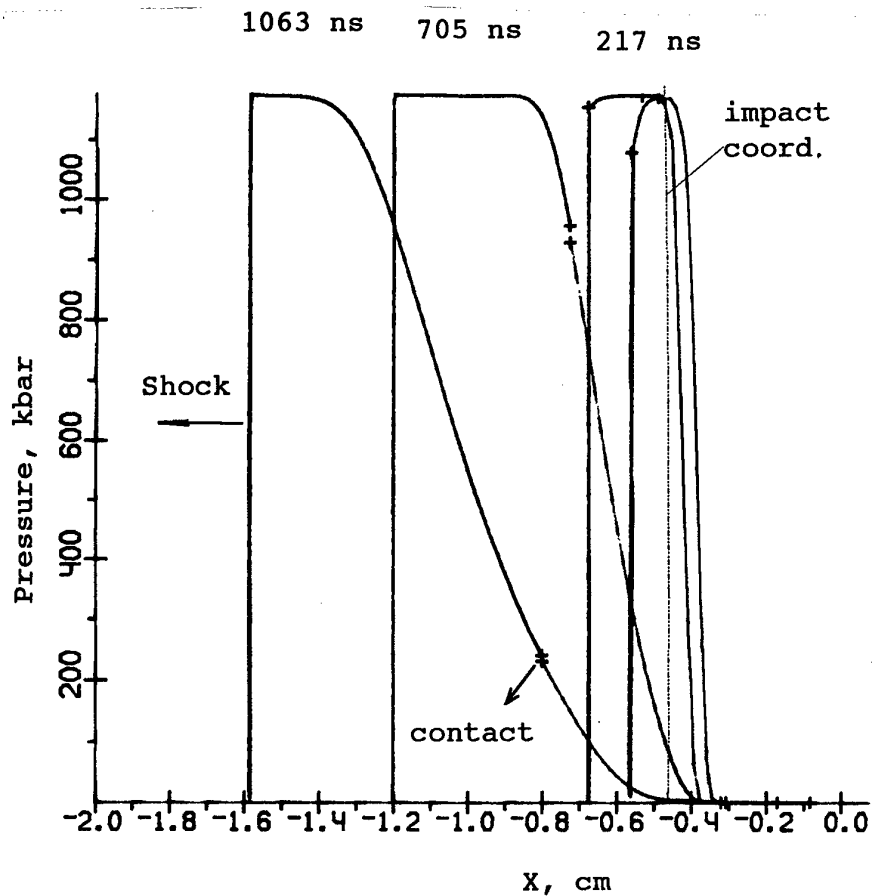


Fig.8 Pressure profiles at different time moments

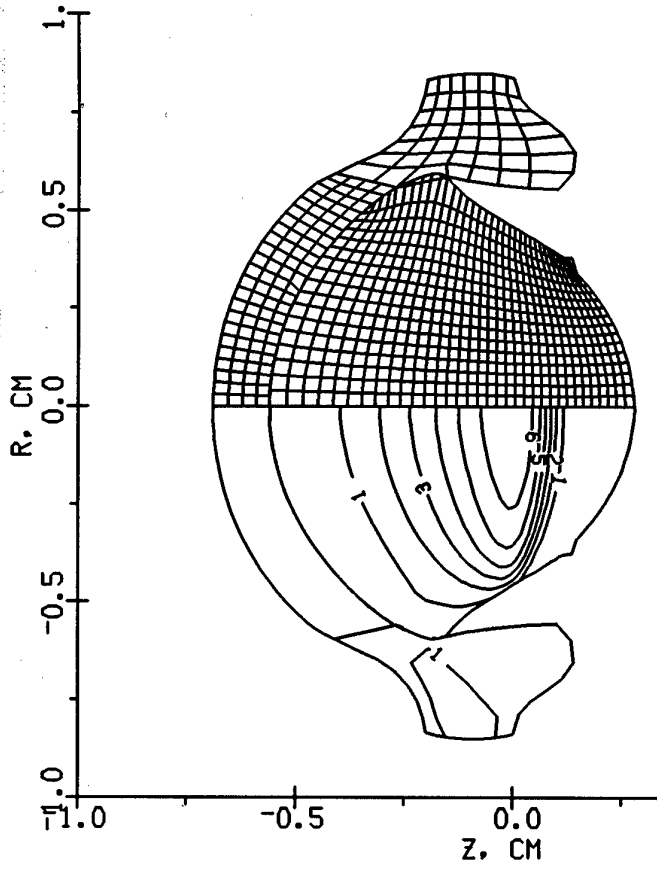


Fig.9 Grid and pressure levels.  
 1- 100 kbar, 2- 200 kbar ...  
 Time: 710 ns

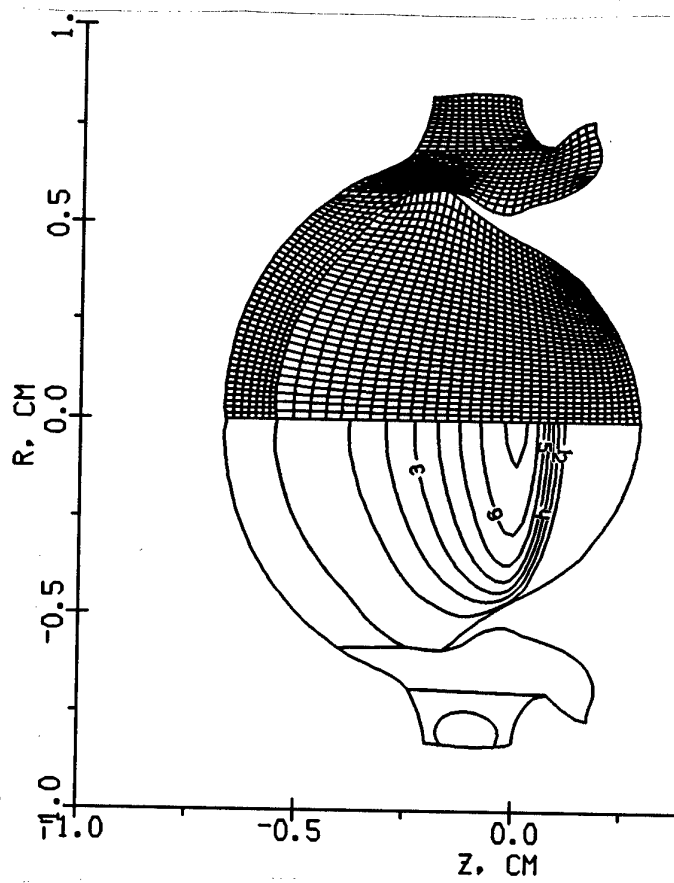


Fig.10 Grid and pressure levels  
 1-100 kbar, 2-200 kbar...

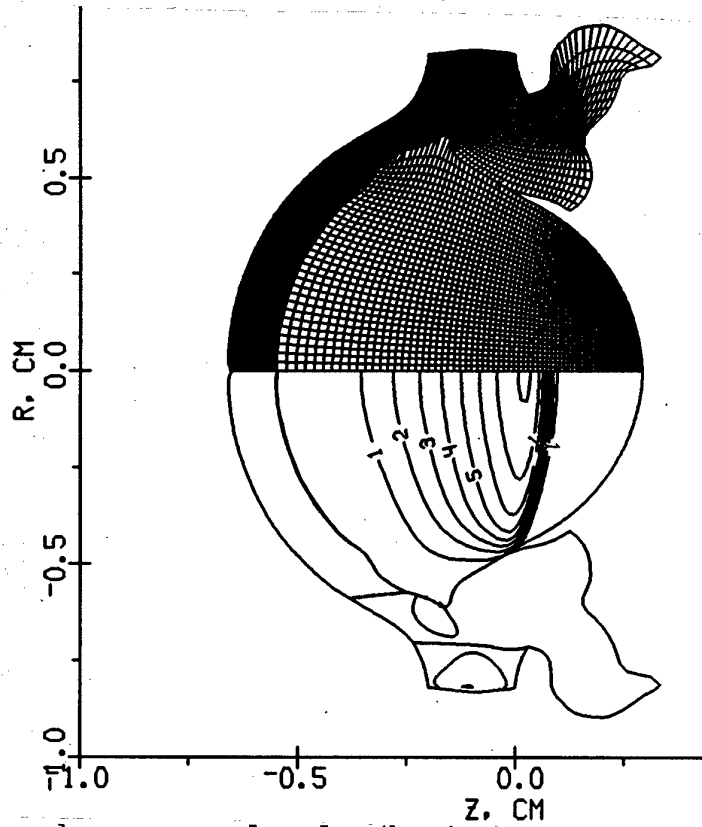


Fig.11 Grid and pressure levels (best accuracy)  
 step 100 kbar, time: 710 ns

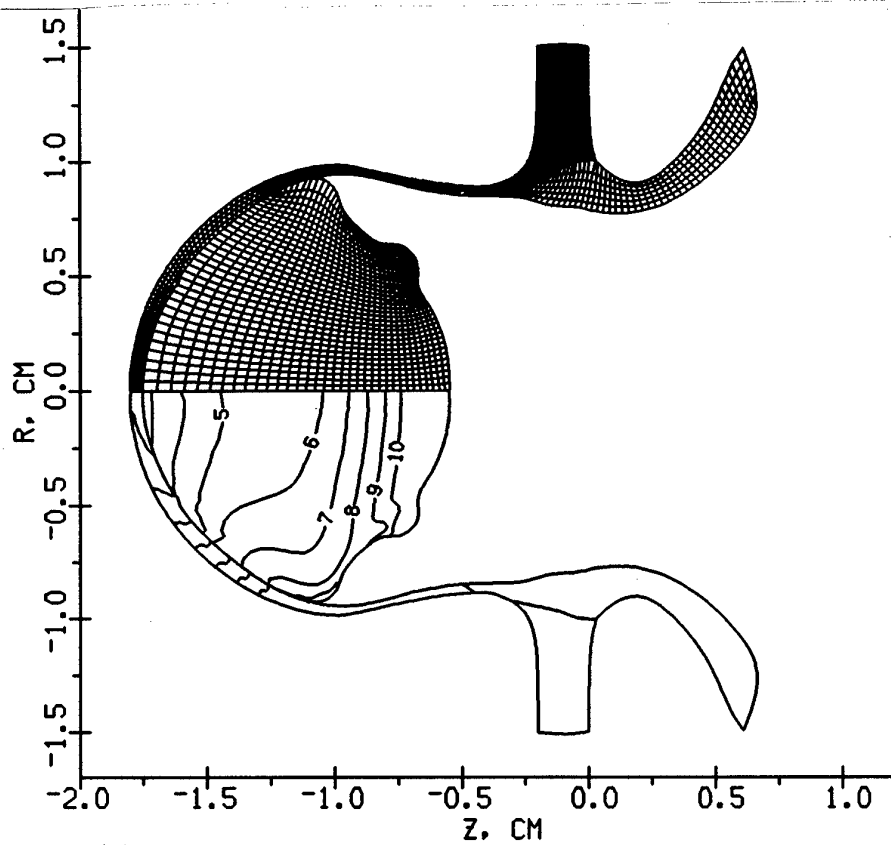


Fig.12 Grid and velocity levels:1-10.6, 2-10.3, 3-9.9, 4-9.6,  
5-9.2, 6-8.8,7-8.5, 8-8.1, 9-7.7, 10-7.4 km/s  
Time: 1900 ns

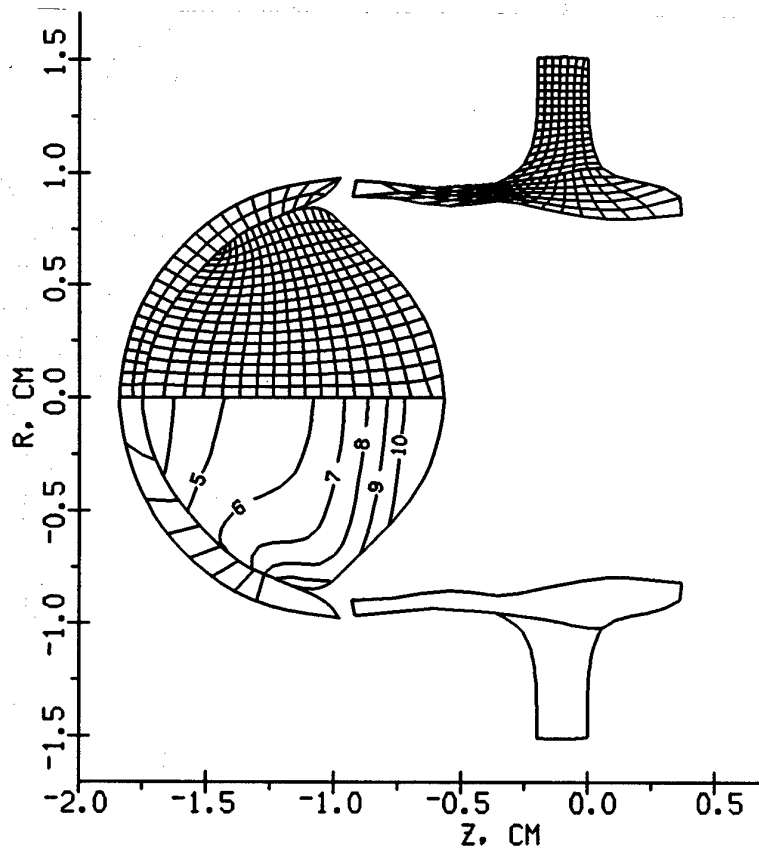


Fig.13 Grid and velocity levels (the same as for fig.12)  
Time: 1900 ns

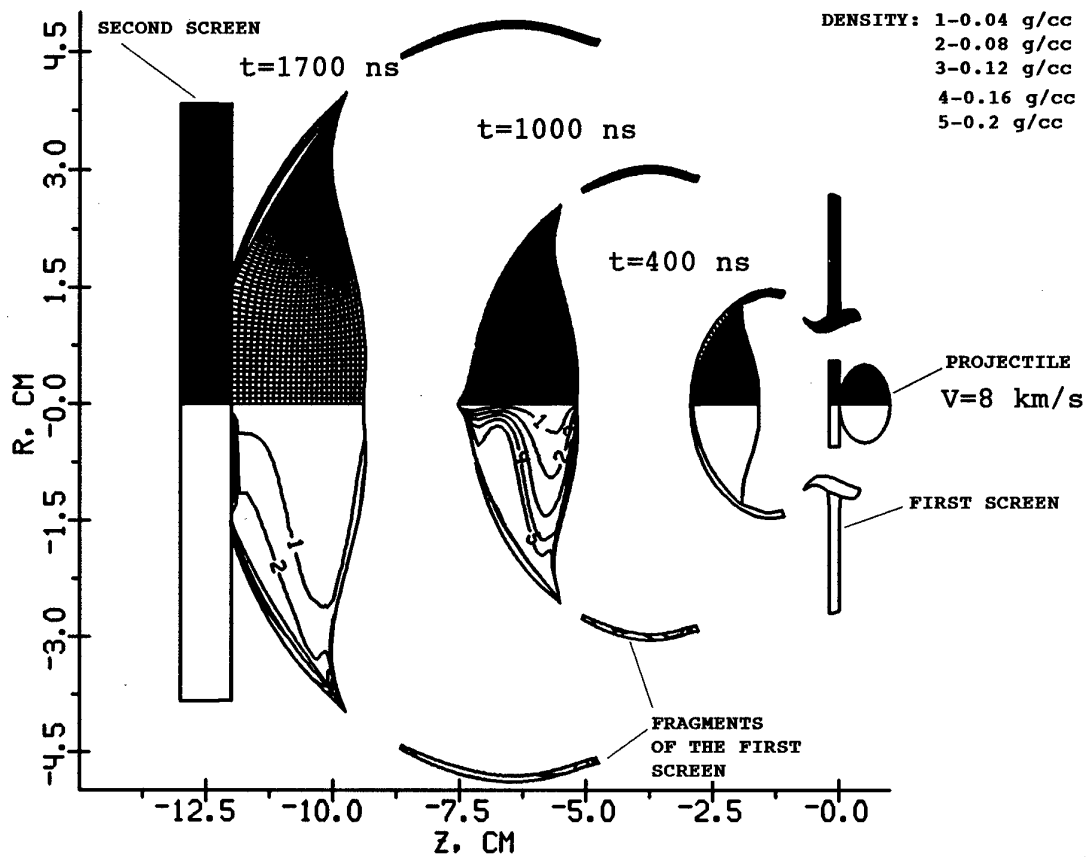


Fig.14 Grids and density levels at different time moments.



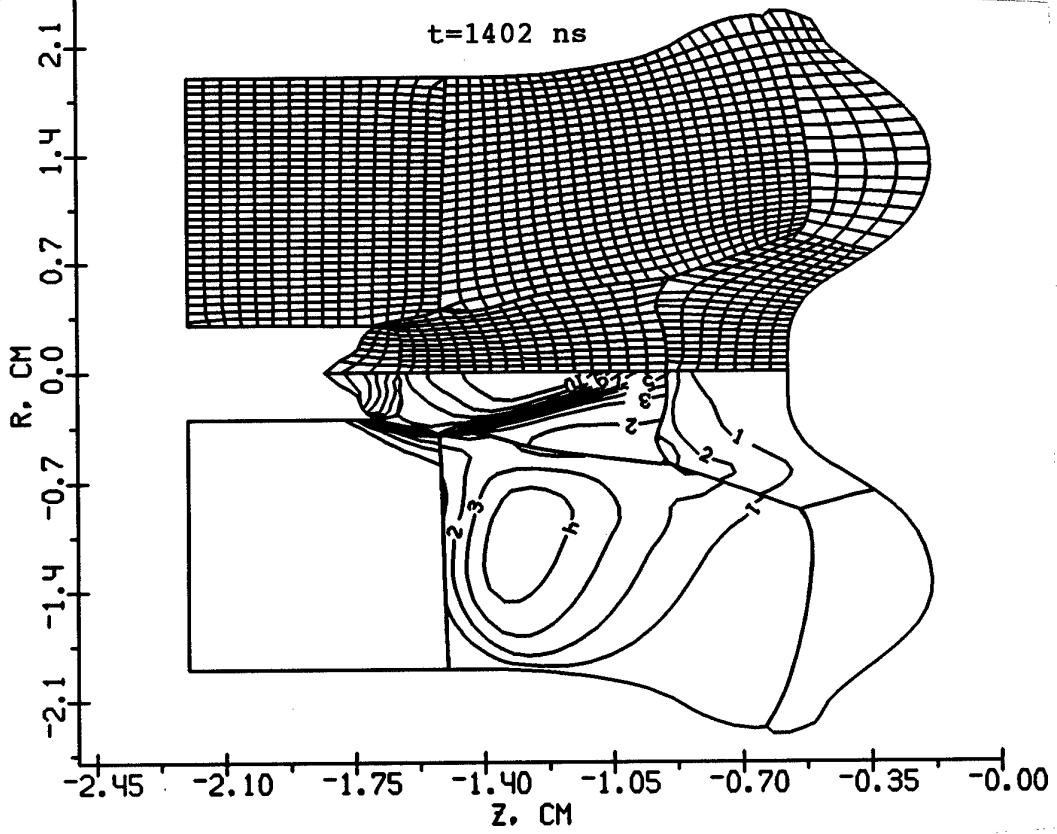


Fig.17 Grid and pressure levels

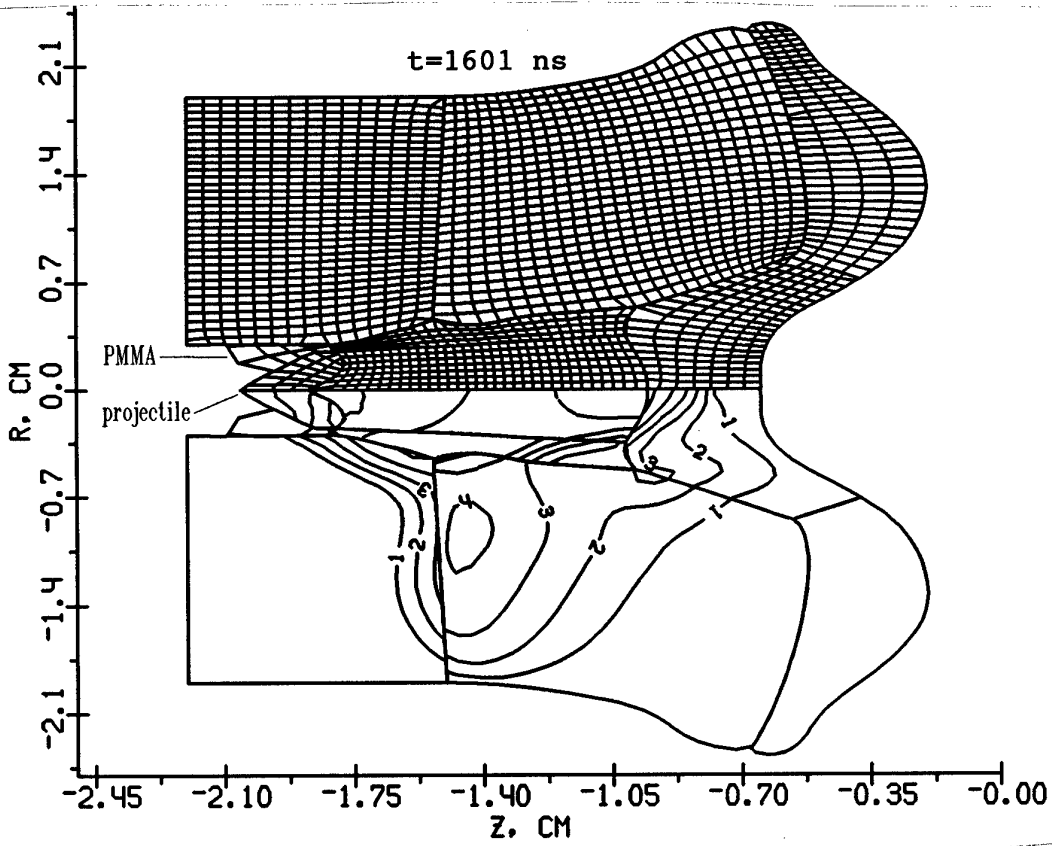


Fig.18 Grid and pressure levels

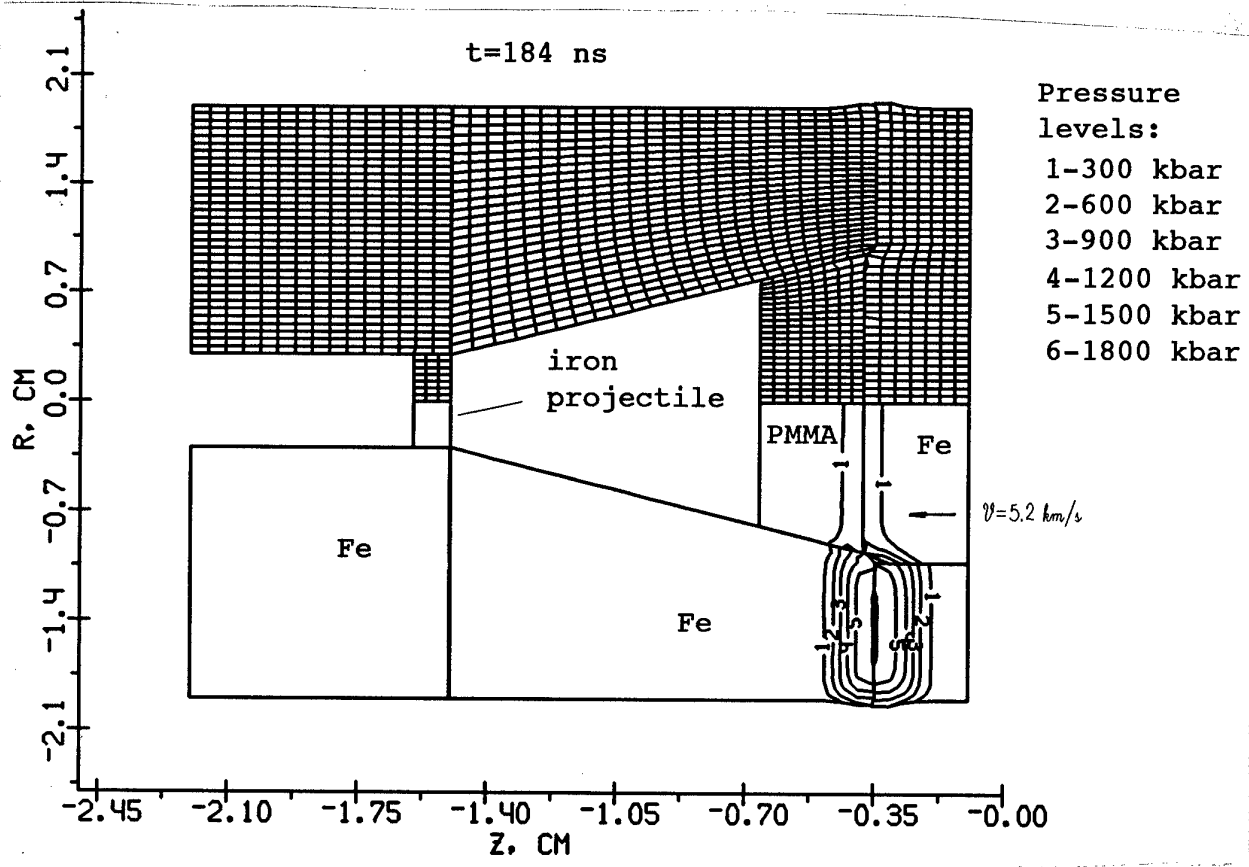


Fig.15 Grid and pressure levels

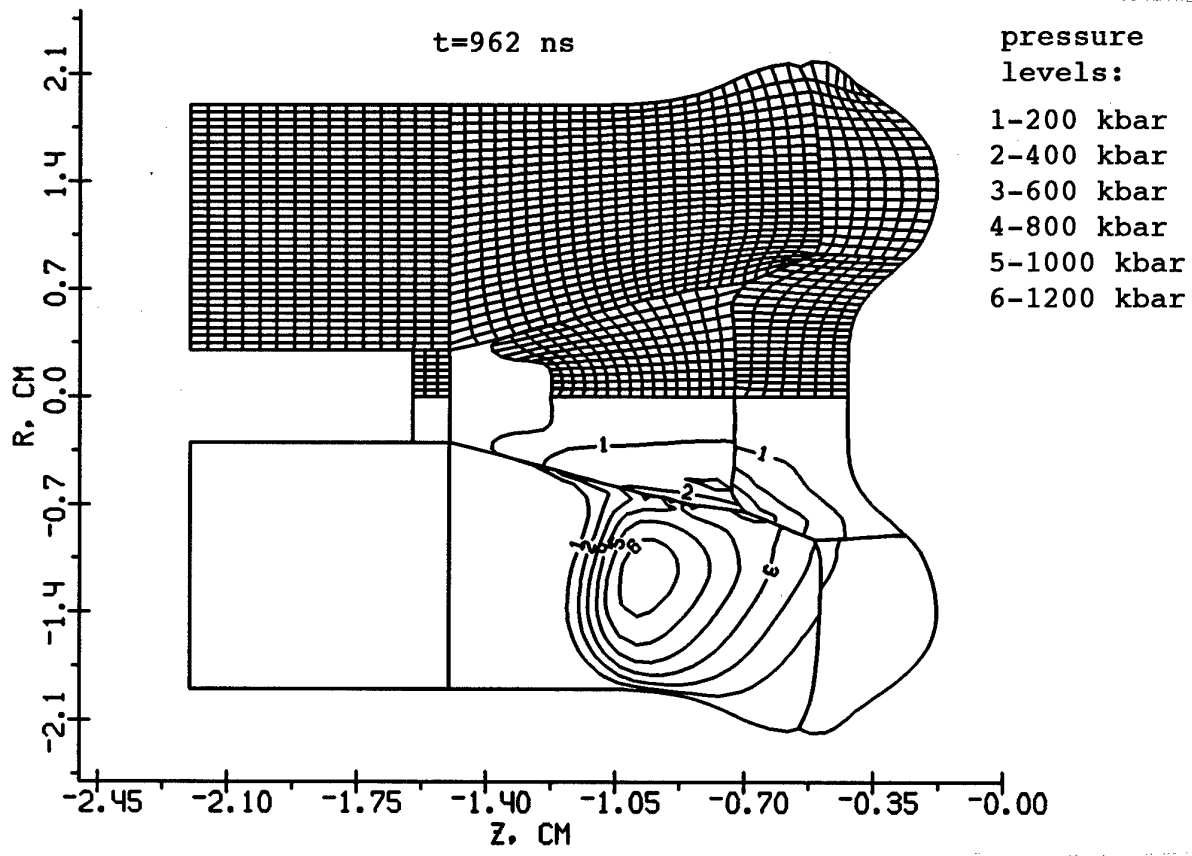


Fig.16 Grid and pressure levels

## V. REFERENCES

1. A.V. Bushman, G.I. Kanel, A.L.Ni, V.E. Fortov, *Thermal Physics and dynamics of Intense Pulse Action*, Inst. of Chemical Physics, Chernogolovka, 1988
2. A.V. Bushman, V.E. Fortov, *Wide-range equations of state for matter under extreme conditions*, Sov.Tech. Rev. **B**. Term. Phys., vol. 1, p.219, 1987
3. M.L.Wilkins *Calculation of elastic-plastic flow*. In:Adler B, Fernbach S, Rotenberg M (eds) *Methods in Computational Physics* vol. 3, p.211, 1964
4. V.A. Agureikin, B.P.Krukov *Individual particle method for calculations of flows of multi-component matter with strong deformations*, Num.meth.cont.mech (russian), Novosibirsk, vol. 17, No. 1, p.17, 1986
5. O.M.Belocerkovski, Yu.M.Davidov *Big particle methods in fluid dynamics.Computational experiment*. (russian) Moscow, Nauka, 1982
6. F.H.Harlow *The particle-in-cell computing method for fluid dynamics* In:Adler B, Fernbach S, Rotenberg M (eds) *Methods in Computational Physics*, vol. 3, p.319, 1964
7. R.F.Stellingwerf, C.A.Wingate *Impact modelling with smooth particle hydrodynamics*, Int.J.Impact Engng, vol. 14, p.707, 1993
8. Fomin V.M., Shapeev V.P., Yanenko N.N. *Modelling of continuum mechanics problems with large deformations*, Comp.Meth.Appl.Mech. Engng, vol.32, p.157, 1982
9. K.-D.Munz, R.Scheider, M.Goez, A.Herschel *Study of numerical approximations of gas flow into vacuum*, KFK report 5237, 1993
10. J.K. Meier *The sensivity of an eulerian hydrocode impact analysis to user-selected impact parameters*, Int.J. Impact Engng vol. 10, p.361, 1990.

11. T.G. Trucano, J.M. McGlaun Hypervelocity impact calculations using CTH: case studies, *Int.J. Impact Engng.*, 10, p.601, 1990
12. W.W. Predebon, C.E. Anderson, J.D. Walker *Inclusion of evolutionary damage measures in Eulerian wavecodes*, *Computational Mechanics*, No. 7, p.221, 1991
13. E.P. Fahrenthold, *Int.J. Impact Engng*, vol. 14, p.229, 1993
14. J.A. Trangenstein, R.B. Pember *Numerical algorithms for strong discontinuities in elastic-plastic solids*, *J. Comp. Phys.*, vol 103, p.63, 1992
15. A. Suresh, M.S. Liou *Osher's scheme for real gases*, *AIAA Jour.*, vol. 29, No. 6, p.920, 1989
16. S.K. Godunov *A finite difference method for the numerical computation of discontinuous solutions of the equations of fluid dynamics* *Mat.Sb.* 47, p.271, 1959
17. S.K. Godunov *Numerical solution of multi-dimensional problems of gas dynamics* (in russian), Nauka, Moscow, 1976
18. A.V. Bushman, V.E. Fortov, I.V. Lomonosov, *Proc. Enrico Fermi School 1989*, Elsevier Publ. 1989
19. O.Yu. Vorobiev, A.L. Ni, A.V. Shutov, V.E. Fortov *Application of Godunov's method with movable grids for calculations of dynamics of condensed matter under intense impulsive actions*, *Modelling in mechanics* (russian), vol. 6, No 4, p.3., 1992
20. A.L. Ni, T.N. Fortova, K.G. Shkadinski, A.V. Shutov, A.V. Utkin *Numerical simulation of interaction of high velocity impactors with condensed targets*, (in russian) Preprint Institute of Chemical Physics, Chernogolovka, 1989

21. J.F. Thompson *Grid generation techniques in computational fluid dynamics*, AIAA Journal, vol. 22, No 11, p.1505, 1984
22. A.V.Bushman, O.Yu. Vorobiev, I.V.Lomonosov et al *Numerical simulation of condensed matter dynamics under the action of directed intense  $\gamma$  radiation*, (in russian) Preprint Institute of Chemical Physics, Chernogolovka, 1990
23. P.Colella, H.Glaz *Efficient solution algorithm for the Riemann problem for real gases*, J.Comp.Phys. vol 59, p.264, 1985.
24. Ja.Cholodov, O.Yu.Vorobiev *Effective methods of integrating 1D gas dynamics problems*, Z.vich.mat. i mat phys. (russian) to be published, 1994
25. C.-D. Munz *On the comparison and construction of two-step schemes for the euler equations*, In.: Finite Approximations in Fluid Mechanics, Ernst Heinrich Hirschel (ed.), Priority REsearch Programme, reports 1983-1985, p.195.
26. G.Moretti *Computation of flows with shocks*, Ann.Rev.Fluid Mech., vol. 19, p.313, 1987

HEDRC REPORT  
contract SPC-93-4075

## 2D HIGH RESOLUTION SHOCK WAVE PHYSICS CODE

9-month technical report

*Second order modification of moving grid hydrocode*

Participants:  
Vorobiev O.Yu.  
Shutov A.V.  
Zharov A.V.  
Ni A.L.  
Fortov V.E.

## Introduction

One of the most important problem of numerical solution of nonlinear hyperbolic conservation equation is to obtain high accuracy of the solution in both discontinuous and continuous regions. In recent years, a lot of so called high resolution schemes have been proposed, for example, second order TVD scheme of Roe [1,2] and Sweby [3]; upwind TVD of Harten [4] and Yee et al. [5]; symmetric TVD of Chakravarthy and Osher [6]; ENO scheme of Harten et al. [7,8], FCT scheme of Zalesak [9] McDonald and Ambrosiano [10]; MUSCL schemes of van Leer [11], Goodman and LeVeque [12], Davis [13], Colella [14], and PPM of Colella and Woodward [15]. The most of schemes mentioned above were originally derived for the case of perfect gas and for 1D geometry (or 2D for fixed Eulerian grids). For numerical simulations of hypervelocity impact problems, when realistic physical models are used, we face with additional problems. This is, for example, a variety of matter properties in different phase states (solid, liquid, gas, plasma), when the compressibility of matter differs up to several orders of magnitude. This difference often gives some unphysical values of variables appearing due to errors of numerical approximation (negative internal energy or density), which lead to a failing of numerical scheme. As it was found in [16], some of Godunov-type second order methods based on approximate Riemann solver are not positively conservative or positively conservative under certain conditions. They can produce non-physical states with negative density or internal energy in rarefaction waves. We based our code on the Godunov's method of numerical integration of Euler equations on a time dependent (so called moving) grid [17]. As it was shown in [16], this scheme is positively conservative for at least in the case of ideal gas EOS.

Let us remind the main principles of this code. In the framework of this approach only the boundaries of numerical grid are moved in Lagrangian fashion. The location of interior grid nodes are determined during grid generation procedure by using of coordinates of boundary nodes. As the material flows through the grid cells there is some diffusion error as well as in any Eulerian method. Nevertheless there exist several possibilities to reduce such errors by generating "near-Lagrangian" grids. In the present version of 2D hydrocode we utilize decomposition of numerical region onto subregions with Lagrangian boundaries, in which grids are generated independently using conformal mapping procedure. This decomposition is provided automatically during the computations. When every subregion consist of only

one cell. This approach resembles Lagrangian method on unstructured quadrilateral mesh. On the other side, such a grid enables all advantages of a regular grid. It is known that the numerical approximation of solution on an orthogonal grid is always better than that one on an arbitrary disturbed grid [17]. The grid generation procedure can be governed by moving the boundary nodes along the boundary. Using such a redistribution of the boundary nodes orthogonal grids are generated in subregions. The other advantage of orthogonal grids is a possibility to simplify a second order extension of Godunov's scheme.

In the present report we consider a second order extension of moving grid code and compare results of calculations of hypervelocity impact problems with shock-fitting calculations. The strategy of shock fitting grids was described in the previous report. Unfortunately, the application of this approach is not possible inside of numerical subregions. It means, that the description of shock wave propagation and interaction inside of disturbed subregion can not be done using shock fitting grids. That is the reason why the second order extension of Godunov's scheme is very important.

### 3. NUMERICAL ALGORITHM

In this report we describe algorithm of computations only briefly. More detailed description one can find, for example, in [18], as well as in the first report. As we have already mentioned, the numerical region is divided into several subregions with Lagrangian boundaries during the computations. Let us consider the main steps of computational algorithm for one subregion.

The first step of computations is the displacement of the boundary of subregion. After shifting the boundary to a new position some segments of the boundary can change their type due to interaction with boundaries of the other subregions. The boundary type determines the boundary condition (what is necessary for Riemann problem initial data) and the law of motion of the boundary. For example, a shock-front boundary moves according to Hugen's principle, rigid wall boundary does not move and so on.

The second step is an iterative procedure of orthogonal grid generation inside of subregion. This procedure is based on the distribution of the boundary nodes. This distribution is performed several times until the grid generated with conformal mapping becomes orthogonal.

The third step is a solution of Riemann problems for inner zones and calculation of fluxes between the neighboring zones. One should remark here,



that for an arbitrary equation of state the Riemann problem can be solved only numerically. Nevertheless, we employ an exact solver of this problem only in vicinity of flow discontinuity. The most of Riemann problem computations are done either in isentropic or in acoustic approximation.

Second order extension of Godunov's scheme can be obtained if we assume a piecewise linear distribution of flow parameters inside of the grid cells. To conserve the monotonicity property of Godunov's scheme we use the "minimum derivative principle" proposed in [19]. The main idea of this principle is to choose the minimum possible derivative when interpolating the values from the zone center to the boundary with the neighboring zone, where the Riemann problem must be solved. If the grid is orthogonal, derivatives only in one direction (either along the grid rows, or along the grid columns) are important when interpolating cell-centered values to the boundaries of the cells. This simplifies the realization of "minimum derivative principle".

#### 4. EXAMPLES OF CALCULATIONS

In the present paper we consider an application of our 2D code to hypervelocity impact problem. One of the most difficult task for any 2D Lagrangian code is to compute hypervelocity penetration of projectile into a thick target. We consider two different approaches to numerical simulation of hypervelocity impact of iron projectile moving with 10 km/s velocity on a thick aluminum target .

First one concludes in a usage of "near-Eulerian" grid, which covers the region of the target where the shock wave propagates.

The second one is fitting of this shock wave by moving the boundary of the grid with shock front velocities obtained by Riemann solver. The second method in fact, is more accurate to resolve the shock front and is more economic, because it does not require a grid in undisturbed regions. On the other hand the shape of numerical region is more complicated and, as a consequence of that, the grid generated is not so orthogonal as in the first case. The results of computations corresponding to these cases together with numerical grids are shown in Fig.1. There were two subregions used in the case of shock-fitting grid. One of them corresponded to the projectile, the other one covered the disturbed region in the target. In the other case (near-Eulerian grid) three subregions were used in computations.

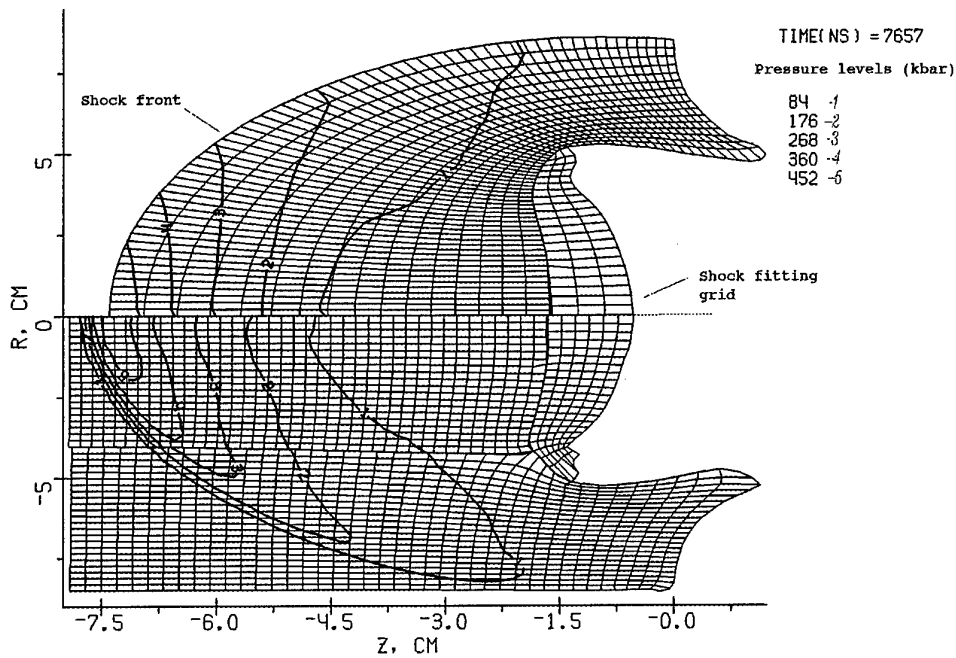


Fig.1 Numerical grid and pressure levels for hypervelocity impact calculations using shock fitting grid (above the axis) and "near-Eulerian" grid (below the axis).

It is known, that first order Godunov's scheme is a very dissipative one. Our experience shows, that this scheme smears out weak discontinuities in the case of realistic EOS much stronger than in the case of perfect gas. Moreover, this dissipation grows in time. Results of computation of hypervelocity impact of iron projectile on aluminum target shown in fig.2-3 confirms this fact. In contrast to the first order scheme, second order calculations exhibit nearly constant width of shock front smoothing.

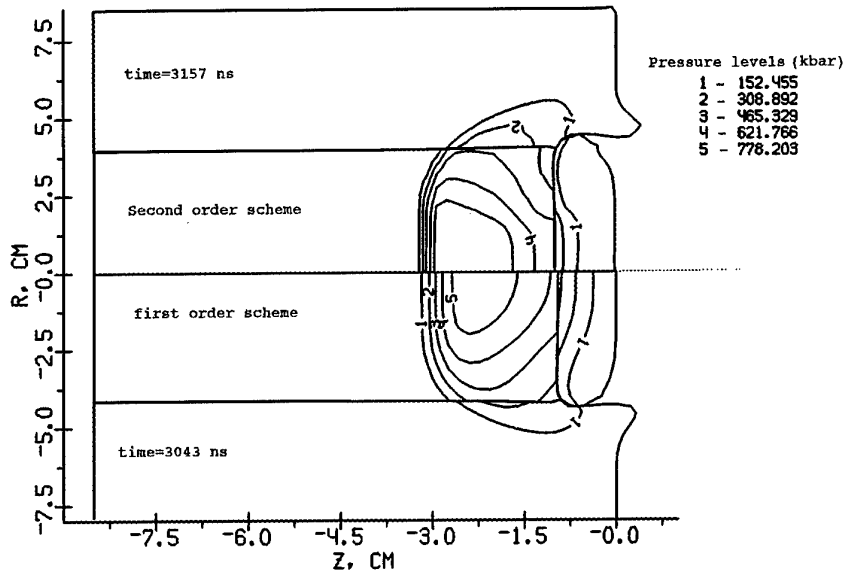


Fig.2 Grid boundaries and levels of constant pressure for the first (below the axis) and second order accuracy calculations of hypervelocity impact of iron projectile (on the right) on an aluminum target.

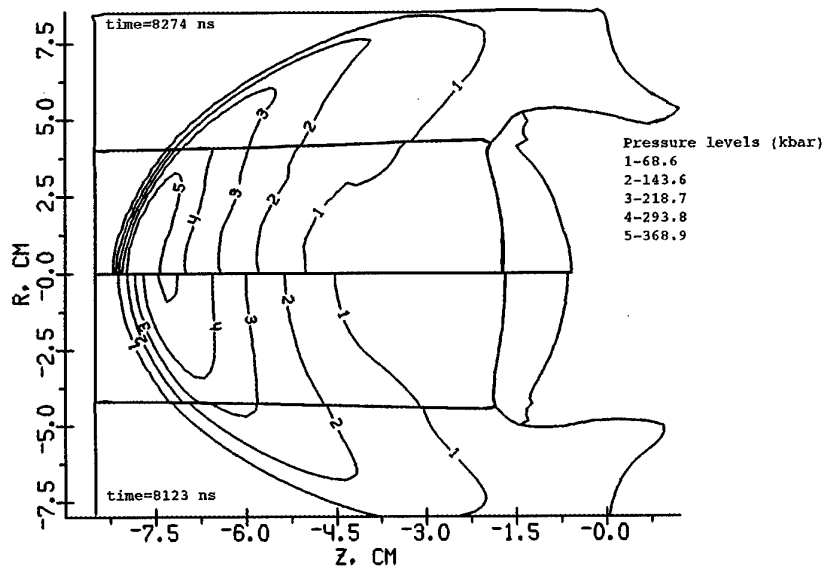


Fig.3 Grid boundaries and levels of constant pressure for the first (below the axis) and second order accuracy calculations of hypervelocity impact of iron projectile (on the right) on an aluminum target.

As it has been shown in [20] for the case of steady gas flow, the second order extension of Godunov's scheme is not so sensitive to distortions of numerical grid as it's first order counterpart. We demonstrate below (Fig.4-5) the results of simulation of hypervelocity impact obtained using the first and the second order Godunov scheme both on the shock fitting grid and on the near-Eulerian grid. Our results generally confirm the conclusions obtained in [20]. For the second order scheme (Fig.5) the difference between the results obtained on the different grids is negligible, while for the first order scheme there is a big difference in the amplitude of the shock wave calculated on the shock fitting and on near-Eulerian grid. It is naturally, that the shock front dissipation is much pronounced in the case of the first order scheme than in the case of the second order one.

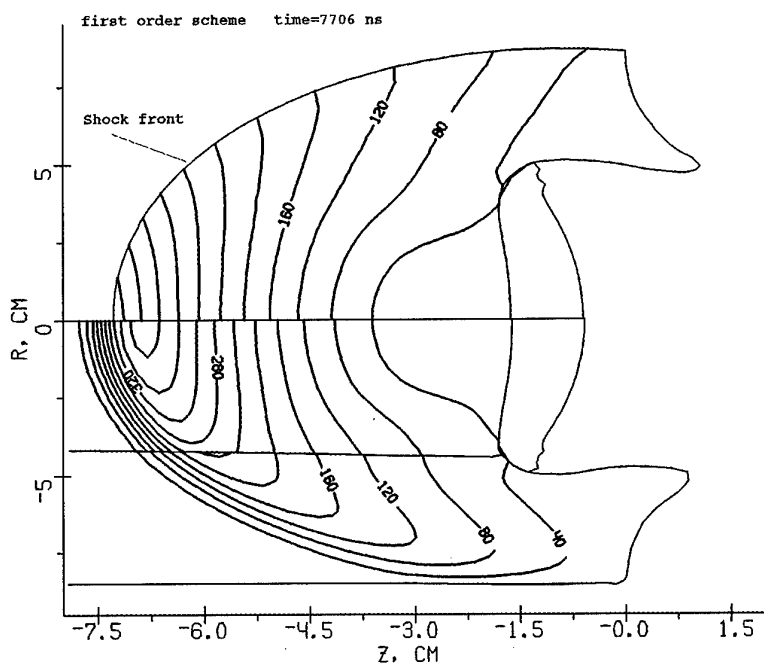


Fig.4 Grid boundaries and pressure levels (in kbars) for shock fitting grid and "near-Eulerian" grid. First order scheme.

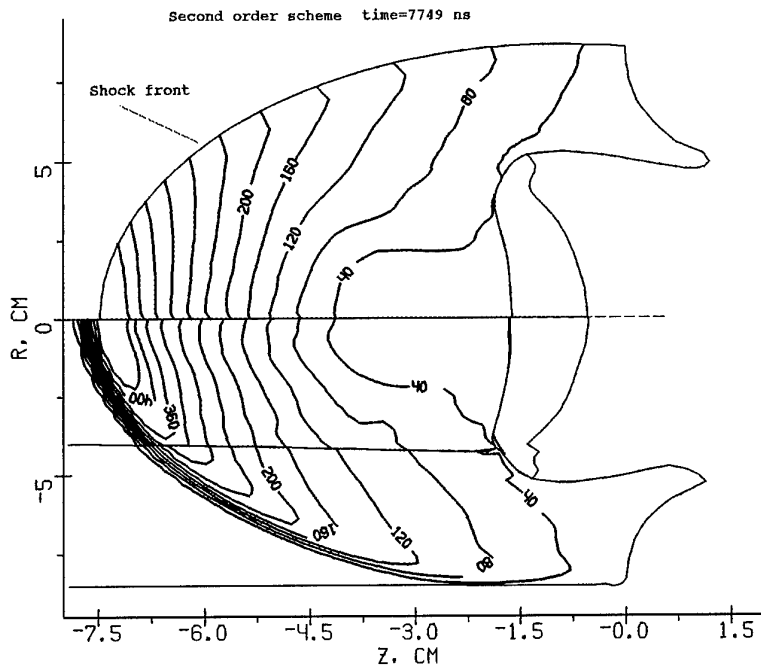


Fig.5 Grid boundaries and pressure levels (in kbars) for shock fitting grid and near-Eulerian grid. Second order scheme.

## CONCLUSIONS

We have considered an application of Godunov's scheme on the moving grids and its second order extension (Kolgan scheme) on the example of hypervelocity impact calculation. We have shown that this scheme coupled with the algorithm of decomposition of numerical region onto subregions shows a good robustness and flexibility for multimaterial problems of computational fluid dynamics with large distortions. The other advantage of decomposition of numerical region of complicated shape is a possibility to generate orthogonal grids in subregions

We have developed second order Godunov's scheme applying Kolgan's algorithm of "minimal derivative". It has been found that Kolgan's scheme is not so sensitive to the form of the moving grid as original Godunov's scheme. The results of second order calculations are much closer to more accurate shock-fitting calculations.

## REFERENCES

- [1] P.L. Roe, *Annu. Rev. Fluid Mech.* 337(1986)

- [2] P.L. Roe, Lectures in Appl. Math. Vol. 22 (Am. Math. Soc., providence, RI , 1985
- [3] P.K.Sweby, SIAM J. Num. Anal. 21,995(1984)
- [4] A. Harten, J.Comput. Phys.49,357(1983)
- [5] H.C.Yee, R.F.Warming, and A. Harten, J.Comput. Phys.57,327(1985)  
ICASE Report No 84-20,June 1984
- [6] S.R.Chakravarthy and S.Osher,"A New Class of High Accuracy TVD Schemes for Hyperbolic conservation Laws",AIAA-98-0363, 1985
- [7] A.Harten and S.Osher,SIAM J.Num.Anal.24,297(1987)
- [8] A.Harten, B.Engquist, S. Osher,S.R.Chakravarthy , "Uniformly High Order Accurate Essentially Non-Oscillatory Schemes", NASA CR-178101,1986
- [9] S.T.Zalesak, J.Comput. Phys.31,335(1979)
- [10] B.E.McDonald and J.Ambrosiano, J.Comput. Phys.56,448(1984)
- [11] B.van Leer, J.Comput. Phys.32,101(1979)
- [12] J.B.Goodman and R. LeVeque, SIAM J. Num. Anal. 25,268(1988)
- [13] S.F.Davis,SIAM J.Sci.Stat.Comput.9.445(1988)
- [14]P.Colella,SIAM J.Sci.Stat.Comput.6.104(1985)
- [15]P.Colella and P.R.Woodward,J.Comp.Phys.54,174(1984)
- [16]B.Einfeldt,C.D.Munz,P.L.Roe,B.Sjoegreen J.Compt.Phys.92,273(1991)
- [17] S.K.Godunov, Numerical solution of multi-dimensional problems of gas dynamics (in russian) (1976) Nauka, Moscow
- [18] O.Yu.Vorobiev, I.N.Lomov,A.V Shutov et al.,Godunov's Scheme on Moving Grids for High Velocity Impact Simulations, to be published in Proc. HVIS94, Santa Fe,NM
- [19] V.P.Kolgan, Scientific Notes of CAGI (in russian),3,68,(1972)
- [20] V.I.Koptchenov, A.V.Kraiko, Zh.Vych.Matem.i Matem Fiz. (in russian) 23,848 (1983)

**HEDRC REPORT**  
contract SPC-93-4075

**2D HIGH RESOLUTION SHOCK WAVE PHYSICS CODE**

6-month technical report

*Application of 2D code to various hypervelocity impact problems*

**Participants:**  
Vorobiev O.Yu.  
Shutov A.V.  
Zharov A.V.  
Ni A.L.  
Fortov V.E.

## *Introduction*

In this report we present applications of previously described moving grid Godunov code to several hypervelocity impact problems. This method employs the exact solution of Riemann problem, therefore it is well suited for construction of "nonhomogeneous" computational algorithms fitting flow singularities. It is clear, that to fit all singularities, which can arise in the flow is rather difficult algorithmic problem especially in multidimensional case. That is why the most of widespread computational methods of shock wave dynamics are based on homogeneous algorithms treating in the same fashion both continuous and discontinuous domains of flow.

To better resolve discontinuities so called high resolution shock-capturing schemes are used. Most of them are second order modifications of Godunov scheme [1], which use approximate Riemann problem solvers [2-5]. One should mention in this context so called ENO schemes (essentially non-oscillatory schemes) which allows one to increase the order of accuracy up to fourth or even more [6-7]. Of course, the higher is the order of accuracy, the more complicated is the computational algorithm. For example, as it was found in [8], the cost of the third-order ENO scheme is four times that of the second-order one. It may appear the second order schemes to be more profitable when using refined mesh than the fourth-order ones.

We have chosen another approach to construction of high resolution shock-wave codes, namely, Godunov scheme on a moving grid. The main principles of this approach were described in [9-10] and in the previous HEDRC report. Note that in the framework of moving grid code shock waves, contacts between different materials and matter-vacuum boundaries, can be easily fitted. By that the grid boundaries coincided with these discontinuities are moved in accordance with the solution of Riemann problem.

In the present report we demonstrate the advantages of moving grid approach for solving four different problems.

The first one is an impact of thin plane projectile on a thin screen. A great difference of longitudinal and transverse dimensions leads to a great number of zones when using a Lagrangian grid, which covers all the projectile and the target. Our method allows one to



compute only those domains where the flow is two-dimensional, that gives a substantial economy of computer's resources.

The second example is the numerical simulation of penetration of a cosmic body moving with hypervelocity into gaseous atmosphere with exponentially increasing density. The typical feature of this problem is the presence of various space scales. For example, the size of the body is much larger than the thickness of compressed gas layer at the face side of the body and on the other side it is much less than the distance which this body passes before it explodes.

The third problem is a debris cloud simulation produced by ball-plate impacts. In this problem the ball and the plate have thicknesses of the same order, that makes it difficult to employ any Lagrangian code because of the great deformations of material. On the other side it is known that Eulerian codes give a great dispersion of mass due to averaging of flow values over the fixed zone intervals. Application of the moving grid code in which the computation grid moves with material near the boundaries and has a minimal advection error in the central grid region allows one to overcome these difficulties.

The last example is a numerical simulation of detonation of charges of finite diameters. It is well known, that a steady detonation can exist only if the size of the explosive is greater than some minimum value. To find this size for a charge of some specified geometry numerous numerical computations are required. When this size is close to the critical one the time which is necessary for setting up a quasi steady detonation regime is very long. It means that we must be able to track the propagation of the front over a long distance. As the region of computation increases with time, a grid refinement is required to maintain some specified level of computation accuracy.

### **Numerical simulation of impact of projectiles with a great D/L ratio**

Impactors with a great D/L ratio (where D is the diameter and L is the thickness) are used in shock-wave experiments in order to simplify their interpretation reducing the last one to 1D case. Nevertheless, the flow becomes two dimensional when the rarefaction waves from the periphery reach the center of the projectile. To account 2D effects at the late stages of interaction 2D simulation is necessary. In the present report we demonstrate one example of

application of moving grid to effective solution of such a problem. In fig.1(a-d) numerical grid and levels of constant density are presented for high velocity impact of 1mm thick aluminum disk on 2mm thick aluminum foil at 8 km/s velocity. The diameter of the disk is 4 cm. In the beginning of computation we specify two small numerical regions. One of them represents the edge of the disk and the other corresponds to the fragment of the foil, which is in contact with this edge. Then we move the boundary segment separating the 1D and 2D flow regions with characteristic velocity towards to the axis of symmetry. The other fragments of the boundary are: free boundaries (back sides of the disk and the foil), contact between the disk and the foil and the front of the shock wave running away from the center. Rarefaction waves coming from the back surfaces of the projectile and the target lead to an expansion of shocked material and to generation of tensile stresses. That is why the contact between the disk and the target disappears. The type of the boundary segments is changed automatically from contact boundary to free one (fig. 1b). For the later times the size of the flow under consideration is much more than initial one (see fig. 1d). The straight line fragment of the boundary separates the flow region where the transversal rarefaction waves are important.

In addition to this example one should note, that there is a lot of problems containing different time and space scales which could be effectively solved using moving grid code, for example, investigation of thin foil acceleration with laser and ion beams, perforation of multilayered spaced shields and so on.

### **Computation of large asteroid penetration in Jupiter's atmosphere**

The problems of asteroid hazard are of great interest, because the number of asteroids moving in vicinity of Earth is increasing with time. An impact of periodic comet Shoemaker-Levy on Jupiter took place recently (in July 1994). The consequences of this impact were observed both from the Earth and space satellites. In this report we demonstrate an example of numerical simulation of the penetration of one comet fragment of 1 km diameter into Jupiter's atmosphere. The asteroid was approximated by a spherical incompressible body moving with a velocity of 60 km/s. Due to its high velocity it passes a distance much more than its diameter before it explodes. As the density of the atmosphere grows with distance the flow is unsteady.

Extremely high velocity of impact leads to heating and ionization of a gas flow after shock compression. Since the flow behind the shock front is responsible for ionization and luminosity of gas, which can be observed an accurate resolution in this region is required. It is clear, that application of Eulerian codes to this problem will lead to a great diffusion of shock front and contact interfaces. Eulerian computations also require a great number of computational zones to cover the regions in which the asteroid moves. That is why Eulerian computations of this problem were performed in 'reverse ballistic' sense using an atmosphere moving towards an initially stationary fragment [11].

To avoid computations in undisturbed domains we surrounded the asteroid region by a thin region of the gas, whose boundary moves with the characteristics velocity. The size of the gas region grows in time but we can exclude from consideration those parts of the gas region, which are far from the asteroid and are not of our interest. The results of computation are shown in fig.2-4. In the beginning (fig.2) of penetration the gas detaches from the back side of asteroid and a gas jet appears moving in the opposite direction. Then we cut off the part of gas region corresponding to this jet (fig.3). Fig.4 presents the results of simulation for the time when the asteroid has passed about 80 km in atmosphere. The pressures at the frontal surface of the asteroid become about 0.3-0.5 kbar, that are close to the strength of material. Further computations require to account for the fracture of matter. In accordance with [12], fragmentation of the asteroid leads to a growth of the heat flux inside it, because of significant increase of the effective surface area. This gives rise to the rapid transformation of the asteroid material from the condensed to gaseous state. If we suppose, that the fracture and fragmentation of asteroid is due to the stress gradient at its surface, we obtain the distance of about 100 km, where the explosion takes place. This agrees with recent observations.

### **Numerical simulation of propagation of debris cloud produced by ball-plate impact.**

The results of a computation of a 20 g spherical lead projectile striking a lead plate is

presented in Fig.5(a,b). The impact velocity for this problem is 6.6 km/s. Fig.6 represents the experimental X-ray photograph of the same problem at the time moment 30  $\mu$  m presented in [13]. Simulation results are in accordance with the experiment. The number of zones used grows during the computation to ensure some specified level of accuracy. The criteria for grid refinement are not purely geometric. When the pressure gradient and the density decrease some coalescence of zones takes place.

Using moving grids demonstrates a substantial economy of required computer memory in comparison with a fixed Eulerian grid. One can estimate that about 10 000 - 20 000 mesh is required to perform computation of this problem using Eulerian grid with the same accuracy.

### **Simulation of detonation in high explosive charges of finite diameter.**

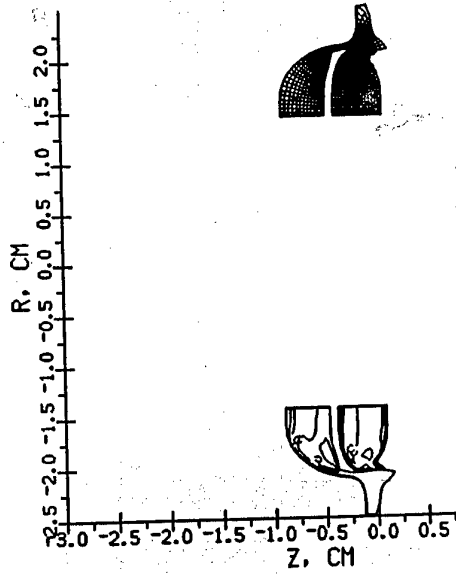
The failure detonation problem is the problem of minimal explosive charge diameter when a self-sustained detonation can exist. We present below an example of determination of this diameter using numerical simulation. The flow is described by Euler equations. The only difference with hypervelocity impact problem is the appearance in the energy equation of a source term which is responsible for heat release. To check whether the detonation becomes steady or not it is necessary to calculate the evolution of detonation process along the distance of at least several (perhaps tens) diameters. As the downstream flow behind the shock is determined by the chemical reaction kinetics and, in particular, by the value of energy release, the shock must be calculated accurately.

The following computational strategy is chosen in accordance with the problems listed above. The computational region represents a curvilinear quadrangle. The sides of the quadrangle are: the leading shock, the segment of contact between detonation products and vacuum, the segment of axis of symmetry, and the fourth one is a segment of straight line between the free surface and the axis of symmetry, which is perpendicular to the axis of symmetry. The velocity of this side is assumed to be directed along the axis and to be equal to  $\max(u+a, D)$ , where  $D$  is the shock velocity at the axis of symmetry and  $u+a$  is the velocity of characteristic

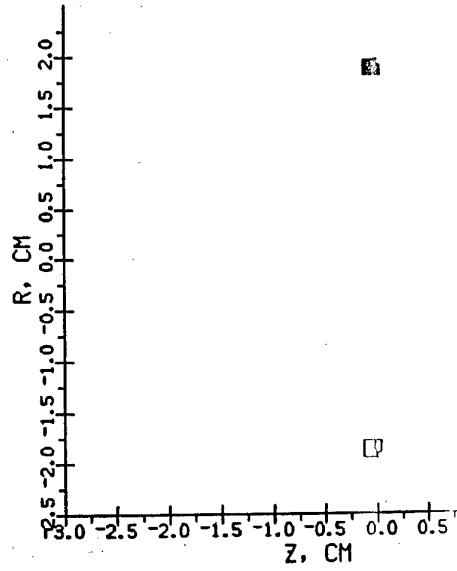
surface moving along the axis and calculated using parameters of the cells adjacent to this side. It means that the boundary moves relative to the matter ahead of it at least with the sonic velocity. Therefore the flow parameters, which determine the fluxes of mass, momentum and energy throughout this side are taken from internal cells. A pressure of 200 kbar, normal density and zero velocity were taken as an initial data for calculations. It was found from simulations, that the critical diameter is somewhere between 2.4 and 3 mm. Results of simulations corresponding to these two cases are shown in Fig.7(a,b) In the case of 2.4 mm diameter detonation decays. Calculations for this diameter were performed with different initial pressures. In all the cases a steady detonation was not obtained. This fact allows to draw a conclusion that the failure diameter of TNT lies within the interval 2.4 and 3 mm. This also agrees with the experiment [14].

## CONCLUSIONS

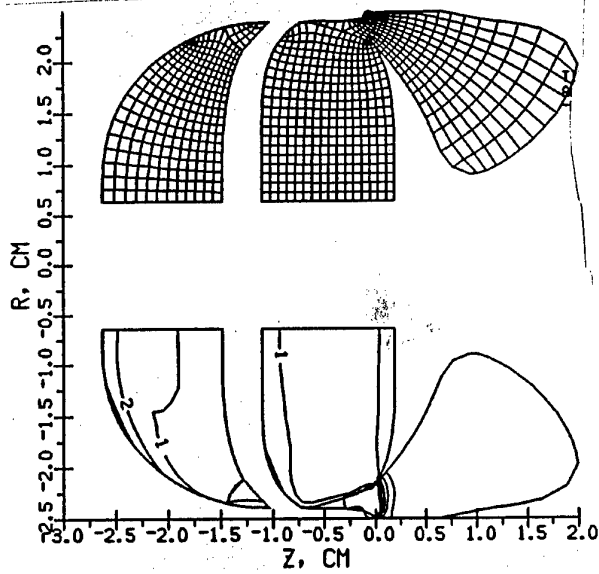
**We have demonstrated the robustness and flexibility of developed 2D code for hypervelocity problem computations. The main advantage of this code in comparison with Eulerian high-order accuracy hydrocodes is an accurate treatment of multimaterial interfaces. On the other side, arbitrary Lagrangian-Eulerian methods (ALE), which utilize lagrangian motion of interfaces and permit an arbitrary mesh motion inside the computation region are not always adapted to dynamically evolving interface shape. It is the main reason to develop ALE codes on unstructured grids [15]. We overcome these difficulties with the help of decomposition of numerical region onto subregions. This decomposition is provided automatically during the computation. By that one can govern this process excluding from computations the regions which are not of our interest.**



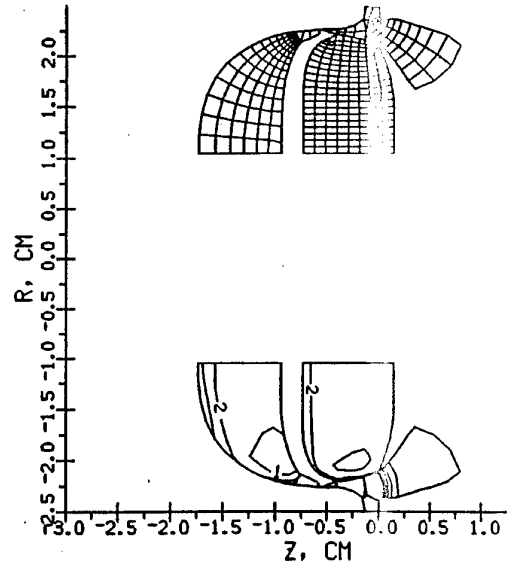
b)



a)



d)



c)

Fig.1(a-d) Numerical grid at different times:  
 a) Time is 51 ns, density level step is 0.5 g/cc  
 b) Time is 1000 ns  
 c) Time is 2010 ns  
 d) Time is 3090 ns

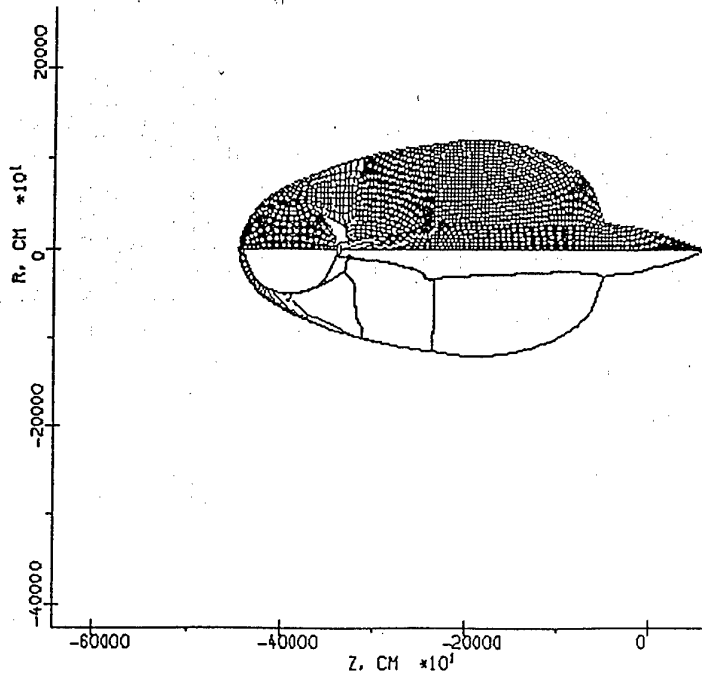


Fig.2. Numerical grid and pressure levels. Pressure level step is 0.001 kbar, maximum pressure is 0.01 kbar. Time is 55  $\mu$ s.

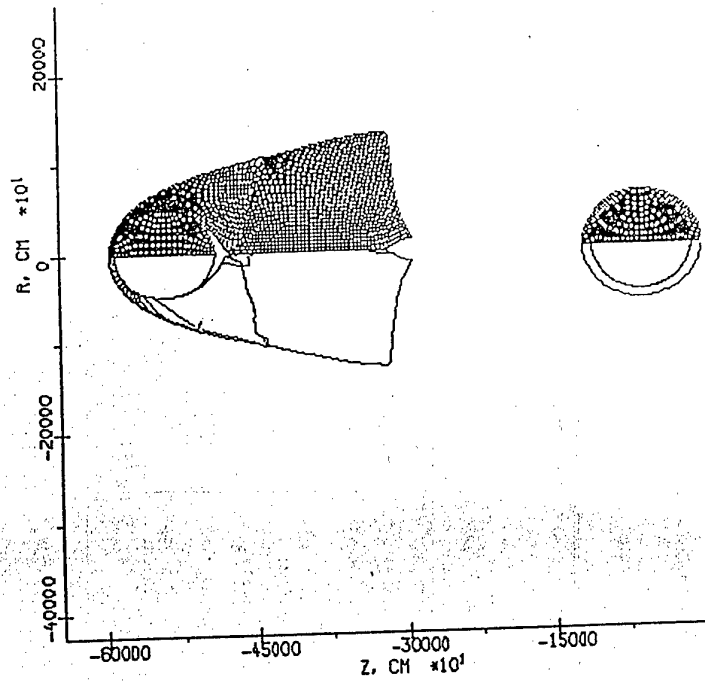


Fig.3. Numerical grid and pressure levels. Pressure level step is 0.001 kbar, maximum pressure is 0.014 kbar. Time is 80  $\mu$ s. Initial configuration is shown on the right side.

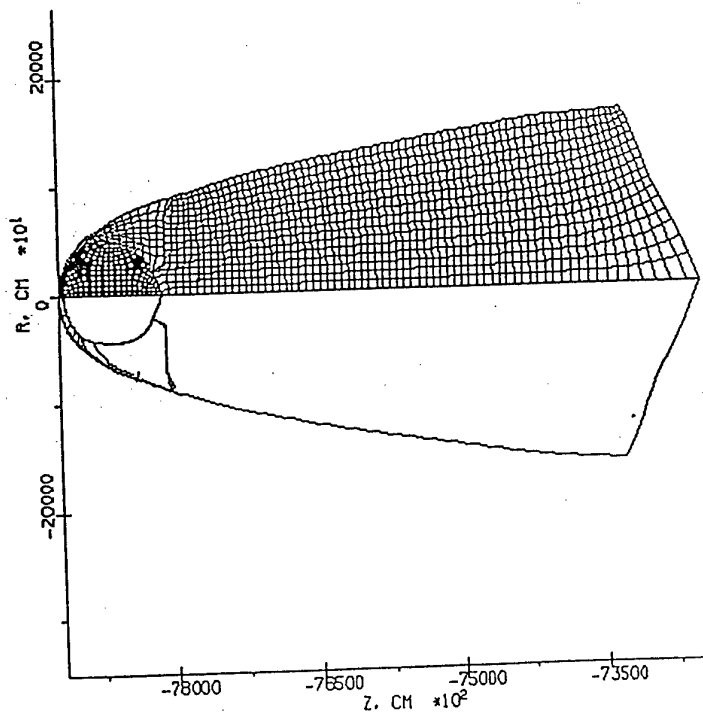


Fig.4. Numerical grid and pressure levels. Pressure level step is 0.06 kbar, maximum pressure is 0.6 kbar. Time is 1.3 s.



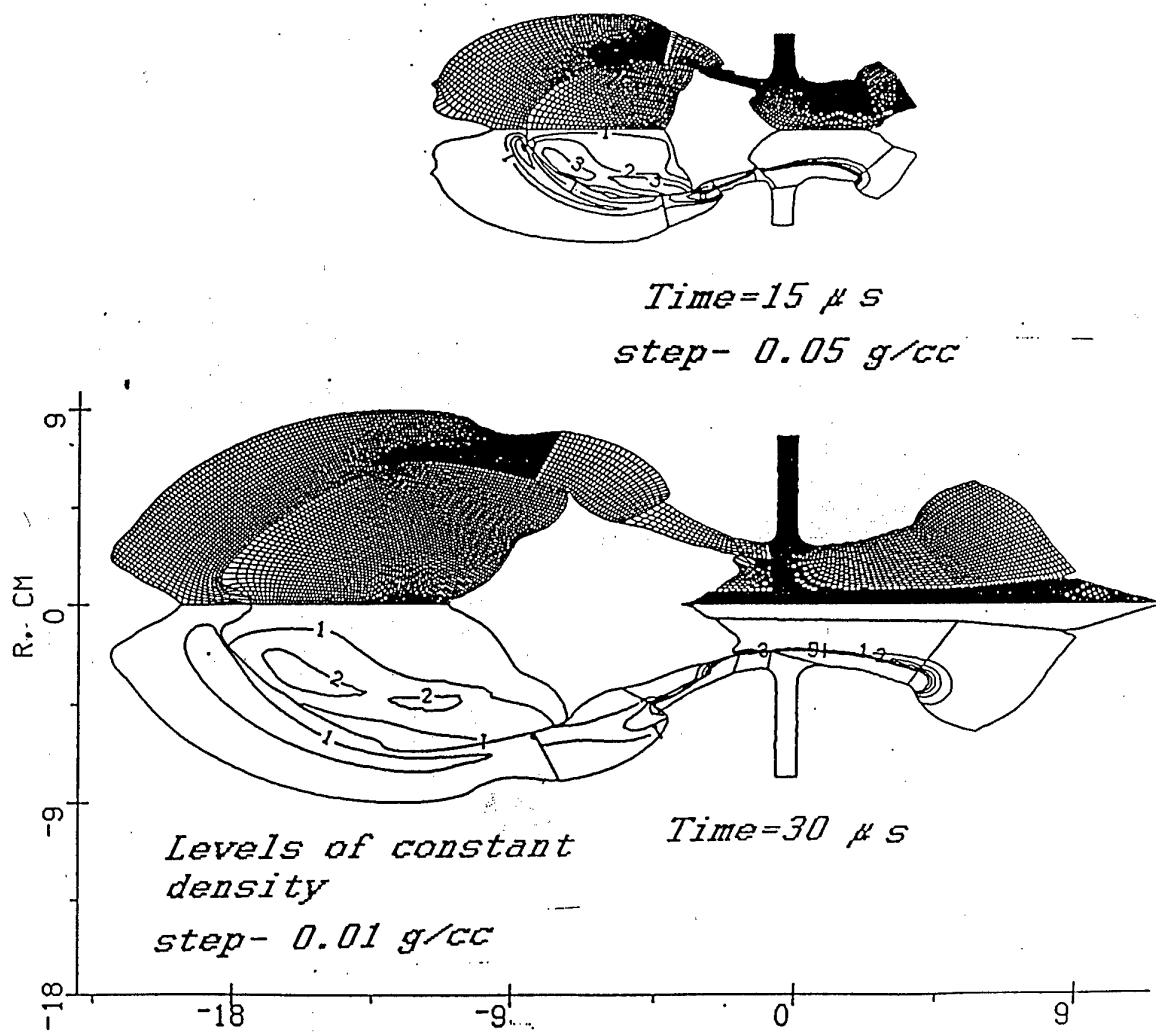


Fig. 5 Numerical grid and levels of constant density.  
 a) Time is  $15 \mu$ s, level step is 0.05 g/cc  
 b) Time is  $30 \mu$ s, level step is 0.01 g/cc

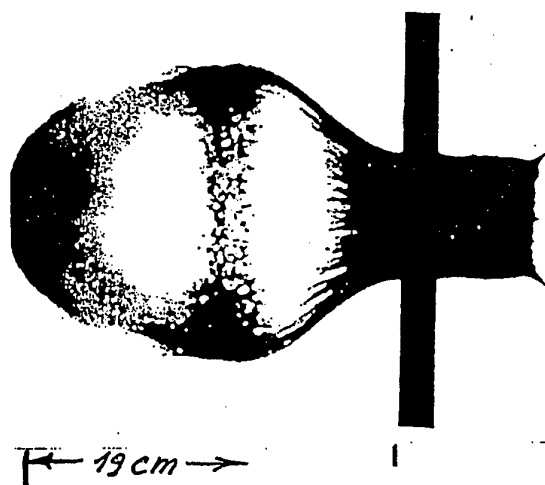
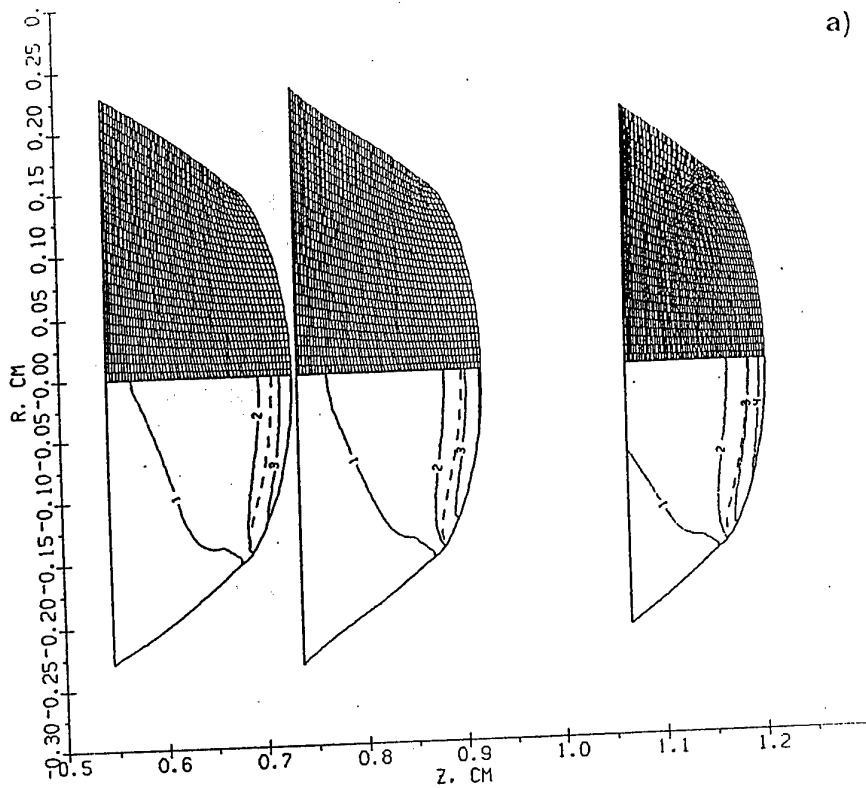
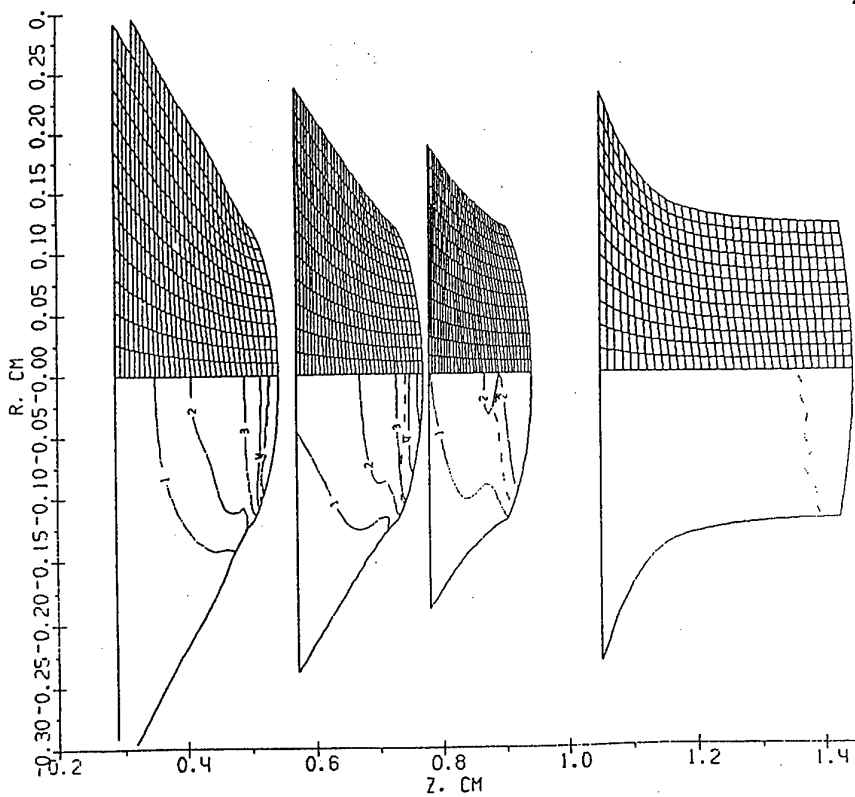


Fig. 6 Experimental X-ray photograph at the time  $30 \mu$ s



a)



b)

**Fig.7(a,b)** Computational grids and levels of constant pressure at different times. The dashed line corresponds to Mach number  $M=1$ .  
 a) diameter is 3 mm, levels step is 40 kbar  
 b) diameter is 2.4 mm, levels step is 20 kbar

## REFERENCES

1. S.K. Godunov (1976) Numerical solution of multi-dimensional problems of gas dynamics (in russian), Nauka, Moscow
2. P.Colella, H.Glaz (1985) Efficient solution algorithm for the Riemann problem for real gases, *J.Comp.Phys.* 59, p.264
3. Ja.Holodov, O.Yu.Vorobiev (1994) Effective methods of integrating 1D gas dynamics problems, *Z.vich.mat. i mat phys.* (russian) to be published
4. J.D. Frey, F.Janicot, X. Garaud, P. Groenenboom, M.Lambert (1993) *Int.J.Impact Engng*, 14, p.255, 1993
5. J.K.Dukowicz (1985) *J.Comput.phys.* 61, pp.119-137.
6. A.Harten (1989) *J.Comput. Phys.* 83, p.148
7. A.Harten and S.Osher (1987) *SIAM J.Numer.Anal.*, 24(2), p.279
8. R.Abgral (1994) *J.Comput Phys.*, 114, p.45
9. O.Yu. Vorobiev, A.L. Ni, A.V. Shutov, V.E. Fortov (1992) Application of Godunov's method with movable grids for calculations of dynamics of condensed matter under intense impulsive actions, *Modelling in mechanics* (russian), 6(4), p.3
10. A.L Ni, T.N.Fortova, K.G.Shkadinski, A.V.Shutov, A.V. Utkin (1989) Numerical simulation of interaction of high velocity impactors with condensed targets, (in russian) Preprint Institute of Chemical Physics, Chernogolovka
11. D.A.Crawford, M.B.Boslough, T.G.Trucano, A.C.Robinson (1994) The impact of comet Shoemaker-Levy 9 on Jupiter, *Shock Waves*, 4, p.47-50.
12. B.Klumov et al. (1994) Collision of the Shoemaker-Levy-9 Comet with Jupiter: Simulation of Long-Term Consequences, *physics-doklady*, 39, pp.486-493
13. Kathleen S.Holian (1990) Hydrodynamics code calculations of debris clouds produced by ball-plate impacts, *Int.J.Impact Engng.* 10, p.231
14. A.V.Utkin, T.N.Fortova, G.I.Kanel, K.G. Shkadinski.(1988) Calculation of Nonideal Detonation in TNT on the Base of Macrokinetics Empirical Equation", *Chemical Physics, Russia*, 7(9), p.1257.
15. J.K.Dukowicz et al. (1989) A General Topology Godunov Method , *J.Comput.Phys.* 82, p.29

### *Brief description of the code*

The language of the code is standard F77 FORTRAN. So it can be easily installed on any computer with f77 compiler. The code consists of the following program modules:

<b>Module:</b>	<b>Function:</b>
STARTT -	input of initial data and transformation of these data into file "NAM".TMP for continuation of calculations by module BIG2T
BIG2T-	carries out calculations, renews data for continuation of calculations (file "NAM".TMP) and records results of the calculation
REP-	modification of the task (possibility to add or delete subregions ). The changed data are rewritten into the file "NAM".TMP
UNFTOF-	transformation of "NAM".TMP from binary file to ASCII file and back (it may be useful for transmission of calculation results from one computer to other one with different binary data presentation)

### *Installation of the code*

To create object modules

1) copy all files \*.FOR and \*.INC to one directory on a hard disk

REMARK: all \*.INC files must be with capital characters

2) compile all \*.FOR files

\* before compilation probably may be necessary:

A) to set function which determines CPU time in seconds in SUBROUTINE ETIME in the file PC.FOR. (to decomment correspondent string may be sufficient)

B) to change parameters in the file BIGPAR.INC (dimensions of arrays)

3) create loading module STARTT, using object files:

startt.o, blocka.o, adi.o, arct.o, big.o, contw.o, univer.o, dat0.o,  
dattst.o, disto.o, jup.o, pc.o, shr.o, spect.o, urst.o, coef.o

4) create loading module BIG2T, using object files:

basica.o, blocka.o, mainxt.o, spect.o, tnew2a.o, urst.o, adi.o, arct.o,  
big.o, buil.o, buil0.o, buil1.o, build.o, contw.o, dat0.o, del.o, disto.o,  
god2.o, grnew.o, jup.o, pc.o, ref.o, shr.o, split.o, split1.o, univer.o,  
coef.o

5) create loading module REP, using object files:

rep.o, blocka.o, spect.o, urst.o, adi.o, arct.o, big.o, contw.o, dat0.o,  
del.o, jup.o, pc.o, ref.o, shr.o, split.o, split1.o, univer.o

\*Note that modules mentioned above (STARTT, BIG2T, REP) can be  
created using makefile. To generate first order accuracy code (BIG1T),  
one should replace tnew2a.\* by tnew1a.\* in the makefile.

#### *Generation of a new initial data file*

1) Chose one of the existing initial data files from the  
file list below

TST2.DAT

VRB1.DAT

VRB2.DAT

VRB3.DAT

.....

2) Copy the chosen file into file "NAM".DAT, where NAM is  
any name consisting of 1-4 symbols  
(the names of all the files created during the computation  
of this problem will include "NAM" as a root word)

3) Correct contents of the file "NAM".DAT with text editor  
using description of initial data file presented  
below

#### *Description of the structure of initial data file NAM.dat*

The initial data file consists of two parts:  
First part contains control information. This part has the same format for all  
files of this type. Let us consider an example shown below, where the  
first part of initial data file TST.DAT is presented.

```

AL/AL U=10.1KM/C
ISPR-LOS-LST-IRD-ISP-IRA-ICM-AIR
  0  1  1  2  1  00  1  0
NBL--MI-ID1-ID2--IK-IGR-ILENPARIVSP
9900  1  10  10  300  10 -10  6  0
----CMM----:-----H3-----:----HDEL----:----T-----:---STABL----:
-1.00000E-03 0.00075E-00 0.01000E+00 1.10000E+05 0.50000E+00

```

The first string is comment. This is usually short information about the problem. (Here this is 10.1 km/s impact of aluminum on aluminum). The next strings consist of title\_strings and contents\_strings. The title\_strings show the names of variables. The contents\_strings are values of these variables. The assignment of the variables is shown in the table

### TABLE

variables:	meaning:
ISPR	controls rebound of different boundary segments 0- calculations without rebound 1- rebound for "contact" type boundaries only 2- rebound for "contacts and rigid walls" type boundaries 3- rebound for all boundary types
LOS	1- cylindrical symmetry 0- plane symmetry
LST	1- there are rigid walls 0- rigid walls are absent
IRD	0- to ignore isp 1- to continue calculations from the restart data 2- to correct in dialog regime the number of time steps after which the splitting of numerical regions into subregions will be switched on
ISP	1- to change in dialog regime the type of " contact " between subregions 0- to do nothing
IRA	energy source (for impact problems ira is equal to 0)
ICM	1- automatical choice of time step 0- --- ----- ---- time step = abs(cmm) * stabl (cmm,stabl see below.)

**NBL** is the number of time steps to do before copying of all flow parameters to output file.

**MI** 1- to search the optimum location of 4 angle tops of rectangular subregion along the boundary

**ID1, ID2** are the numbers of time steps to do before the data record for restart(id1- before the first record)

**IK** is the maximum number of time steps to do.

**IGR** is the number of time steps to do before printing packed information about all subregion's boundaries.

**ILEN** is the number of time steps to do before the next graphic data record.  
If ilen less 0 then data for the graphics will be written in time step= $\text{abs}(\text{ilen} * \text{cmm})$  in nanoseconds. (cmm parameter described below)

**PAR** is the number of flow parameters which must be written for graphics data. (from 5 to 7 parameters)

**IVSP** if ivsp is not equal to 0 then ivsp is input parameter for subroutine AUTOSP, which changes types of " contact " between subregions automatically .  
This automatical regimes must be programmed by user for the concrete task in subroutine AUTOSP.

**CMM** is parameter which determines time step (stt)  
 $\text{stt} = \text{cmm} * \text{stabl}$  if  $\text{cmm} > 0$ .  
If  $\text{cmm} < 0$ , then cmm will be read from restart or  $\text{cmm} = \text{abs}(\text{cmm})$  in case of initial data.

**H3** space precision.(H3 equals to 0.1 of cell size)  
H3 is widely used in the code as a characteristic size.

**HDEL**  
The boundary section with length  $< \text{hdel} * (\text{cell size})$  will be combined with neighboring one.

**T** time cpu limit in seconds

**STABL** stability coefficient  $\text{stt} = \text{cmm} * \text{stabl}$

---

The second part of the initial data file includes an information about geometric configurations of the problem to be solved. The information may

be prepared using so called UNIVERSAL INPUT. In this case the first string in the second part of the initial data file must be UNIVER.....

One Universal input starting with UNIVER..and finishing with UNIEND specifies only one subregion (numerical block).

To specify several subregions one must use this block of input strings several times.

The boundaries of numerical subregion are specified in accordance with the following rules:

1) If the problem contains the rigid walls and shock fronts they must be specified right after the string UNIVER....

For example, in the case of rigid wall the input looks like this

UNIVER.....

RIGIDRD

IWALL, INW, ITP, AW, BW, CW;STRAIGHT LINE:F=INW\*(AW\*X+BW\*Y-CW)=0.

1 , -1 , 1, 0. , 1., 0.

-1 , -1 , 1, 0. , 1., 0.

Here the second string (after UNIVER) starting as RIGIDRD indicates to the beginning of wall specification, which is finished when the first parameter (IWALL) equals to some negative value (-1 in this example). In the example presented above the rigid wall specified is the straight line (ITP=1) and input parameters are the coefficients which determine it's orientation. There are following types of walls

ITP=1-rigid wall specified by the straight line

ITP=2-rigid wall specified by the circle

ITP=3- "transparent" wall (matter can flow out through this wall)

To specify the front one must put the string starting as FRNTREAD either after the UNIVER... or after the rigid wall specification. The front specification looks like the following

FRNTREAD

c1 --- read of front information

ifr,ityp, | the\_number\_of\_front, the\_type\_of\_front

icont, | the\_number\_of\_contour

a,b,c, | the contour is straight line  $a*x+b*y-c=0$  ! icont=nomco+1

ibeg\_end, | 1-begin,2-end

-1

Here the expressions on the right from | are comments. The front input is finished when ifr equals to some negative value (-1 in this example). The beginning and the end of the front move along the straight lines (called contour). There are not more than two contours corresponding to the same front. The sequence of the numbers of the contours specified must be increasing. Every contour corresponds either to the beginning of



the front (ibeg\_end=1) or to the end. Using such an input several fronts can be specified. There are several front types considered (the\_type\_of\_front). The main of them are

- 1- shock front in undisturbed solid media
- 2-shock front in undisturbed porous media
- 3- front of onedimensionality

Specification of all fronts and walls must be closed by the string  
END.....

2) The next two strings

5., 0., 0.,::--USRT--,---VSTR---,VPOL  
12,::--NUMBER OF URS

give the velocity components (USRT, VSTR), porosity of the subregion (VPOL) and number of material (EOS). Then the boundary segments must be specified. Boundary orientation is counter-clockwise. The boundary segment can be straight line, circle or some other arbitrary curve specified in the table form. The next string gives the coordinates of the first point of the boundary.

0.,0.,::X0,Y0 - THE LOCATION OF THE FIRST POINT FOR A BOUNDARY (CM)

If the first boundary segment is a straight line, then the next two strings are

**STRAIGHT 1**

0.,1., XE,YE,:: IS COORDINATES OF THE END OF THE STRAIGHT SEGMENT (CM)

If the next segment is a fragment of a circle then must be

**CIRCLE**

XC,YC,ALF,:: IS THE CENTER OF THE CIRCLE(CM),ANGLE (0-360 grad)

The boundary segment can be any arbitrary curve. In this case it is specified using the table input

**TABLE**

XE,YE,:: IS THE NODES COORDINATES

..... , TABLE INPUT UNTIL INPUT ERROR OCCURES  
END OF THE TABLE

The specification of the boundary of a subregion is closed by the string

**REGEND**

The four angles of subregion must be determined for the purpose of grid generation, when the boundary of the subregion is specified. The angles input looks like this

#### 1---2---3---4 ANGLES LOCATION

I1,I2,I3,I4,;; TO FIND 4 ANGLES OF THE RECTANGULAR REGION USING  
CORRESPONDENT BOUNDARY SEGMENTS NUMBERS I1,I2,I3,I4

In the example of input shown below

,,5,;;  
the ANGLES with numbers 1,2,4 are determined automatically and the angle 3 is found in the beginning of the boundary segment number 5. Initially all the boundary segments have the type of "FREE BOUNDARY". If one needs to assign some other boundary type to the boundary segment the following strings are necessary:

#### BOUNDARY TYPE INPUT

Then depending on the boundary type can be:

a)in the case of rigid wall

**RIGID** ,;CHANGES "FREE" TYPE BY "RIGID"  
**IREG,IRG** ,; IREG-NUMBER OF BOUNDARY SEGMENT  
IRG-NUMBER OF RIGID WALL

b)in the case of shock front

**FRONT** ,;CHANGES "FREE" TYPE BY "FRONT"  
**IREG,IFR** ,; IREG-NUMBER OF BOUNDARY SEGMENT  
IFR-NUMBER OF FRONT

c) in the case of contact discontinuity

**CONTACT** ,;CHANGES "FREE" TYPE BY "CONTACT"  
**IREG,N1,IREG1**,; IREG-NUMBER OF BOUNDARY SEGMENT FOR CURRENT SUBREGION, N1-  
NUMBER OF SUBREGION WHICH IS IN CONTACT, IREG1-NUMBER OF BOUNDARY  
SEGMENT FOR N1 SUBREGION

The input of data for the current subregion is closed by

**UNIEND**

#### Remark:

We have described UNIVERSAL INPUT in the text above. If there are special program for more simple input for concrete configuration then the name of this program is the first string in the second part of the input data.

For example:

**DATST1** ; -NAME OF THE PROGRAM WHICH TREATS INPUT DATA

### *How to run the code*

- 1) Run the module STARTT in the directory containing file "NAM".DAT
- 2) Type "NAM" when the question "ENTER DATA NAME" appears

module STARTT will create the files:

"NAM".TMP- for following calculations

"NAM"000.DAT- first file for graphics

"NAM".CFG- file containing some parameters (if this file does not exist)

An example of CFG file is presented below

```
-----VRB2.CFG-----  
1.          , PLIM [bar]           line 1  
2.7104001E-05, RLIM [G/(CM**3)]   line 2  
13.93920   , EPSGAS [M/C]        line3  
278.7840   , EPSCON [M/C]        line4  
9.9999998E-03, ALMIN              line5  
0.3000000  , SINCOND              line6  
2.0000000E-02, ALMN               line7  
9.9999998E-03, SHISAMI            line8  
5.0000001E-02, SHISAMA            line9  
0.7000000  , TET                  line10  
0.0000000  , ADP                   line11  
-----
```

In this file the first two strings are minimal pressure and density, the next two strings are accuracy of calculation of wave velocities for the cases of gas EOS and table EOS correspondingly. Parameters ALMIN, SINCOND (SINCOND is changing from 0 to 1), ALMN are responsible for the movement of boundary nodes on the boundary of "special" type. SHISAMI and SHISAMA are minimum and maximum shift of the boundary nodes during the procedure of boundary node distribution (in relative units). TET is a parameter determining the convergence of grid generation (TET>0) and ADP is a level of grid adaptation to solution. In the present version of the code adaptation is not included (ADP=0)

When the STARTT finishes its work the following message appears

THE NUMBER OF PICTURE =0

3) Run the module BIG2T (or BIG1T) to continue calculations

4) Reply the questions appearing on the screen

To avoid the grid tangle in the cases of large deformations to split the numerical regions into subregions is recommended. The most frequently appearing question concerning that is

IF YOU DON'T WANT TO SPLIT SUBREGION \*

**ENTER** number of steps without splitting analysis

Enter 0 on this question if you want to split subregion, which the program suggests to split. Then press enter to continue computations.

The question **ENTER N,M ACCORDING TO THE STENCIL** means that you can change the type of contact between subregions N and M. Enter -1,1 to ignore this (and -1,1 for the next question)

The program periodically creates the files "NAM"xxx.DAT for graphics and renews file "NAM".TMP for restart.

When the program has done the calculations it starts the dialogue from the beginning (asking "ENTER DATA NAME"). To continue the computations of the same problem enter the same name NAM.

- 5) Analyze the results of computation using graphics modules. For this purpose created graph files "NAM"\*\*\*.DAT (and k"NAM"\*\*\*.DAT) must be copied to IBM PC Then they can be depicted on the screen using and written in TIF file using GR.EXE (See the manual for GR.EXE)
- 6) Continue calculations (point 3) if it is necessary
- 7) Change configuration of the task,if it is necessary if you want to change configuration you must create the file D"NAM".DAT (see description of the file) and run the program REP

### *Brief manual for GR.EXE*

*Executing module GR.EXE shows the results of computation on the screen of IBM PC (DOS is required) and writes the pictures shown on the screen in TIF format. Besides the resulting files "NAME"\*\*\*.DAT to be shown, one more file K"NAME".DAT is necessary to determine the limits of the picture. This file can be created anytime by coping already existing files of such type. After running GR.EXE one need to answer the questions in the dialog.*

- 1) Type the root name of \*.DAT files to be plotted ("NAME")
- 2) Enter the number of picture N (file "NAME"N.DAT will be plotted)
- 3) Choose the flow parameter to be plotted (1-density, 2-pressure, 3-porosity, 4,5-velocities, 6-energy)
- 4) Choose the type of picture (I-levels of constant values and numerical grid, I2-levels of constant values for two different flow parameters, DY-cross sections along the axis of symmetry, DX- perpendicular to the axis)

5) When the picture is shown on the screen one can plot over this picture another pictures (if the axes are not plotted yet). For this purpose enter negative number  $-N$  (where  $N$  is the number of picture to be plotted)

6) To finish plotting enter any character (for example '.') and axes will be shown. Then type enter, the name of the TIF file where this picture will be saved and CTRL-C to leave the program.

7) REMARK: When using DY or DX options (plotting cross sections) use CTRL-Z to return back for plotting pictures after the question  
 $I = \text{INPUT Y/X COORDINATE FOR SECTION.}$

There is an example of GR.EXE execution presented on the picture below

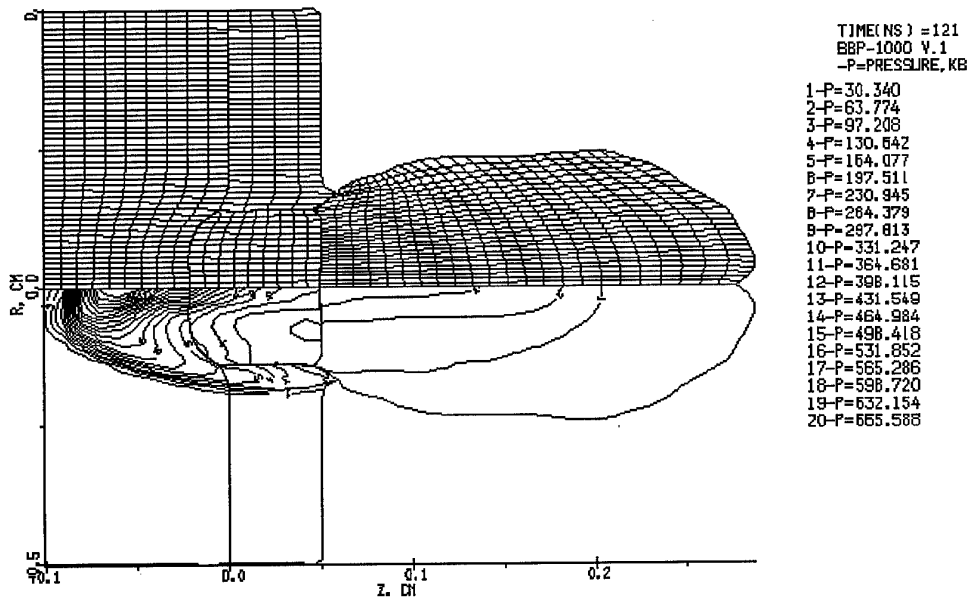


Figure .1 An Example of GR.EXE plot

*Example of initial data files*

Let us consider some demonstrative examples of initial data generation for hypervelocity impact problems

EXAMPLE 1: initial data file VRB3.DAT

Impact of W projectile on Al target  
 JSPR-LOS-LST-IRD-ISP-IRA-ICM-AIR  
 1 1 1 2 1 00 1 0  
 NBL--MI-ID1-ID2--IK-IGR-ILENPARIVSP  
 9900 1 30 30 300 30-500 6 0  
 ----CMM----:----H3----:----HDEL---:----T-----:----STABL---:  
 -1.00000E-03 0.02000E-00 0.06000E+00 1.10000E+05 0.60000E+00  
 UNIVER ; -NAME OF PROGRAM WHICH TREATS INPUT DATA  
 RIGIDRD ; READING AXIS AND RIGID WALLS  
 C IWALL, INW, ITP, AW, BW, CW ;STRAIGHT LINE: F=AW\*X+BW\*Y-CW=0.  
 1 , -1, 1, 0. , 1., 0.

```

-1 , -1 , 1, 0. , 1., 0. exit,A,A,A,A
END
-5., 0., 0.,:--USRT--,---VSTR---,VPOL
44,:--NUMBER OF EOS
0.,0.,: X0,Y0 - THE LOCATION OF THE FIRST POINT FOR THE BOUNDARY (CM)
STRAIGHT 1
1.,0., XE,YE,: COORDINATES OF THE END OF THE STRAIGHT SEGMENT (CM)
STRAIGHT 2
1.,4., XE,YE,: COORDINATES OF THE END OF THE STRAIGHT SEGMENT (CM)
STRAIGHT 3
0.,4., XE,YE,: COORDINATES OF THE END OF THE STRAIGHT SEGMENT (CM)
STRAIGHT 4
0.,0., XE,YE,: COORDINATES OF THE END OF THE STRAIGHT SEGMENT (CM)
REGEND
c-1-2-3-4
1,2,3,4,
BOUNDARY TYPE INPUT
RIGID ,CHANGING "FREE" TYPE BY "RIGID"
1,1,; IREG-NUMBER OF BOUNDARY SEGMENT,IRG-NUMBER OF RIGID WALL
UNIEND 1
UNIVER , -NAME OF PROGRAM WHICH TREATS INPUT DATA
END
0., 0., 0.,:--USRT--,---VSTR---,VPOL
41, :--NUMBER OF EOS
-8.5,0.,: X0,Y0 - THE LOCATION OF THE FIRST POINT FOR THE BOUNDARY (CM)
STRAIGHT 1
0.,0., XE,YE,: COORDINATES OF THE END OF THE STRAIGHT SEGMENT (CM)
TABLE 1
0.,0.,
0.,8.5,
0.,8.5,
-8.5,8.5,
-8.5,8.5,
-8.5,0.,
-8.5,0.,
END OF TABLE
REGEND
1---2---3---4
1,2,,,
BOUNDARY TYPE INPUT
RIGID
1,1,
UNIEND 2
ENDINPUT

```

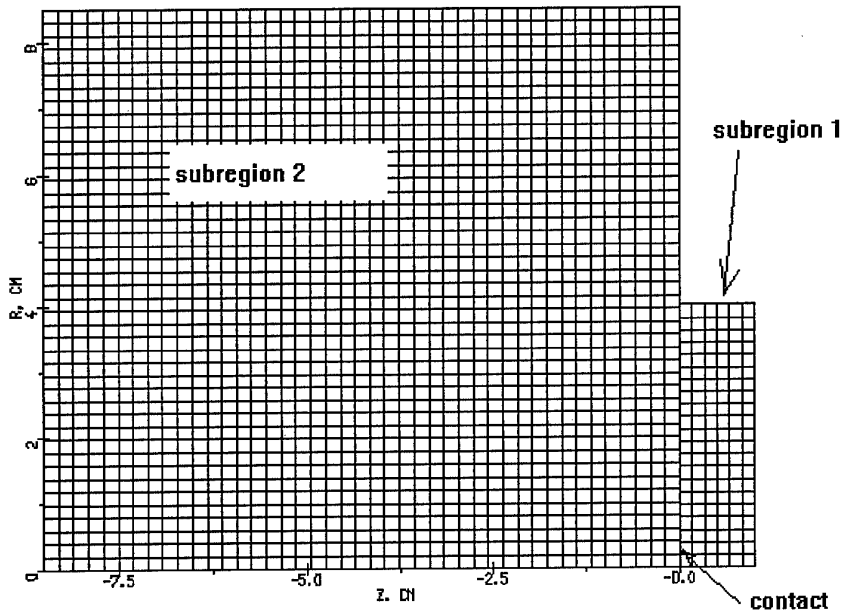


Fig.1 Initial configuration for initial data file VRB3.DAT

EXAMPLE 2: initial data file VRB2.DAT

IMPACT with shock fitting

JSPR-LOS-LST-IRD-ISP-IRA-ICM-AIR

1 1 1 2 1 00 1 0

NBL--MI-ID1-ID2--IK-IGR-ILENPARIVSP

9900 1 30 30 300 30-500 6 0

----CMM---:-----H3---:----HDEL---:----T-----:---STABL---:

-1.00000E-03 0.02000E-00 0.06000E+00 1.10000E+05 0.60000E+00

UNIVER ; ; -NAME OF PROGRAM WHICH TREATS INPUT DATA

FRNTREAD ,

C1 --- read of the front information

1,1, ;c2 ifr,ityp ,: the\_number\_of\_front, the\_type\_of\_front

1, ;c3 icont,: the\_number\_of\_contour

1.,0.,0., ;c4 a,b,c,: the contour is straight line  $a*x+b*y-c=0$  !

icont=nomco+1

1, ;c5 ibeg\_end,: 1-begin,2-end

-1, ;c6 end

RIGIDRD , ; READ OF AXIS AND RIGID WALLS

C IWALL, INW, ITP, AW, BW, CW ;STRAIGHT LINE:  $F=AW*X+BW*Y-CW=0$ .

1 , -1 , 1 , 0. , 1., 0.

-1 , -1 , 1 , 0. , 1., 0. exit,A,A,A,A

END

-5., 0., 0.,:--USRT--:--VSTR---,VPOL

44, :--NUMBER OF EOS

0., 0., :: X0,Y0 - THE LOCATION OF THE FIRST POINT FOR THE BOUNDARY (CM)

STRAIGHT 1

1.,0., XE,YE,: ARE COORDINATES OF THE END OF THE STRAIGHT SEGMENT (CM)

STRAIGHT 2

1.,4., XE,YE,:: ARE COORDINATES OF THE END OF THE  
 STRAIGHT SEGMENT (CM)  
 STRAIGHT 3  
 0.,4., XE,YE,:: ARE COORDINATES OF THE END OF THE STRAIGHT SEGMENT (CM)  
 STRAIGHT 4  
 0.,0., XE,YE,:: ARE COORDINATES OF THE END OF THE STRAIGHT SEGMENT (CM)  
 REGEND  
   1---2---3---4 ANGLE LOCATION  
   1,2,3,4,  
 BOUNDARY TYPE INPUT  
 RIGID ;,YOU WILL CHANGE "FREE" TYPE ON "RIGID"  
   1,1,; IREG-NUMBER OF BOUNDARY SEGMENT,IRG-NUMBER OF RIGID WALL  
 UNIEND 1  
 UNIVER ;, -NAME OF PROGRAM WHICH TREATS INPUT DATA  
 END  
   0., 0., 0.,::--USRT--,---VSTR---,VPOL  
 41, ::--NUMBER OF EOS  
   -0.25, 0., :: X0,Y0 - THE LOCATION OF THE FIRST POINT FOR THE BOUNDARY (CM)  
 STRAIGHT 1  
   0.,0., XE,YE,:: ARE COORDINATES OF THE END OF THE STRAIGHT SEGMENT (CM)  
 STRAIGHT 2  
   0.,4.1, XE,YE,:: ARE COORDINATES OF THE END OF THE STRAIGHT SEGMENT (CM)  
 TABLE 3  
   0.,4.1, XE,YE,:: ARE COORDINATES OF THE END OF THE STRAIGHT SEGMENT (CM)  
   -0.,4.1, XE,YE,:: ARE COORDINATES OF THE END OF THE STRAIGHT SEGMENT (CM)  
   -0.25,3.0, XE,YE,:: ARE COORDINATES OF THE END OF THE STRAIGHT SEGMENT (CM)  
   -0.25,3.0, XE,YE,:: ARE COORDINATES OF THE END OF THE STRAIGHT SEGMENT (CM)  
   -0.25,0., XE,YE,:: ARE COORDINATES OF THE END OF THE STRAIGHT SEGMENT (CM)  
   -0.25,0., XE,YE,:: ARE COORDINATES OF THE END OF THE STRAIGHT SEGMENT (CM)  
 END OF TABLE  
 REGEND  
   1---2---3---4 ANGLE LOCATION  
   1,2,3,,  
 BOUNDARY TYPE INPUT  
 RIGID ;,YOU WILL CHANGE "FREE" TYPE ON "RIGID"  
   1,1,; IREG-NUMBER OF BOUNDARY SEGMENT,IRG-NUMBER OF RIGID WALL  
 FRONT  
   3,1,; IREG-NUMBER OF BOUNDARY SEGMENT,IRG-NUMBER OF FRONT  
 UNIEND 2  
 ENDINPUT

Note: Boundary specified by TABLE is considered as *one* boundary segment !!!



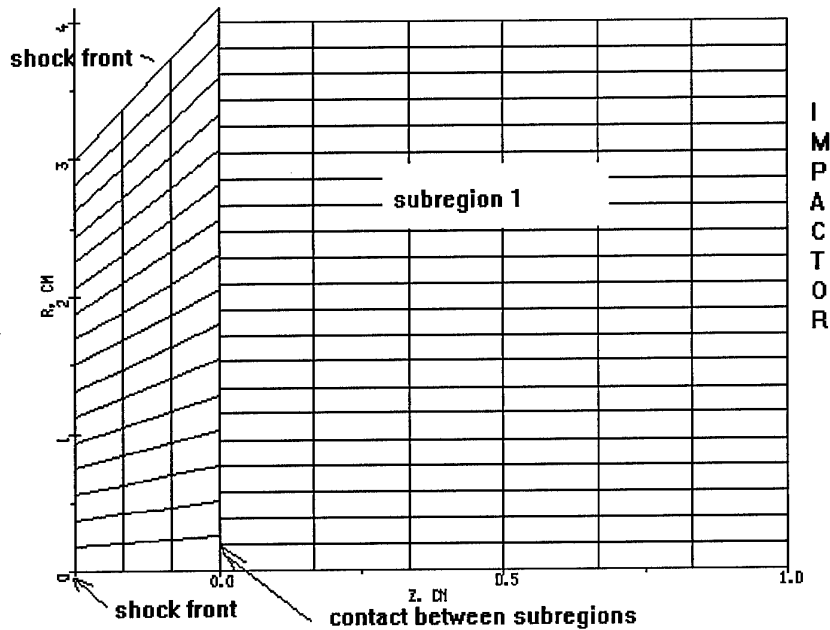


Fig.2 Initial configuration for initial data file VRB2.DAT

## *Strategy of computations and some useful details*

### Grid splitting

To prevent the code failure in grid generation, please, avoid numerical subregion being of complicated shape. In the most of cases when it is necessary, the program analyses the form of regions and offers the ways of dividing them into subregions. Nevertheless, one can split any numerical region running module *REP.OUT*. This module requires the data file *D"name".DAT*, where action is specified. In the case of splitting the first two strings in *D"name".DAT* must be

**SPLSUB**

**ENDINPUT**

Then running *REP.OUT* one should answer the following equations:

- 1) Enter the number of the region to be split
- 2) Enter option to refine the grid in the subregion (0-no refinement, 1-refinement along i- index, 2-along j index, 3- along both)
- 3) Enter option to make the grid rough (answers are similar as for 2))
- 4) Enter 1-to split along i grid line, 2-to split along j grid line, 0-no splitting.

If you put 1 or 2 on the question 4) there will be one more question:

- 5) Enter the number of i(or j) line along which the region will be split.
- To leave dialog enter any negative number of the region.

### Removal of numerical region N

*Sometimes it is desirable to delete the numerical region which is not interesting. To do this put the following four strings into the file*

*D"name".DAT:*

*DELSUB*

*N*

*-1*

*ENDINPUT*

*where N- is the number of subregion to be deleted.*

*Then run REP.OUT again.*

### Addition of a new numerical subregion

*The code allows one to include into consideration additional numerical regions as soon as it is required (for example in the case of an impact on multilayered spaced target). To do this put all information about these regions into D"nam".dat according to initial data format (starting from*

*UNIVER*

*and ending with*

*ENDINPUT.*

*Then run REP.OUT and a new TMP file will be generated. After that proceed with doing computations with BIG2T.OUT.*

### Changing boundary type.

*Sometimes it is necessary to change the type of boundary between subregions. For example, newly appearing subregions (after splitting procedure) have so called "special" type of boundaries between each other. To change this boundary into contact type is possible running BIG2T.OUT*

*.For this purpose:*

*1) Put IRD=1 and ISP=1 in "NAME".DAT*

*2) Run BIG2T.OUT and enter the following answers on the questions:*

*N1,N2*

*N1,N2,M*

*N2,N1,M*

*-1,1*

*-1,1*

*Here N1 and N2 are the numbers of subregions where the boundary type is to be changed from current type to contact (if M=0) or to "special" boundary (if M=4).*

## What does it mean and What to do if

Output print: ???CHANGE CM??? - one of the mesh rows (or columns) becomes too thin to satisfy the Courant stability condition. In this case program blocks this row with the neighboring one during the flow parameter recalculation to the next time step.

Output print: DJCO(2) - This output usually occurs after splitting procedure. One should stop computations and repeat it once again by BIG2T without splitting of subregion at the same moment. One can do it several steps later.

Output print: CATCH STOP - something is happened. Press enter to continue computations.

## GENERAL RECOMMENDATIONS

A. Do not split subregions without necessity !!

B. Changing parameters SHISAMI and SHISAMA one can influence the grid generation. You can do the grid more orthogonal making them greater and more uniform making them less. If you have some problems with the grid, for example, in the case when the grid has strongly different cell dimensions in different parts of the numerical region, please, decrease these parameters to generate more uniform grid.

C. Please, look periodically at your results using graphics  
If you use PC computer you can run CINEMA.EXE in the directory where are your graphic files NAME\*.DAT are.

GOOD LUCK